Theoretical Study of Phase Separation and Thermoreversible Gelation in Aqueous Solutions of Temperature-Sensitive Polymers

Yukinori Okada

2007

Theoretical Study of Phase Separation and Thermoreversible Gelation in Aqueous Solutions of Temperature-Sensitive Polymers

Yukinori Okada

2007

Contents

Chapter 1

Introduction

1.1 Overview

Liquid-liquid phase separation and thermoreversible gelation are two of the most characteristic phase transition phenomena in polymer solutions. To clarify their molecular mechanisms is very important not only for basic scientific research of polymers but also for their industrial applications. So far, these problems have been intensively studied by various methods such as experimental, theoretical, and computational methods. In early stage of theoretical study in 1940s, P. J. Flory and W. H. Stockmayer developed a statistical reaction theory of gelation. In the same period, Flory established the statistical thermodynamic theory of polymer solutions, which enabled us to analyze phase separation phenomena in polymer solutions. Studies of interference between phase separation and gelation, however, started much later in 1990s, and the problem has not completely been solved even in these days.

Aqueous water-soluble polymers attract interest from the viewpoint of global environment protection. Water-soluble polymers reveal interesting properties such as phase separation at high temperature, swelling by water adsorption etc. Their molecular mechanisms have not however been described. Hydration plays an important role for phase separation at high temperature. Water-soluble polymers form hydrogen bonds with water molecules (bound water) at low temperature, i.e., *polymers wear cloths made by water.* Thus, polymer chain dissolves in water. At high temperature, dehydration occurs due to thermal motion, i.e., *polymer chain takes off its cloth of water*, being driven into low solubility. Then, liquid-liquid phase separation follows due to aggregation of polymer chains. The shape of phase separation region depends on the side chain of the polymer. Poly (*N*-isopropylacrylamide) (referred to as PNIPAM), which is well known as thermosensitive polymer, separates into two liquid phases when temperature is raised to approximately 31°C. The cloud point curve of PNIPAM depends only weakly on both molecular weight and the concentration. In the case of poly (ethylene oxide) (referred to as PEO), however, phase separation region expands when the molecular weight becomes higher. Thus, there is a great difference in their molecular mechanisms of phase separation.

Hydrophobic groups represented by alkyl groups, aggregates with each other by hydrophobic interaction in water. Then networks and micelles are formed. Gelation and phase separation are interfered by hydrophobic association between surfactants and polymers when surfactants are introduced into aqueous associating polymer solutions. Various hydrophobically modified water-soluble polymers (commonly named as associating polymers) are synthesized and studied their thermodynamic properties. It is much interesting in the case of telechelic associating polymers which carry hydrophobic groups at both chain ends. Due to coexistence of hydration on the main chain and hydrophobic aggregation by the end chains, flower micelles are formed at low temperature in dilute regime, while three dimensional networks are formed at concentrated regime, being accompanied with phase separation at high temperature. Study on the molecular mechanism of phase transitions under coexisting, or competing hydration and hydrophobic aggregation in polymer solutions has not been reported yet.

In polycondensation system, water molecules reacts with polymers, thus they can be regarded as active solvent. In the case of monomers that have more than three reactive sites, branched polymers are formed during polycondensation, thus phase separation is promoted due to the loss of the mixing entropy by the decrease in the degrees of translational motion. Such phase separation is called *gelation induced phase separation.* Gelation induced phase separation in polycondensation, such as esterification, sol/gel reaction in tetra- ethoxysilane, etc is very important, thus they are studied in both academic science and industrial engineering. Polymerization takes place either in a closed vessel or an open vessel. The controllable parameters in these vessels are the temperature and volume. Thus vapour pressure is usually not a controllable parameter. If the reaction is confined under a constant vapour pressure, controlling phase separation and gelation is easier. Therefore, it is important to find the fundamental principle of pressure-controlled thermoreversible gelation. There is also an important study for both reaction mechanism and gelation induced phase separation to find the relation between time-dependent properties (reaction paths) and the initial condition of the reactive solutions, i.e., the initial temperature and composition. In this thesis, the author reports theoretical and compu-

tational studies on these problems that he has done during the past three years of the doctoral research.

In the rest of this chapter, the author briefly describes the outline of the general theoretical framework, and motivation of this thesis and the related studies.

1.2 Theoretical Researches on Solutions of Associating Polymers

In this section, the author shows the statistical-mechanical theory of associating polymer solutions and theoretical study of phase separation in water-soluble polymer solutions with focus on hydration. The classical theories of sol/gel transition are also described.

1.2.1 Statistical-Mechanical Theory of Associating Polymer Solutions

Let us study the statistical-mechanical theory of associating polymer solutions[1]. This thesis is based on it.

Let us start from the lattice theory in a binary mixture system. The system volume V is divided into cells of size a, thus the total number of cell Ω is defined by $\Omega \equiv V/a^3$. There are two types of molecules in this system - A molecule and B molecule with the degree of polymerization n_A and n_B, respectively. The monomer of A molecule and B molecule have same size. The solution is assumed incompressibility of the solution. The cluster which consists of the number l of the A molecules and m of the B molecules is expressed by an (l, m)-mer, then the number of the (l, m)-mers is N_{lm}. Thus, $(1, 0)$ and $(0, 1)$ clusters are un-reacted A molecule and B molecule, respectively. Now, Ω can be rewritten by

$$\Omega = \sum_{l,m} (n_A l + n_B m) N_{lm}. \tag{1.1}$$

The number density and volume fraction of the (l, m)-mers are given by

$$\nu_{lm} = \frac{N_{lm}}{\Omega} \tag{1.2}$$

$$\phi_{lm} = (n_A l + n_B m)\nu_{lm} = \frac{(n_A l + n_B m)N_{lm}}{\Omega}, \tag{1.3}$$

respectively. In the postgel regime where gel networks exist, the number of A and B molecules belonging to gel networks are defined by N_A^G and N_B^G, respectively. Thus, the number density and volume fraction are expressed by

$$\nu_A^G \equiv \frac{N_A^G}{\Omega} \qquad \nu_B^G \equiv \frac{N_B^G}{\Omega} \tag{1.4}$$

$$\phi_A^G \equiv n_A \nu_A^G = \frac{n_A N_A^G}{\Omega} \qquad \phi_B^G \equiv n_B \nu_B^G = \frac{n_B N_B^G}{\Omega}. \tag{1.5}$$

Ω is given by

$$\Omega = \sum_{l,m} (n_A l + n_B m) N_{lm} + n_A N_A^G + n_B N_B^G. \tag{1.6}$$

The volume fraction of sol part are given by

$$\phi_A^S \equiv n_A \sum_{l,m} l \nu_{lm} \qquad \phi_B^S \equiv n_B \sum_{l,m} m \nu_{lm}. \tag{1.7}$$

We have to note the relations that

$$\phi_A = \phi_A^S + \phi_A^G \tag{1.8}$$

$$\phi_B = \phi_B^S + \phi_B^G \tag{1.9}$$

$$\phi_A + \phi_B = 1. \tag{1.10}$$

If we assume ϕ_A as an independent parameter, ϕ_A can be rewritten to the simple expression ϕ.

Let us discuss the free energy. The free energy difference ΔF from the standard reference state can be divided into two terms,

$$\Delta F = \Delta F_{\text{rea}} + \Delta F_{\text{mix}}. \tag{1.11}$$

ΔF_{rea} is the free energy difference of reaction between the standard reference state and the ideal state that has real number distribution of clusters by reaction with A molecules and B molecules.

$$\beta \Delta F_{\text{rea}} = \sum_{l,m} (\Delta_{lm} N_{lm} + \delta_A N_A^G + \delta_B N_B^G), \tag{1.12}$$

where $\beta \equiv 1/k_B T$, and

$$\Delta_{lm} \equiv \beta(\mu_{lm}^\circ - l\mu_{10}^\circ - m\mu_{01}^\circ). \tag{1.13}$$

is the free energy when an (l,m)-mer is formed by the number l of A molecules and m of B molecules. μ° shows internal free energy, δ_A, δ_B are the free energy change when an isolated molecule bonds with the gel networks, then expressed as a function of volume fraction ϕ.

ΔF_{mix} is the free energy difference of mixing between the ideal state and the real state. According to the Flory-Huggins theory[2, 3], ΔF_{mix} is given by

$$\beta\Delta F_{\mathrm{mix}} = \sum_{l,m} N_{lm} \ln \phi_{lm} + \chi\phi(1-\phi), \tag{1.14}$$

where χ is the Flory's χ-parameter that is the interaction between A molecule and B molecule. Eq.(1.11) has both the bonding term ΔF_{rea} and the repulsive term ΔF_{mix}, thus there is a lot of interesting phenomenon in such associating polymer solutions.

The chemical potential of the (l,m)-mers $\Delta\mu_{lm}$ is given by

$$\begin{aligned}\beta\Delta\mu_{lm} \equiv \beta\left(\frac{\partial\Delta F}{\partial N_{lm}}\right)_{T,N_{l'm'},\cdots} =& 1 + \Delta_{lm} + \ln\phi_{lm} - (n_A l + n_B m)\nu^S \\ &+ \chi[n_A l(1-\phi) + n_B m\phi - (n_A l + n_B m)\phi(1-\phi)] \\ &+ [n_A l(1-\phi) - n_B m\phi][\delta'_A(\phi)\nu_A^G - \delta'_B(\phi)\nu_B^G],\end{aligned} \tag{1.15}$$

where

$$\nu^S \equiv \sum_{l,m} \nu_{lm} \tag{1.16}$$

is the total number of sol clusters. From Eq.(1.15), the chemical potentials of isolated molecules are expressed by

$$\frac{\beta\Delta\mu_{10}}{n_A} = \frac{1+\ln\phi_{10}}{n_A} - \nu^S + \chi(1-\phi)^2 + [\delta'_A(\phi)\nu_A^G - \delta'_B(\phi)\nu_B^G](1-\phi) \tag{1.17}$$

$$\frac{\beta\Delta\mu_{01}}{n_B} = \frac{1+\ln\phi_{01}}{n_B} - \nu^S + \chi\phi^2 - [\delta'_A(\phi)\nu_A^G - \delta'_B(\phi)\nu_B^G]\phi, \tag{1.18}$$

respectively. The chemical potential of A and B molecules in gel networks are expressed by

$$\frac{\beta\Delta\mu_A^G}{n_A} = \frac{\delta_A}{n_A} - \nu^S + \chi(1-\phi)^2 + [\delta'_A(\phi)\nu_A^G - \delta'_B(\phi)\nu_B^G](1-\phi) \tag{1.19}$$

$$\frac{\beta\Delta\mu_B^G}{n_B} = \frac{\delta_B}{n_B} - \nu^S + \chi\phi^2 - [\delta'_A(\phi)\nu_A^G - \delta'_B(\phi)\nu_B^G]\phi. \tag{1.20}$$

We next derive the distribution function from chemical potential. In the case of nongelling system or at pregel regime, then $\phi^G = 0$. From the thermoequilibrium condition for association (multiple equilibria),

$$\Delta\mu_{lm} = l\Delta\mu_{10} + m\Delta\mu_{01}. \tag{1.21}$$

Thus, the volume fraction of the (l, m)-mers is given by

$$\phi_{lm} = K_{lm}\phi_{10}^{l}\phi_{01}^{m}, \tag{1.22}$$

where

$$K_{lm} \equiv \exp(l + m - 1 - \Delta_{lm}) \tag{1.23}$$

is the equilibrium constant for association that is given as a function of temperature. The total number density and the volume fraction of sol part are given by

$$\nu^S(\phi_{10}, \phi_{01}) = \sum_{l,m} \frac{\phi_{lm}}{n_A l + n_B m} = \sum_{l,m} \frac{K_{lm}}{n_A l + n_B m}\phi_{10}^{l}\phi_{01}^{m}, \tag{1.24}$$

$$\phi^S(\phi_{10}, \phi_{01}) = \sum_{l,m} \phi_{lm} = \sum_{l,m} K_{lm}\phi_{10}^{l}\phi_{01}^{m}. \tag{1.25}$$

ϕ_{10} and ϕ_{01} are expressed as a function of ϕ by solving Eqs.(1.26) and (1.27),

$$n_A\phi_{10}\frac{\partial\nu^S}{\partial\phi_{10}} = \phi \tag{1.26}$$

$$n_B\phi_{01}\frac{\partial\nu^S}{\partial\phi_{01}} = 1 - \phi. \tag{1.27}$$

Let us discuss sol/gel transition, Eq.(1.25) is a double series equation and monotonous increasing series. Thus, there are boundary lines of convergence region. If $\phi^S < 1$ on this boundary line and inside convergence region, the gel networks exist in this solution. Thus, sol/gel transition line is given by

$$\phi^S(\phi_A^*, \phi_B^*) = 1. \tag{1.28}$$

At the postgel regime, the equilibrium condition for association between an isolate molecule and a gel network are given by

$$\Delta\mu_A \equiv \Delta\mu_{10} = \Delta\mu_A^G \qquad \Delta\mu_B \equiv \Delta\mu_{01} = \Delta\mu_B^G. \tag{1.29}$$

Then,

$$\ln \phi_{10} = \delta_A(\phi) - 1 \qquad \ln \phi_{01} = \delta_B(\phi) - 1. \tag{1.30}$$

Thus, ϕ_A, ϕ_B are given as a function of $\delta_A(\phi), \delta_B(\phi)$, respectively.

Binodal Condition

The binodal condition where solution separates into two different macroscopic phase at a giving temperature T is given by

$$\Delta\mu_A(\phi', T) = \Delta\mu_A(\phi'', T), \tag{1.31}$$

$$\Delta\mu_B(\phi', T) = \Delta\mu_B(\phi'', T), \tag{1.32}$$

where ϕ', ϕ'' are the volume fraction of A molecules in rich B phase, and in rich A phase, respectively. Thus, ϕ', ϕ'' are given by solving the simultaneous equations (1.31) and (1.32). The curve which ϕ' and ϕ'' are plotted on the temperature-concentration plane is called binodal curve.

Spinodal Condition

The spinodal condition where is the boundary between stable/unstable region is given by

$$\frac{\partial(\Delta\mu_A/n_A - \Delta\mu_B/n_B)}{\partial\phi} = 0. \tag{1.33}$$

Then,

$$\frac{\kappa_A(\phi)}{n_A\phi} + \frac{\kappa_B(\phi)}{n_B(1-\phi)} - 2\chi = 0. \tag{1.34}$$

where

$$\kappa_A \equiv \phi_A \frac{d}{d\phi_A}\left(1 + \phi_A^G \frac{d}{d\phi_A}\right)\ln \phi_{10} = \phi \frac{d}{d\phi}\left(1 + \phi_A^G \frac{d}{d\phi}\right)\ln \phi_{10} \tag{1.35}$$

$$\kappa_B \equiv \phi_B \frac{d}{d\phi_B}\left(1 + \phi_B^G \frac{d}{d\phi_B}\right)\ln \phi_{01} = -(1-\phi)\frac{d}{d\phi}\left(1 - \phi_B^G \frac{d}{d\phi}\right)\ln \phi_{01}. \tag{1.36}$$

1.2.2 Statistical Theory in Aqueous Solutions of Poly (Ethylene Oxide)

Matsuyama *et al.*[4] (referred to as MT) theoretically studied phase separation in a binary mixture of polymer and solvent which were capable of forming thermoreversible bonds each other by pairwise association. The binodal curves from this theory fitted very well the experimental data in aqueous solutions of PEO by Saeki *et al.*[5]. In this section, the author shows this MT theory applying to PEO/water systems.

MT is employed to a model solution in which the number N_1 of polymer chains with degree of polymerization (referred to as DP) n are mixed with the number N_0 of water molecules, and a polymer chain has n functional site, then it is based on the lattice-theoretical picture of polymer solutions. Each of unit cell can accommodate either a water molecule or a statistical repeat unit of the polymer, thus total number of cells is given by $\Omega = N_0 + nN_1$. The type of hydrated clusters are expressed by $(1, m)$ type, where is $m = 0, 1, \cdots, n$. Then, the free energy change is divided into two terms,

$$\Delta F = \Delta F_{\text{mix}} + \Delta F_{\text{rea}}. \tag{1.37}$$

According to the lattice theory of Flory-Huggins[2, 3], the free energy difference of mixing ΔF_{mix} is given by

$$\beta \Delta F_{\text{mix}} = N_0 \ln \phi_0 + \sum_{m=0}^{n} N_{1m} \ln \phi_{1m} + \Omega \chi \phi (1 - \phi), \tag{1.38}$$

where $N_0, \phi_0 \equiv N_0/\Omega$ are the number of the free water molecules and their volume fraction, N_{1m}, ϕ_{1m} are the number of the $(1, m)$-mers and their volume fraction, χ is the water-polymer interaction parameter, $\phi = nN_1/\Omega = \sum_{m=0}^{n} n\phi_{1m}/(n + m)$ is the total volume fraction of the polymers, and $\beta \equiv 1/k_B T$, respectively.

$$\beta \Delta F_{\text{rea}} = \sum_{m=1}^{n} \Delta_m N_{1m}, \tag{1.39}$$

where Δ_m is the free energy difference in the formation of an $m-$mer from a bare polymer chain and the number m of the water molecules, then, given by

$$\Delta_m \equiv \beta(\mu^{\circ}_{1m} - \mu^{\circ}_{10} - m\mu^{\circ}_{01}). \tag{1.40}$$

The chemical potential of the free water μ_0, m–mer μ_{1m} are given by

$$\beta\mu_0 = \beta\frac{\partial F}{\partial N_0} = \beta\mu_0^\circ + \ln\phi_0 + 1 - \left(\phi_0 + \frac{\phi}{n}\right) + \chi\phi^2, \tag{1.41}$$

$$\beta\mu_{1m} = \beta\frac{\partial F}{\partial N_{1m}} = \beta\mu_{1m}^\circ + \ln\phi_{1m} + 1 - (n+m)\left(\phi_0 + \frac{\phi}{n}\right) + n\chi\left[(1-\phi)^2 + \frac{m}{n}\phi^2\right]. \tag{1.42}$$

The multiple chemical equilibria condition is given by

$$\Delta\mu_{1m} = \Delta\mu_{10} + m\Delta\mu_0. \tag{1.43}$$

Thus, submitting Eqs.(1.41) and (1.42) into Eq.(1.43), the volume fraction of the m–mers is given by

$$\phi_{1m} = K_m\phi_{10}(\phi_0)^m, \tag{1.44}$$

where $K_m = \exp(m - \Delta_m)$ is the association constant.

Δ_m consists of three terms - the combinatorial entropy ΔS_{comb}, the configurational entropy ΔS_{dis}, and the free energy of bonding (enthalpy term), thus, Δ_m is given by

$$\Delta_m = -\frac{1}{k_B}(\Delta S_{\text{comb}} + \Delta S_{\text{dis}}) + \beta\Delta f_0 m. \tag{1.45}$$

If each bond between polymer and water is both isolate and random, then ΔS_{comb} is given by

$$\Delta S_{\text{comb}} = k_B \ln W_m = k_B \ln({}_nC_m), \tag{1.46}$$

where W_m is the number of ways to select m functional groups out of n on a polymer chain.

ΔS_{dis} for an m–mer formation is given by

$$\Delta S_{\text{dis}} = S_{\text{dis}}(n+m) - S_{\text{dis}}(n) - mS_{\text{dis}}(1) \tag{1.47}$$

$$= k_B \ln\left[\frac{n+m}{n}\left\{\frac{\sigma(z-1)^2}{ze}\right\}^m\right]. \tag{1.48}$$

$S_{\text{dis}}(n)$ is given by from "entropy of disorientation",

$$S_{\text{dis}}(n) = k_B \ln\left[\frac{nz(z-1)^{n-2}}{\sigma e^{n-1}}\right], \tag{1.49}$$

where z is the coordination number of a quasilattice, σ is the symmetry number of the cluster.

From Eqs.(1.45), (1.46), and(1.49), K_m is given by

$$K_m = \frac{n+m}{n} {}_nC_m \lambda(T)^m, \tag{1.50}$$

where $\lambda(T) \equiv [\sigma(z-1)^2/ez]e^{-\beta\Delta f_0}$ is the association constant.

By the normalization condition together with multiple equilibria, the volume fraction ϕ_0 is given as a function of ϕ and $\lambda(T)$,

$$\phi_0 = \frac{1}{2\lambda}[(1-2\phi)\lambda - 1 + \sqrt{D(\phi)}], \tag{1.51}$$

where

$$D(\phi) \equiv [(1-2\phi)\lambda - 1]^2 + 4\lambda(1-\phi). \tag{1.52}$$

Now, Eqs.(1.41) and (1.42) are also expressed as a function of ϕ and $\lambda(T)$. The spinodal condition is given by

$$\frac{\partial(\Delta\mu_{10}/n - \Delta\mu_0)}{\partial\phi} = \frac{1}{n\phi} + \frac{\phi_0 - 1}{\phi_0\phi}\left(\frac{d\phi_0}{d\phi}\right) - 2\chi = 0. \tag{1.53}$$

For numerical calculation, the reduced temperature τ is introduced by the definition $\tau \equiv 1 - \Theta_0/T$, where Θ_0 is the reference theta temperature, Θ_0 satisfying $\chi(\Theta_0) = 1/2$. $\chi(T)$ is expressed as the conventional Schultz-Flory form $\chi(T) = 1/2 - \psi\tau$ for the χ-parameter[6] and $\lambda(T) = \lambda_0 \exp(|\epsilon + \Delta\epsilon|/k_BT) = \lambda_0 \exp[\gamma(1-\tau)]$, where λ_0 gives the entropy part of the binding free energy, and $\gamma \equiv |\epsilon + \Delta\epsilon|/k_B\Theta_0$ gives the binding energy measured relative to the thermal energy at the reference theta temperature.

Figure 1.1 shows the phase diagram in PEO/water systems. Phase separation region expands with the increase of DP n. The parameters are used to fit the experimental data by S. Saeki *et al.*[5]: $\psi = 1, \Theta_0 = 730K, \gamma = 6, \lambda_0 = 1.66 \times 10^{-5}$.

1.2.3 Classical Theory of Sol/Gel Transition

It is important to predict molecular weight distribution of products from the extent of reaction in polycondensation reaction of multi functional molecules such as $Si(OEt)_4/H_2O/EtOH$ system. There are two assumptions when we theoretically study this relation;

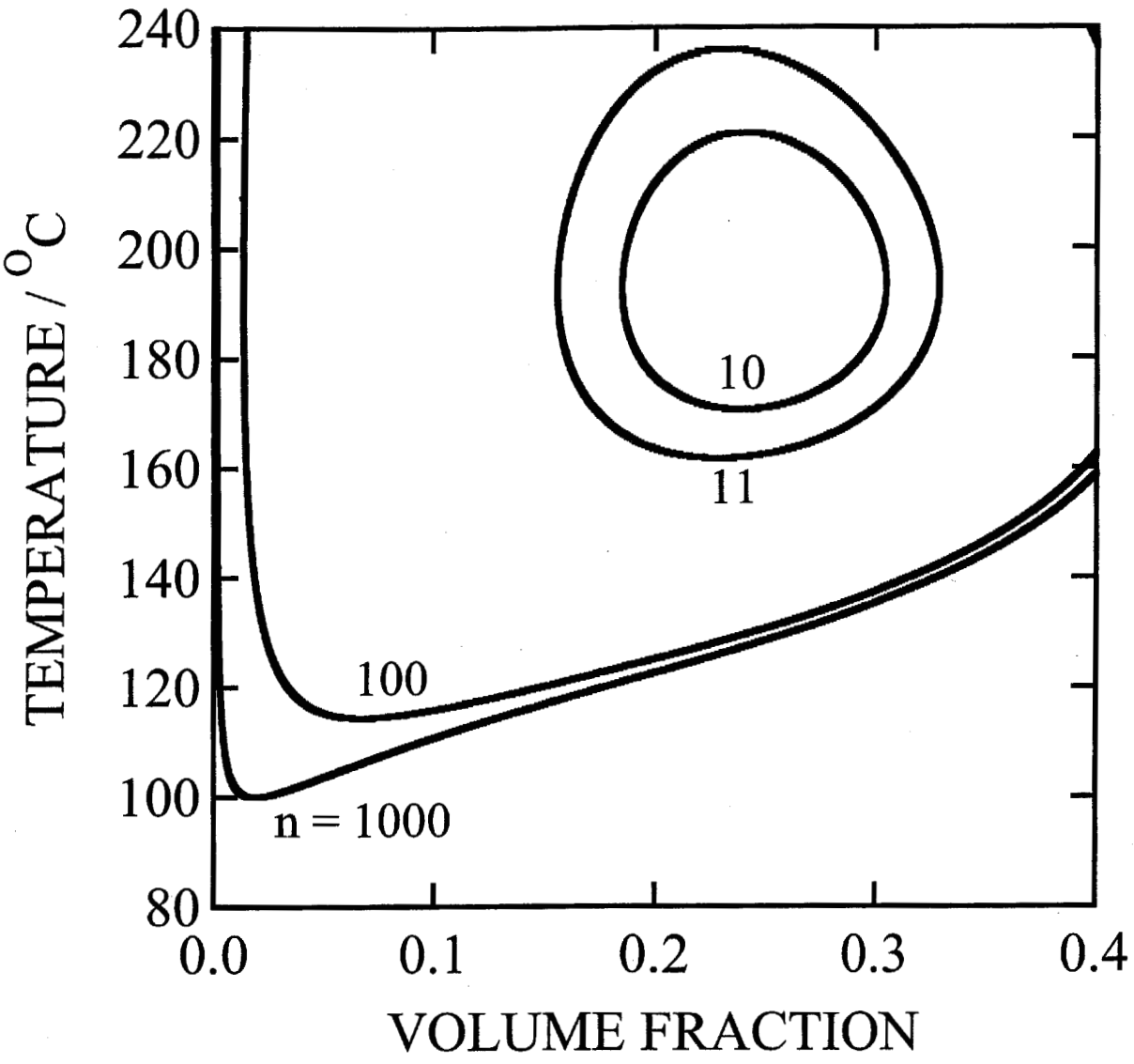

Figure 1.1: Phase diagram of PEO/water system computed by MT theory.

(1) All functional groups have equal reactivity during the reaction.

(2) Internal loop in all clusters is forbidden, i.e., all clusters take Cayley's tree structure.

In this section, the author shows the classical theories of gelation by Flory[7, 8] and Stockmayer [9] on the basis of these assumptions.

Gel Point and Degree of Polymerization

Gel is a cluster with infinite molecular weight. Gel point is defined mathematically where weight-average degree of polymerization diverges, thus the condition is given by

$$\bar{M}_w = \infty. \tag{1.54}$$

Then, the geometrical definition is that cluster grows to macroscopic size.

Let us study molecular weight distribution in the case of polymerization in homogeneous system of "A" molecule with f functional groups. The number of A molecules in the system is N. In an m-mer, the number of reacted and un-reacted functional groups are $2(m-1)$ and $fm - 2(m-1) = fm - 2m + 2$, respectively. The total number of un-reacted sites is given by $fN(1-\alpha)$ where α is the conversion of functional groups. The ratio of un-reacted sites in m-mers for all un-reacted sites is given by

$$P_m = \frac{fm - 2m + 2}{fN(1-\alpha)} N_m, \tag{1.55}$$

where N_m is the number of the m-mers. P_m is also expressed by

$$P_m = \omega'_m \alpha^{m-1} (1-\alpha)^{fm-2m+1}, \tag{1.56}$$

where ω'_m is the number of different ways to form an m-mer from the number m of the A molecules. Thus, ω'_m is given by

$$\omega'_m = \frac{(fm-m)!}{m!(fm-2m+1)!}. \tag{1.57}$$

Thus,

$$N_m = N \frac{f(1-\alpha)^2}{\alpha} \omega_m \beta^m, \tag{1.58}$$

where $\omega_m \equiv (fm - m)!/m!(fm - 2m + 2)!$ and $\beta = \alpha(1 - \alpha)^{f-2}$. The number of bonds in the system is $fN\alpha/2$. The number of monomers is decreased by one when one bond is formed, i.e., a monomer aggregates to a cluster, thus the total number of clusters M is given by

$$M \equiv \sum_m N_m = N - \frac{fN\alpha}{2} = N\left(1 - \frac{f\alpha}{2}\right). \tag{1.59}$$

Then the number-distribution of molecular weight f_m is given by

$$f_m \equiv \frac{N_m}{M} = \frac{f(1-\alpha)^2}{\alpha(1 - f\alpha/2)}\omega_m\beta^m. \tag{1.60}$$

The number-average degree of polymerization $< m >_n$ is given by

$$< m >_n \sum_{m=1}^{\infty} mf_m = \frac{f(1-\alpha^2)}{\alpha(1 - f\alpha/2)} \sum_{m=1}^{\infty} m\omega_m\beta^m = \frac{1}{1 - f\alpha/2}. \tag{1.61}$$

The weight-distribution of molecular weight w_m is given by

$$w_m \equiv \frac{mN_m}{\sum_m mN_m} = \frac{f(1-\alpha)^2}{\alpha} m\omega_m\beta^m. \tag{1.62}$$

The weight-average degree of polymerization $< m >_w$ is given by

$$< m >_w = \sum_{m=1}^{\infty} mw_m = \frac{f(1-\alpha^2)}{\alpha} \sum_{m=1}^{\infty} m^2\omega_m\beta^m = \frac{1+\alpha}{1 - (f-1)\alpha}. \tag{1.63}$$

Let us go back to the gel point. By comparison Eq.(1.54) with Eq.(1.63), the conversion α^* at gel point is defined by

$$\alpha^* \equiv \frac{1}{f-1}. \tag{1.64}$$

At gel point, the number-average degree of polymerization $< m >_n$ has still finite value (see Figure1.2),

$$< m >_n = \frac{2(f-1)}{f-2}. \tag{1.65}$$

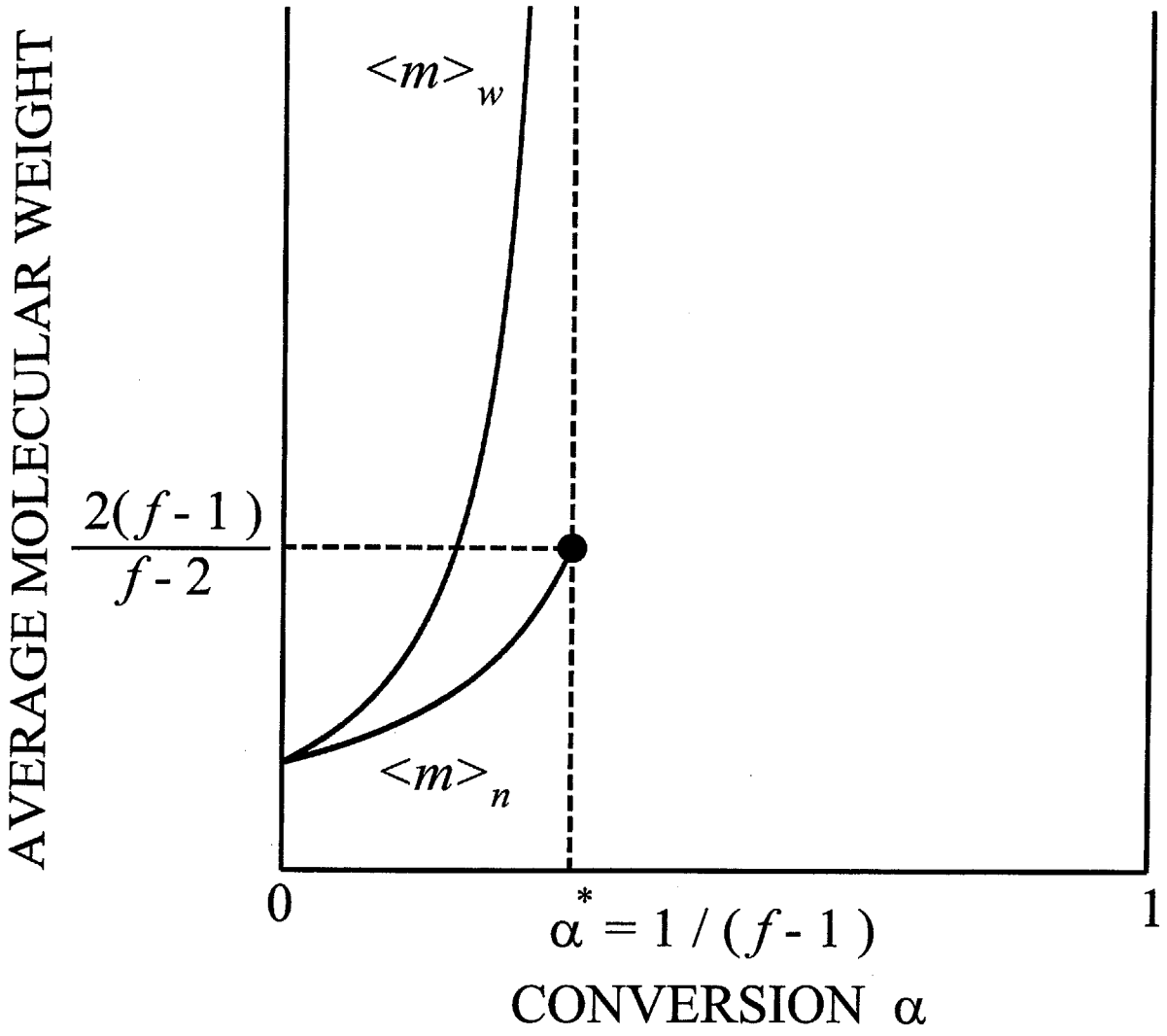

Figure 1.2: Average molecular weight $< m >_n$ and $< m >_w$ as a function of the conversion α

Postgel Regime

There are two treatments at postgel regime - Stockmayer's treatment[9] and Flory's treatment[7, 8]. Let us study Stockmayer's treatment first.

We can regard gel cluster as m-mers at $m \to \infty$ if we assume tree statistics at postgel regime. Thus, the conversion α^G of the gel clusters is given by

$$\alpha^G = \lim_{m\to\infty} \frac{2(m-1)}{fm} = \frac{2}{m}. \tag{1.66}$$

We assume that the finite size clusters bond to the gel clusters with the conversion of sol clusters $\alpha^S = \alpha^*$ at postgel regime ($\alpha > \alpha^*$). The conversion α of all functional groups is given by

$$\alpha = w_S\alpha^S + w_G\alpha^G = \alpha^*(1 - w_G) + \frac{2}{f}w_G, \tag{1.67}$$

where w_S, w_G are weight fraction of sol and gel clusters, respectively, thus $w_S + w_G = 1$. Then, w_G is a liner function that is given by

$$w_G = \frac{(f-1)\alpha - 1}{1 - 2/f}. \tag{1.68}$$

From Eq.(1.68), $w_G = 1$ at $\alpha = 2/f < 1$. Thus, all monomers belong to the gel clusters before the reaction is terminated $\alpha = 1$ (see Figure 1.3 (a)).

On the contrary, Flory interpreted from his following result that circle formation is permitted in the gel network. The weight fraction of the gel w_G is given by

$$w_G = 1 - \frac{(1-\alpha)^2\alpha'}{(1-\alpha')^2\alpha}. \tag{1.69}$$

This derivation is shown in the following sentences. At postgel regime ($\alpha > \alpha^*$), α' and α are the solutions of the equation $\beta \equiv \alpha(1-\alpha)^{f-2}$. Thus,

$$\alpha(1-\alpha)^{f-2} = \alpha'(1-\alpha')^{f-2}. \tag{1.70}$$

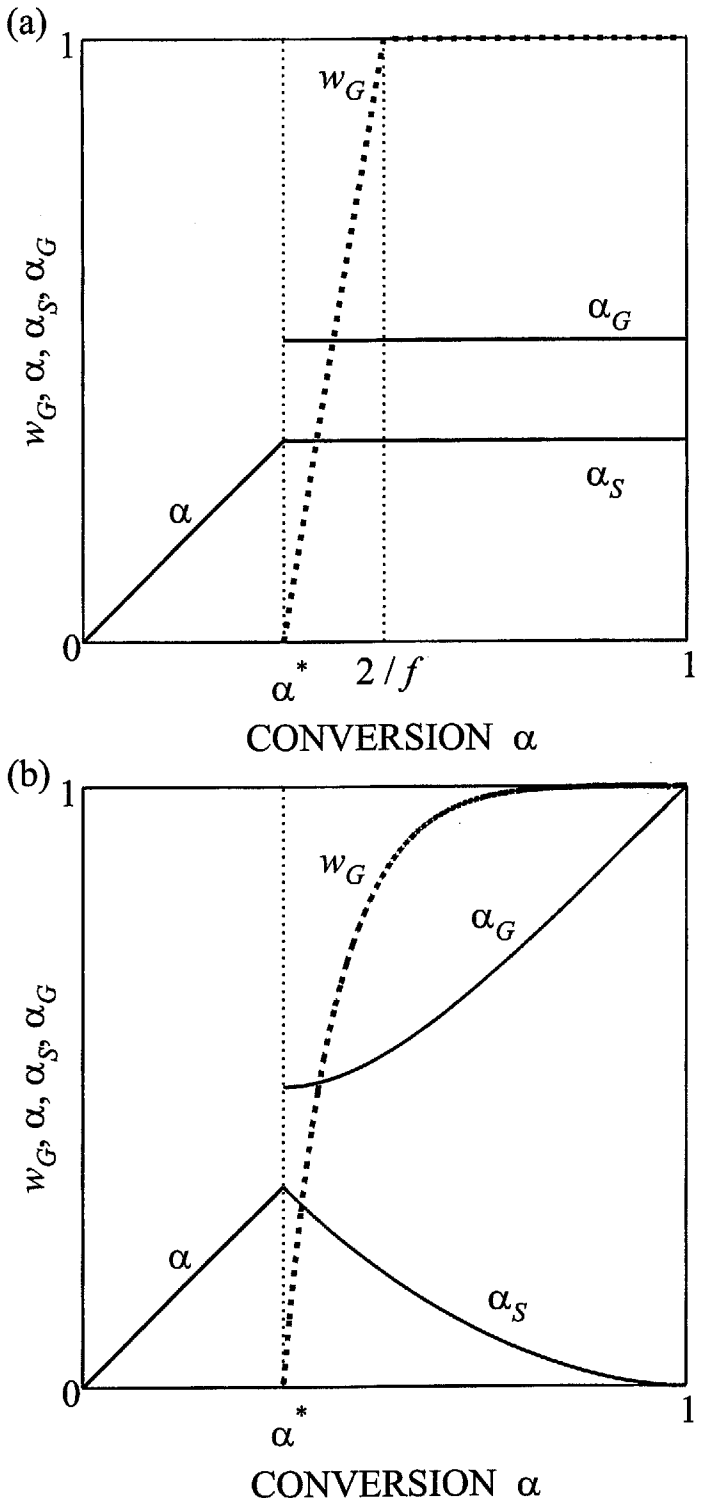

Figure 1.3: Conversion $\alpha, \alpha_S, \alpha_G$ and gel fraction w_G as a function of conversion α in the case of $f = 4$. (a) Stockmayer's treatment, (b) Flory's treatment.

α' is the small root of this equation. The weight distribution of the finite size clusters in the sol is given by substituting α' into α in Eq.(1.62) ($\alpha^S = \alpha'$). The weight fraction of the sol is given by

$$w_S = \sum_m w_m = \frac{(1-\alpha)^2\alpha'}{(1-\alpha')^2\alpha}. \tag{1.71}$$

Thus, Eq.(1.69) is derived. α is given by

$$\alpha = w_S\alpha' + w_G\alpha^G. \tag{1.72}$$

From this equation, α^G is larger than $2/f$, thus circle formation must be permitted in the gel network at Flory's treatment. In Figure 1.3 (b), all monomers belong to gel clusters at $\alpha = 1$.

1.3 Several Studies of Phase Separation and Thermoreversible Gelation in Solutions of Associating Polymers

1.3.1 Phase Separation in Water-Soluble Polymer Solutions

Aqueous Solutions of Thermosensitive Poly (*N*-isopropylacrylamide)

There are many studies of phase separation in PNIPAM solutions.

In 1960s, M. Heskins *et al.*[10] made the phase diagrams of the cloud points on the temperature-concentration plane in PNIPAM/water solutions by visual observation. The M_n of PEO samples were 290,000 and 1,000,000. From the diagrams, the flat LCST curve was observed and the LCST was determined 31°C. There was an endothermic peak near phase separation temperature by DSC measurement that showed the deformation of hydrogen bonds between PNIPAMs and water molecules. The aggregation due to the formation of nonpolar and intermolecular hydrogen bonds played an important role in phase separation by viscosity, sedimentation, and light-scattering studies. The ordering effect of hydrogen bonds between amide groups on PNIPAM chain and water molecules was weakening as the temperature was raised, then this effect contributed the stability of the two-phase system.

In the latter half of 1980s, the study of phase separation in PNIPAM solutions began to thrive. S. Fujishige *et al.*[11] was determined the phase separation temperature of aqueous solu-

tions of PNIPAM, Poly (*N*-isopropylmethacrylamide) (referred to as PNIPMAM), and methylcellulose by dynamic light scattering measurement. In the case of PNIPAM, phase separation was both sharp and thermoreversible compared to PNIPMAM and methylcellulose. The phase separation temperature was 31°C, then it didn't almost depend on both the molecular weight and the concentration. There was a coil-globule transition near 31°C by static light scattering measurement. Then they suggested the molecular mechanism of phase separation in aqueous PNIPAM solutions that the initial stage of phase separation was the coil-globule transition, this is then followed by the onset of aggregation of isopropyl groups on the surface of globular particles by hydrophobic interaction.

In 1990s, K. C. Tam *et al.*[12] also suggested the molecular mechanism by rheological measurement. As temperature increased from 20°C to 40°C, the viscosity decreased until 28°C (Region I), then increased sharply from 28°C to 31°C (Region II), decreased again (Region III). They explained this behavior that at Region I, the "water cage" surrounding the isopropyl groups in PNIPAMs was disrupted by the Brownian motion of the molecules, thus the interaction between each isopropyl group was stronger, at Region II, the viscosity was increased by the aggregation of each isopropyl group leading to an apparent increase in molecular weight near LCST, in Region III, PNIPAM chains formed colloidal particles. C. Wu *et al.*[13] studied the coil-globule transition of PNIPAM chain in the dilute solution by laser light scattering measurements. They reported that the mechanism of phase separation could be divided into two steps - PNIPAM chain first collapsed and globule was formed , then the globules were aggregated each other.

In 2000s, Azevedo *et al.*[14] measured the cloud points and spinodal points on the temperature-concentration plane in PNIPAM(M_w = 615, 000)/water solutions by laser light scattering. The cloud point curve was very flat, thus it didn't almost depend on the concentration. The spinodal curve, however, depended on the concentration in the dilute region. The cloud point and spinodal point temperatures were 32°C and 33-50°C, respectively. They also studied the pressure effects of cloud point and spinodal point. The cloud point temperature increased as pressure increased. The opposite was observed for the spinodal point temperature. The cloud

point temperature did not increase at more than 400MPa. L. P. N. Rebelo *et al.*[15] measured the cloud points on the temperature-pressure plane. The cloud point curve was a convex curve and the pressure dependence was negligibly. A. Milewska *et al.*[16] also studied the molecular dependence of cloud point. The cloud point didn't almost depend on the molecular weight except in the case of low $M_w = 14,400$.

Aqueous Solutions of Poly (Ethylene Oxide)

There are several studies of phase separation in PEO solutions.

In 1950s, G. N. Malcolm *et al.*[17] made the phase diagrams of the cloud points on the temperature-concentration plane in PEO/water solutions by visual observation. The M_n of PEO samples were 3,000 and 5,000. From the phase diagram, there were two phase separation regions - one was *closed-loop* type at low concentration and high temperature, and the other was *dome* type at high concentration and low temperature. The phase separation region expanded at high M_n. The LCST of $M_n = 3,000$ and 5,000 samples were 170 °C and 130 °C, respectively. They also observed cloud points in poly (propylene oxide) (referred to as PPO) ($M_n = 400$)/water solutions. The LCST curves of PPO samples were very flat compared to PEO samples.

In 1970s, S. Saeki *et al.*[5] also measured the cloud points in PEO ($M_\eta = 2,180-1,020,000$) /water and /*t*−butyl acetate solutions. The molecular weight dependence of LCST and UCST had the same tendency of Malcolm's study. In the case of PEO/*t*−butyl acetate, if M_η was more than 719,000, the phase separation region made *hour glass* type. They also studied the pressure dependence of LCST $(dT/dP)_C$. $(dT/dP)_C$ in PEO ($M_\eta = 1,020,000$)/water and /*t*−butyl acetate over the pressure range of 0-50 atm were 0.004, 0.4-0.6 °C/atm, respectively, thus, in the case of PEO/water, the pressure dependence of LCST was negligibly.

In 1980s, G. Karlstrom[18] calculated the phase diagram of PEO/water solutions by using the Flory-Huggins theory with focus on the change of gauche-trans orientation around the C-C bond and C-O bond. The agreement with Saeki *et al*'s experiment[5] was semiquantitative.

In 1990s, A. Matsuyama *et al.*[4] calculated the phase diagram of PEO/water with focus on hydration between the oxygen atoms on PEO chain and water molecules. The detail of this study has already shown in the previous section. Theoretical calculation fitted very well the experimental data by Saeki *et al.* Thus, the phase separation in PEO/water was caused by hydration/dehydration. K. Tasaki[19] showed this mechanism by molecular dynamics simulation that a PEO chain took a loose helical conformation (11/2 helix) in aqueous solution , whose pitch ($\simeq$ 1.7 nm) just fitted the size of a water molecule for adsorption by hydrogen bonds through the two hydrogen atoms on a water molecule.

1.3.2 Phase Separation in Aqueous Solutions of Hydrophobically Modified Water-Soluble Polymers

E. Alami *et al.*[20, 21, 22] measured the cloud points in aqueous solutions of hydrophobically end-capped poly (ethylene oxide) (referred to as HM-PEO) by visual observation. The end groups of alkyl chain were fixed at -$C_{12}H_{25}$. The molecular weight dependence of cloud point was that the cloud point shifted to lower temperature as the molecular weight of PEO was lower. The drop of the cloud point temperature was approximately 100°C if PEO was introduced alkyl chains at both ends of PEO. They also showed the mechanism of association in HM-PEO chain as the concentration of HM-PEO was increased. (1) At an initial critical concentration C_1, alkyl chains began to associate each other with a very small aggregation number. The aggregation number was larger as the concentration was increased. (2) At cmc (critical micelle concentration), hydrophobic microdomains, or micelles were formed, but three dimensional networks were not formed by no significant enhancement of the viscosity was observed. (3) The viscosity is significantly increased due to the overlap of the aggregates at C_η. A order-disorder transition was induced by a further increase in concentration. (4) At about 50%, large aggregates were formed in which the spherical micelles are organized in a cubic lattice.

P. Kujawa *et al.*[23, 24] studied phase separation in aqueous solutions of hydrophobically modified poly (*N*-isopropylacrylamide) (referred to as HM-PNIPAM) with -$C_{16}H_{33}$ by light scattering measurement. The M_n of PNIPAM was changed from 12,400 g/mol to 49,000. From

the phase diagram on the temperature-concentration plane, the cloud point shifted to lower temperature as the molecular weight was smaller or the concentration of PNIPAM was increased. The tendency was same as HM-PEO solutions. The drop of the cloud point temperature, however was about only 5-10°C if alkyl chain was introduced at both ends of PNIPAM. They also determined the coil-globule transition temperature (T_M) by DSC measurement. The T_M was higher than the cloud point, thus, they suggested the mechanism of phase separation as temperature increased. (1) At room temperature (15-20°C), polymer chains associated in the form of noninteracting flower micelles. A flower micelle consisted of 16-27 HM-PNIPAM chains, PNIPAM was hydrated. (2) At the cloud point, the flower micelles associated via the intermicellar bridge chains. (3) At T_M, PNIPAM chains were dehydrated, and collapse. The micelles aggregated each other forming mesoglobules with large association number.

The group of Y. Einaga[25, 26, 27, 28, 29] measured the cloud points in aqueous solutions of diblock poly (ethylene oxide)-alkyl chain as the length of PEO or alkyl groups were changed. The cloud point temperature shifted to lower temperature and the micellar size became larger as the molecular weight of PEO became smaller or alkyl chain became larger. The upper critical solution temperature (UCST) was also appeared in long length of alkyl group.

F. Lafleche *et al.*[30, 31] studied the phase behavior in the mixture of HM-PEO and single end-capped PEO (as surfactant) by static and dynamic light scattering and rheological measurements. HM-PEO and single end-capped PEO had the same hydrophilic-lipophilic balance (HLB). Cloud point shifted to lower temperature as the weight fraction f increased. The HM-PEO and surfactant formed micelles, the number of the hydrophobic groups per micelles was independent of the weight fraction f of HM-PEO. The exclude-volume interaction between micelles was reduced but the molar mass and hydrodynamic radius of micelle was not changed as the temperature increased. From rheological study, the formation of a transient network of bridging micelles that enhanced the viscosity played an important role in the mechanical properties. A transition from soft gel to hard gel (nonflowing gel) appeared at the dense regime due to the jam of close packed micelles. This transition showed strongly temperature dependent but almost independent of the fraction f.

1.3.3 Phase Separation and Gelation in Reactive Solutions

Q. Trans-Cong *et al.*[32] observed the change of crosslinking structure and morphology as ultraviolet irradiation time changed in the case of styrene-chloromethyl styrene copolymer and poly (vinyl methyl ether) (referred as PVME) were crosslinked via dimerization of anthracene. In this experiment, it was reported that the cross-linking reaction in the rich PVME blend proceeded faster and in the case of the same ratio of copolymer and PVME, phase separation occurred preventing cross-linking reaction as time passed.

E. Girard-Reydet *et al.*[33, 34, 35, 36, 37] measured the conversion, gelation time, and phase separation time in polycondensation reaction of diglycidyl ether of bisphenol A as epoxy monomer and 4.4'-diamino-3,3'-dimethyl dicyclohexylmethane or 4,4'-diaminodiphenyl sulfone as diamine monomer in THF or poly (vinyl chloride) solvent. They also draw time-temperature transformation (TTT) diagram of the cloud points, gelation, vitrification, and degradation by light scattering, DSC, and rheological measurements.

T. Kyu *et al.*[38] studied the dynamics of time-dependent phase separation in polymerization system, consisting of carboxyl terminated polybutadiene acrylonitrile/epoxy/methylene dianiline by time-resolved light scattering measurement. They also theoretically calculated time-dependent phase diagram in this system by their new theory combining the Cahn-Hilliard kinetics equation[39] and polymerization kinetics and the solution moved gradually from the metastable to the unstable region due to that the nucleation took place initially in the metastable region and then crossed over to the spinodal region called "nucleation initiated spinodal decomposition (NISD)".

A. Ponton *et al.*[40] measured the gelation time in the typical polycondensation system - $Si(OMe)_4$/ $MeOH/H_2O$ by rheological measurements according to the Winter's criterion[41, 42]. The gelation time t_g decreased with an increase of initial concentration of $Si(OMe)_4$ or hydrolysis molar ratio, then t_g was well-described by a power low. An apparent activation energy E_a was determined from the t_g with temperature T using the equation[43] $\ln t_g = \ln C + E_a/RT$ (where C was a prefactor, R was the gas constant, respectively). E_a was independent of the initial monomer concentration.

S. Sakka *et al.*[44] studied phase separation and gelation at equilibrium condition (terminated reaction) in the typical polycondensation system - $Si(OEt)_4/EtOH/H_2O$ with the change of the ternary ratio. From the triangular phase diagram, they divided into six regions with focus on the shape of fibrous gel.

M. Ohkura *et al.*[45, 46] studied the gelation rate that was reciprocal gelation time in atactic poly (vinyl alcohol) in a mixture of dimethyl sulphoxide and water by ball-dropping method. They expressed the gelation rate as a combination of temperature-dependent function and concentration-dependent function.

J. W. Cho *et al.*[47] studied the gelation mechanism in poly (vinylidene fluoride) gels in γ–butyrolactone. They suggested that gelation was caused by liquid-liquid phase separation from the formation of transparent gel. They also estimated the critical polymer concentration for gel formation.

S. Mal *et al.*[48, 49, 50] studied the gelation process in thermoreversible poly (vinylidene fluoride) (referred to as PVF_2) gels with focus on the formation of crystallite. The X-ray diffraction patterns of the dried gels indicated that α crystallites were formed in the gel process. They estimated the heat of reaction to produce 1mol of cross-links applying to the Eldridge-Ferry equation[51], then they showed that there were about three to six crystallites per crosslink in the gel. Their result was compared to the percolation theory[52, 53] in three-dimensional lattice and the nucleation rate equation[54], then they concluded that gelation rate of PVF_2 was good agreement with the percolation theory and the gelation process was a nucleation-controlled process with crystallites primarily acting points of crosslink.

1.4 Outline of This Thesis

The purpose of this study is to (1) study phase separation and thermoreversible gelation in water-soluble polymer and aqueous associating polymer solutions by developing thermodynamic theory of hydration and hydrophobic aggregation, this theory is able to apply to reversible reaction such as polycondensation, thus (2) find out the principle of sol/gel transition in vapour

pressure controlled polycondensation system, (3) calculate time-dependent phase diagram and conversion diagram solving rate equations for conversion and reactivity in aqueous associative and reactive solutions. These theories and principles are general theories which are able to be applied to more complex solutions.

In chapter 2, the author theoretically studies the solution properties in aqueous water-soluble polymer solutions focusing on hydration.

In chapter 3, the author studies the thermodynamic properties in aqueous associating polymer that the polymer studied in chapter 2 is employed as main chain introducing various hydrophobic groups. The author improve the theory in chapter 2 considering hydrophobic interactions.

In chapter 4, the author theoretically studies the principles that sol/gel transition point shifts artificially by controlling the vapour pressure of active solvent.

In chapter 5, the author suggests a new analytical method that time dependence of association and reaction are shown by dynamic phase diagrams solving time evolution equations from the kinetic point of view in polymer solutions.

Bibliography

[1] Tanaka, F. in *Molecular Gels*, edited by Weiss, G.; Terech, P. (Kluwer Academic Pub., London, 2004), Chapter.1.

[2] Flory, P. J.; *J. Chem. Phys.* **1942**, *10*, 51.

[3] Huggins, M. L.; *J. Phys. Chem.* **1942**, *46*, 151.

[4] Matsuyama, A.; Tanaka, F. *Phys. Rev. Lett.* **1990**, *65*, 341.

[5] Saeki, S.; Kuwahara, N.; Nakata, M.; Kaneko, M. *Polymer* **1976**, *17*, 685.

[6] Schultz, A. R.; Flory, P. J. *J. Am. Chem. Soc.* **1952**, *74*, 4760.

[7] Flory, P. J. *Principles of Polymer Chemistry*; Cornell University Press: Ithaca, NY 1953; Chapter.IX.

[8] Flory, P. J. *J. Am. Chem. Soc.* **1941**, *63*, 3091; 3096.

[9] Stockmayer, W. H. *J. Chem. Phys.* **1943**, *11* 45; **1944**, *12*, 125.

[10] Heskins, M.; Guillet, J. E. *J. Macromol. Sci.* **1968**, *A2*, 1441.

[11] Fujishige, S.; Kubota, K.; Ando, I. *J. Phys. Chem.* **1989**, *93*, 3311.

[12] Tam, K. C.; Wu, X. Y.; Pelton, R. H. *Polymer* **1992**, *33*, 436.

[13] Wu, C.; Zhou, S. *Macromolecules* **1995**, *28*, 8381.

[14] de Azevedo, R. G.; Rebelo, L. P. N.; Ramos, A. M.; Szydlowski, J.; de Sousa, H. C.; Klein, J. *Fluid Phase Equilib.* **2001**, *185*, 189.

[15] Rebelo, L. P. N.; Visak, Z. P.; de Sousa, H. C.; Szydlowski, J.; de Azevedo, R. G.; Ramos, A. M.; Najdanovic-Visak, V.; da Ponte M. N.; Klein, J. *Macromolecules* **2002**, *35*, 1887.

[16] Milewska, A.; Szydlowski, J.; Rebelo, L. P. N. *J. Polym. Sci., Part B: Polym. Phys.* **2003**, *41*, 1219.

[17] Malcolm, G. N.; Rowlinson, J. S. *Trans. Faraday Soc.* **1953**, *53*, 921.

[18] Karlström, G. *J. Phys. Chem.* **1985**, *89*, 4962.

[19] Tasaki, K. *J. Am. Chem Soc.* **1996**, *118*, 8459.

[20] Alami, E.; Almgren, M.; Brown, W. *Macromolecules* **1996**, *29*, 5026.

[21] Alami, E.; Rawiso, M.; Isel, F.; Beinert, G.; Binana-Limbele, W.; François, J. *Adv. Chem. Series* (American Chemical Society, Washington DC, 1996), Vol. 248, p.343.

[22] Alami, E.; Almgren, M.; Brown, W.; Francois, J. *Macromolecules* **1996**, **29**, 2229.

[23] Kujawa, P.; Watanabe, H.; Tanaka, F.; Winnik, F. M. *Eur. Phys. J. E* **2005**, *17*, 129.

[24] Kujawa, P.; Tanaka, F.; Winnik, F. M. *Macromolecules* **2006**, *39*, 3048.

[25] Yoshimura, S.; Shirai, S.; Einaga, Y. *J. Phys. Chem. B* **2004**, *108*, 15477.

[26] Hamada, N.; Einaga, Y. *J. Phys. Chem. B* **2005**, *109*, 6990.

[27] Imanishi, K.; Einaga, Y. *J. Phys. Chem. B* **2005**, *109*, 7574.

[28] Einaga, Y.; Kusumoto, A.; Noda, A. *Polym. J.* **2005**, *27*, 368.

[29] Shirai, S.; Einaga, Y. *Polym. J.* **2005**, *37*, 913.

[30] Lafléche, F.; Durand, D.; Nicolai, T. *Macromolecules* **2003**, *36*, 1331.

[31] Lafléche, F.; Nicolai, T.; Durard, D.; Gnanou, Y.; Taton, D. *Macromolecules* **2003**, *36*, 1341.

[32] Tran-Cong, Q.; Harada, A. *Phys. Rev. Lett.* **1996**, *76*, 1162.

[33] Verchere, D.; Sautereau, H.; Pascault, J. P.; Riccardi, C. C.; Moschiar, S. M.; Williams, R. J. J. *Macromolecules* **1990**, *23*, 725.

[34] Girard-Reydet, E.; Riccardi, C. C.; Sautereau, H.; Pascault, J. P.; *Macromolecules* **1995**, *28*, 7608.

[35] Riccardi, C. C.; Borrajo, J.; Williams, R. J. J.; Sautereau, H.; Girard-Reydet, E.; Sautereau, H.; Pascault, J. P.; *J. Polym. Sci. B* **1996**, *34*, 349.

[36] Girard-Reydet, E.; Sautereau, H.; Pascault, J. P.; Keates, P.; Navard, P.; Thollet, G.; Vigier, G. *Polymer* **1998**, *39*, 2269.

[37] Girard-Reydet, E.; Pascault, J. P. *Macromolecules* **2000**, *33*, 3084.

[38] Kyu, T.; Lee, J. H. *Phys. Rev. Lett.* **1996**, *76*, 3746.

[39] Cahn, J. W.; Hilliard, J. E. *J. Chem. Phys.* **1958**, *28*, 258.

[40] Ponton, A.; Warlus, S.; Griesmar, P. *J. Colloid and Interface Sci.* **2002**, *249*, 209.

[41] Chambon, F.; Winter, H. H. *J. Rheol.* **1987**, *31*, 683.

[42] de Rosa, M. E.; Winter, H. H. *Rheol. Acta.J.* **1994**, *33*, 220.

[43] Oyanguren, P. A.; Williams, R. J. *J. Appl. Poly. Sci.* **1993**, *47*, 1361.

[44] Sakka, S.; Kozuka, H. *J. Non-Crystal. Solids* **1988**, *100*, 142.

[45] Ohkura, M.; Kanaya, T.; Kaji, K. *Polymer* **1992**, *33*, 3686.

[46] Ohkura, M.; Kanaya, T.; Kaji, K. *Polymer* **1992**, *33*, 5044.

[47] Cho, J. W.; Song, H. Y.; Kim, S. Y. *Polymer* **1993**, *34*, 1024.

[48] Mal, S.; Maiti, P.; Nandi, A. K. *Macromolecules* **1995**, *28*, 2371.

[49] Mal, S.; Nandi, A. K. *Polymer* **1998**, *30*, 6301.

[50] Mal, S.; Nandi, A. K. *Langmuir* **1998**, *14*, 2238.

[51] Eldridge, J. E.; Ferry, J. D. *J. Phys. Chem.* **1954**, *58*, 992.

[52] Zallen, R. *The Physics of Amorphous Solids*; John Wiely & Sons: New York, 1983; p.135.

[53] Stuffer, D.; Coniglio, A.; Adam, M. In *Advances in Polymer Science*; Dusek, K., Ed.; Springer-Verlag: Berlin 1982; Vol.44, p.103.

[54] Mandelkern, L. *Crystallization of Polymers*; McGraw-Hill Book Co.; New York 1964; p.278.

Chapter 2

Molecular Mechanism of Sharp Phase Separation in Aqueous Solutions of Temperature-Sensitive Polymers

2.1 Introduction

Phase diagrams of water-soluble polymers often exhibit peculiar phase separation. For instance, aqueous poly(ethylene oxide) (referred to as PEO) solutions show closed-loop phase separation region (*miscibility loop*) at intermediate temperatures[1, 2, 3]. The miscibility loop expands with the polymer molecular weight, and its lower critical solution temperature (LCST) approaches an inverted theta temperature in the limit of infinite molecular weight[2]. There is a competition in forming polymer-water hydrogen bonds and water-water hydrogen bonds. The hydrogen-bond networks in water are, however, not so strong in the temperature region of loop-shaped phase separation (typically 100~200 °C) that indirect interaction between the neighboring water molecules on a chain via water hydrogen-bond network is expected to be weak. The water molecules are therefore *randomly* and *independently* adsorbed into the pockets of the helices. Later, the pressure effect was studied on the basis of the similar picture[4] such that the effective number of hydrogen-bonding sites along a polymer chain is reduced by pressure.

In contrast to PEO, other water-soluble polymers such as poly(*N*-isopropylacrylamide) (referred to as PNIPAM) show very flat LCST behavior whose cloud-point lines and spinodal lines are horizontal up to 20 wt% of polymer concentration and almost independent of the molecular weight[5, 6, 7, 8, 9]. Poly(propylene oxide) oligomers also show similar phase behavior[1]. The phase separation region takes a shape like the bottom part of a square, so that in what follows we refer to it as *miscibility square*. Obviously, the miscibility square cannot be explained by *random* adsorption of water molecules onto a polymer chain. But, if we introduce positive correlation between the neighboring hydrogen bonds along the polymer chain, i.e., if adsorption of a water molecule onto a site next to the already adsorbed one is preferential, phase separation may take place in a narrow temperature region. For PNIPAM, it is in fact the case because the hydrogen-bonding site (amide group) is blocked by a large hydrophobic group (isopropyl group). The random coil parts sharply turn into collapsed globules on approaching the phase separation temperature[6], so that hydrogen-bonding is easier at the boundary between

an adsorbed water sequence and a collapsed coil. Such a steric hindrance by hydrophobic isopropyl side groups is the main origin of the strong correlation between the neighboring water molecules. The purpose of this chapter is to show theoretically that formation of sequential hydrogen bonds along the polymer chain, or *cooperative hydration*, in fact leads to miscibility square behavior of aqueous polymer solutions by so called *domino effect*. We calculate the fraction θ of bound water molecules and their average contiguous length $\bar{\zeta}_w$ as functions of the temperature and the polymer concentration, and derive flat LCST phase diagrams. We compare the results with the recent experimental data on PNIPAM solutions by paying special attention to the molecular-weight dependence.

2.2 Statistical-Mechanical Theory of Aqueous Polymer Solutions

2.2.1 Free Energy of the Model Solutions

We consider a model solution in which the number N_1 of polymer chains with degree of polymerization (referred to as DP) n are mixed with the number N_0 of water molecules. We are based on the lattice-theoretical picture of polymer solutions, and divide the system volume V into cells of size a, each of which can accommodate either a water molecule or a statistical repeat unit of the polymer. We assume incompressibility of the solution, so that we have $\Omega = N_0 + nN_1$, where $\Omega \equiv V/a^3$ is the total number of cells. To describe adsorption of water, let $\mathbf{i} \equiv \{i_1, i_2, \cdots\}$ be the index specifying the polymer chain carrying the number i_ζ of sequences that consist of a run of hydrogen-bonded ζ consecutive water molecules, and let $N(\mathbf{i})$ be the number of such polymer-water complexes whose type is specified by $\mathbf{i}$ (see Figure 2.1). The total number of water molecules on a chain specified by $\mathbf{i}$ is given by $\sum \zeta i_\zeta$, and the DP of a complex is given by $n(\mathbf{i}) \equiv n[1 + \theta(\mathbf{i})]$, where

$$\theta(\mathbf{i}) \equiv \sum_\zeta \frac{\zeta i_\zeta}{n} \tag{2.1}$$

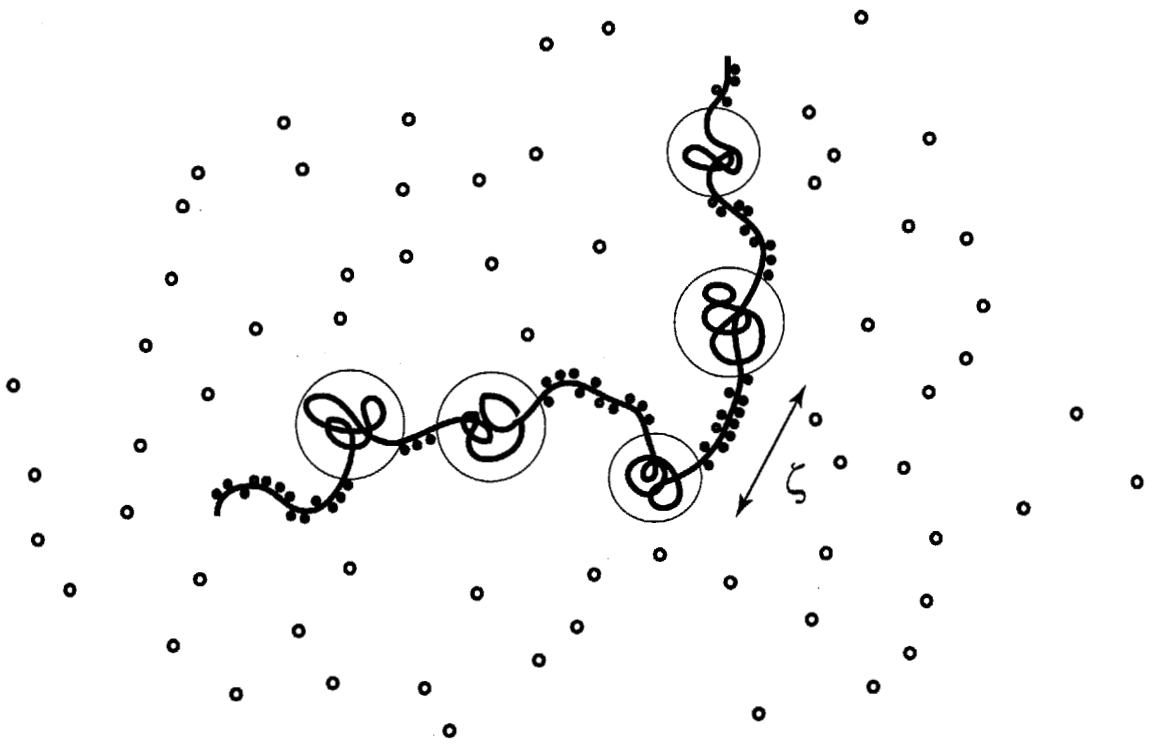

Figure 2.1: Sequential hydrogen bonds formed along the polymer chain due to the cooperative interaction between the nearest-neighboring bound water molecules. The type of polymer-water associated complex is specified by the index $\mathbf{j} \equiv (j_1, j_2, \cdots)$, where j_ζ is the number of sequences that consist of a run of hydrogen-bonded ζ consecutive water molecules. The average length of sequences sharply reduces as temperature approaches LCST from below. The random-coil parts (thin circles) are collapsed near LCST.

is the fraction of the bound water molecules counted relative to the DP of a polymer. Then, the free energy of mixing is given by

$$\beta\Delta F = N_{\rm fw}\ln\phi_{\rm fw} + \sum_{\mathbf{i}} N(\mathbf{i})\ln\phi(\mathbf{i}) + \beta\sum_{\mathbf{i}}\Delta A(\mathbf{i})N(\mathbf{i}) + \chi\phi(1-\phi)\Omega, \tag{2.2}$$

where $\phi(\mathbf{i}) \equiv n(\mathbf{i})N(\mathbf{i})/\Omega$ is the volume fraction of the complex $\mathbf{i}$, $N_{\rm fw}$ is the number of free water molecules in the solution, and $\phi_{\rm fw} \equiv N_{\rm fw}/\Omega$ is their volume fraction, $\Delta A(\mathbf{i})$ is the conformational free energy to form a complex of the type $\mathbf{i}$ measured relative to the reference conformation $\mathbf{i}_0 \equiv \{0, 0, \cdots\}$ where no water molecule is adsorbed. The total volume of the solution is now written as $\Omega = \sum_{\mathbf{i}} n(\mathbf{i})N(\mathbf{i}) + N_{\rm fw}$. The number density of the complexes specified by $\mathbf{i}$ is given by $\nu(\mathbf{i}) = N(\mathbf{i})/\Omega$.

We next derive the chemical potential for the free water and for the associated complex by differentiating the free energy. We find

$$\beta\Delta\mu_{\rm fw} = \left(\frac{\partial\beta\Delta F}{\partial N_{\rm fw}}\right)_{T,N(\mathbf{i})} = 1 + \ln\phi_{\rm fw} - \nu^S + \chi\phi^2 \tag{2.3}$$

for the free water, and

$$\beta\Delta\mu(\mathbf{i}) = \left(\frac{\partial\beta\Delta F}{\partial N(\mathbf{i})}\right)_{T,N_{\rm fw}} = 1 + \beta\Delta A(\mathbf{i}) + \ln\phi(\mathbf{i}) - n(\mathbf{i})\nu^S + \chi[n(1-\phi) + n\theta(\mathbf{i})\phi - n(\mathbf{i})\phi(1-\phi)] \tag{2.4}$$

for the associated complex of the type $\mathbf{i}$, where

$$\nu^S \equiv \nu_{\rm fw} + \sum_{\mathbf{i}}\nu(\mathbf{i}) \tag{2.5}$$

is the total number of molecules that possess translational degree of freedom.

2.2.2 Equilibrium Conditions and Number of Bound Water Molecules

We assume the association equilibrium and give the conditions

$$\Delta\mu(\mathbf{i}) = \Delta\mu(\mathbf{i}_0) + n\theta(\mathbf{i})\Delta\mu_{\rm fw} \tag{2.6}$$

to find the equilibrium distribution of associated complexes. Then, we find

$$\nu(\mathbf{i}) = K_{\rm H}(\mathbf{i})\nu(\mathbf{i}_0)\phi_{\rm fw}^{n\theta(\mathbf{i})} \tag{2.7}$$

for the number density of the complexes specified by **i**, where

$$K_{\mathrm{H}}(\mathbf{i}) \equiv \frac{\exp[n\theta(\mathbf{i}) - \beta\Delta A(\mathbf{i})]}{1 + \theta(\mathbf{i})} \tag{2.8}$$

is the association equilibrium constant. The total polymer volume fraction ϕ is then given by

$$\phi = \phi(\mathbf{i_0}) g_0(\phi_{\mathrm{fw}}), \tag{2.9}$$

and the total volume fraction of water is given by

$$1 - \phi = \phi_{\mathrm{fw}} + \phi(\mathbf{i_0}) g_1(\phi_{\mathrm{fw}}). \tag{2.10}$$

Here, new functions $g(y)$ are defined by

$$g_0(y) \equiv \sum_{\mathbf{i}} K_{\mathrm{H}}(\mathbf{i}) y^{n\theta(\mathbf{j})}, \tag{2.11}$$

$$g_1(y) \equiv \sum_{\mathbf{i}} \theta(\mathbf{i}) K_{\mathrm{H}}(\mathbf{i}) y^{n\theta(\mathbf{i})}. \tag{2.12}$$

These coupled equations should be solved for $\phi(\mathbf{i_0})$ and ϕ_{fw} to find the cluster distribution function in terms of the polymer volume fraction and the temperature. Upon eliminating $\phi(\mathbf{i_0})$, the second equation is transformed to

$$1 - \phi = \phi_{\mathrm{fw}} + \phi G(\phi_{\mathrm{fw}}), \tag{2.13}$$

where the function G is defined by

$$G(y) = \frac{g_1(y)}{g_0(y)} = \frac{\partial \ln g_0(y)}{n \partial \ln y}. \tag{2.14}$$

The total number ν^S of free water molecules and associated complex is given by

$$\nu^S = \phi_{\mathrm{fw}} + \frac{\phi}{n}. \tag{2.15}$$

From the Gibbs-Dühem relation for the free energy of mixing $f \equiv \Delta F/\Omega = \phi_{\mathrm{fw}}\Delta\mu_{\mathrm{fw}} + \sum \nu(\mathbf{i})\Delta\mu(\mathbf{i})$ with help of the reaction equilibrium conditions, we find

$$f = f_{\mathrm{FH}} + f_{\mathrm{AS}}, \tag{2.16}$$

where

$$\beta f_{\mathrm{FH}}(\phi, T) = (1-\phi)\ln(1-\phi) + \frac{\phi}{n}\ln\phi + \chi\phi(1-\phi) \tag{2.17}$$

is the usual Flory-Huggins mixing free energy, and

$$\beta f_{\mathrm{AS}}(\phi, T) = \frac{\phi}{n}\ln\frac{\phi(\mathbf{i}_0)}{\phi} + (1-\phi)\ln\frac{\phi_{\mathrm{fw}}}{1-\phi} + 1 - \phi - \phi_{\mathrm{fw}} \tag{2.18}$$

is the additional free energy due to hydrogen bonding association. This part can be written in the form

$$\beta f_{\mathrm{AS}}(\phi, T) = -\frac{\phi}{n}\ln g_0(\phi_{\mathrm{fw}}) + (1-\phi)\ln\frac{1-\phi G(\phi_{\mathrm{fw}})}{1-\phi} + \phi G(\phi_{\mathrm{fw}}) \tag{2.19}$$

by the substitution of the relations (2.9) and (2.10).

The free energy of association can be regarded as the renormalization of the χ-parameter. The original χ-parameter due to van der Waals type contact interaction is modified to $\chi + \Delta\chi$ by hydrogen-bonding association, where the renormalization part

$$\Delta\chi(\phi, T) \equiv \frac{\beta f_{\mathrm{AS}}(\phi, T)}{\phi(1-\phi)} \tag{2.20}$$

depends on the polymer concentration in a complex way. The appearance of peculiar-shaped phase separation regions on the phase plane originates in this effective interaction term.

An attempt to derive the phase diagram of PNIPAM solution by using effective interaction parameter $\chi_{\mathrm{eff}}(T, \phi)$ was made by Baulin and Halperin[10]. They used, however, an empirical power expansion formula by Afroze *et al.*[11] with many numerical coefficients, whose molecular origin is completely unknown. Although our above renormalization formula due to hydrogen bonding depends implicitly upon the concentration, we can expand it in power series in the dilute regime, and directly compare the result with the experimental measurements on the second virial coefficient of the osmotic pressure. We will discuss this point in the final section of this chapter.

2.2.3 Spinodal Condition and Osmotic Pressure

The osmotic pressure π can be found by the thermodynamic relation $\pi a^3 = -\Delta\mu_{\rm fw}$ and is given by

$$\beta\pi a^3 = -\beta\Delta\mu_{\rm fw} = -1 - \ln[1 - \phi - \phi G(\phi_{\rm fw})] + \left[1 - \phi - \phi G(\phi_{\rm fw}) + \frac{\phi}{n}\right] - \chi\phi^2, \tag{2.21}$$

By expanding the function $G(y)$ in powers of the concentration as $G(y) = G_0 + G_1\phi + \cdots$, we find the second virial coefficient in the form

$$A_2 = \frac{1}{2}(1 + G_0)^2 - \chi, \tag{2.22}$$

where G_0 is the value of $G(y)$ in the limit of infinite dilution.

The spinodal condition is found by differentiating the osmotic pressure once more by the concentration. We find

$$\frac{1}{n\phi} + \frac{\kappa(\phi)}{1 - \phi} - 2\chi = 0, \tag{2.23}$$

where

$$\kappa(\phi) \equiv \frac{[1 + G(\phi_{\rm fw})]^2(1 - \phi)}{[1 + \phi G'(\phi_{\rm fw})]\phi_{\rm fw}} \tag{2.24}$$

gives the effect of hydration. The volume fraction $\phi_{\rm fw}$ of free water is assumed to be solved as a function of the total polymer volume fraction ϕ and substituted into this function κ. Hence κ is regarded as a function of ϕ.

2.2.4 Cooperative Hydration

Let us now proceed to the study on the models of association. If water molecules are independently and randomly hydrogen bonded onto the polymer chain, as was studied previously[12], the index **i** can be replaced by the number m of the bound water molecules, and $K_{\rm H}(\mathbf{i})$ is replaced by $K_m = (1 + m/n)_n C_m \mu^m$, where ${}_nC_m = n!/m!(n-m)!$ is the number of different ways to choose m hydrogen bonding sites from the number n of the total available sites, and $\mu(T) \equiv \exp(-\beta\Delta f_0)$ is the association constant (Δf_0 being the free energy of one hydrogen bond). The functions appearing in thermodynamic properties are given by $g_0(y) = (1 + y)^n, g_1(y) = y(1 + y)^{n-1}$ and

$G(y) = y/(1+y)$, where $y \equiv \mu\phi_{\rm fw}$ is the reduced concentration of the free water. All results reduce to those found in our previous study on phase diagrams of PEO solutions[12].

Now, let us move onto cooperative hydration. The equilibrium constant is most generally written as

$$K_{\rm H}(\mathbf{i}) = \omega(\mathbf{i}) \prod_{\zeta=1}^{n} \eta_\zeta{}^{i_\zeta}, \tag{2.25}$$

where

$$\omega(\mathbf{i}) \equiv \frac{(n - \sum_\zeta \zeta i_\zeta)!}{\prod_\zeta i_\zeta! [n - \sum_\zeta (\zeta+1) i_\zeta]!} \tag{2.26}$$

is now the number of different ways to select sequences specified by $\mathbf{i}$ from a chain, and η_ζ is the statistical weight for a single water sequence of the length ζ formed on a reference coil[13].

Since summing up all possible types $\mathbf{i}$ in the above functions is mathematically difficult, we replace the sum by the contribution from the most probable type $\mathbf{i}^*$ (*one-mode approximation*). The necessary functions are then given by

$$g_0(y) = \omega(\mathbf{i}^*) \prod_{\zeta=1}^{n} (\eta_\zeta y^\zeta)^{i_\zeta}, \tag{2.27}$$

and $g_1(y) = \theta(\mathbf{i}^*) g_0(y)$, and $G(y) = \theta(\mathbf{i}^*)$. The function G reduces to the coverage θ of the bound water in the type $\mathbf{i}^*$.

The most probable type, or sequence distribution, can be found by minimizing the free energy $f_{\rm AS}$ by changing $\mathbf{i}$, i.e., by the condition $\partial f_{\rm AS}/\partial j_\zeta = 0$. We find that it is given by

$$\frac{i_\zeta}{n} = (1-\theta) t \eta_\zeta q^\zeta, \tag{2.28}$$

where q is defined by the equation

$$q \equiv (1 - \phi - \theta\phi) t \exp[R(\theta, \phi)]. \tag{2.29}$$

Here, the function $R(\theta, \phi) \equiv \theta\phi/(1-\phi-\theta\phi)$ gives the ratio of the total number of bound water molecules to that of the free ones. The parameter t is given by $t \equiv 1 - \nu/(1-\theta)$. Substituting this distribution function (2.28) into the definitions of θ and ν, we find

$$\theta(q) = [1 - \theta(q)] t(q) V_1(q) \tag{2.30}$$

and

$$\nu(q) = [1 - \theta(q)]t(q)V_0(q), \tag{2.31}$$

and hence

$$t(q) = \frac{1}{1 + V_0(q)}. \tag{2.32}$$

Here new functions V are defined by

$$V_0(q) \equiv \sum_{\zeta} \eta_\zeta q^\zeta, \quad \text{and} \tag{2.33}$$

$$V_1(q) \equiv \sum_{\zeta} \zeta \eta_\zeta q^\zeta. \tag{2.34}$$

Now, θ and t must be regarded as functions of q, so that Eq.(2.29) is an equation for the unknown variable q to be solved in terms of the concentration ϕ.

The κ function in our spinodal condition Eq.(2.23) now takes the form

$$\kappa(q;\phi) = \frac{1 + (1-\theta)QR}{1 + (1-\theta)QR^2}(1+\theta)^2(1+R), \tag{2.35}$$

where

$$Q(q) \equiv \theta(q) - [1 - \theta(q)]\bar{\zeta}_w(q), \tag{2.36}$$

and

$$\bar{\zeta}_w(q) \equiv \frac{V_1(q)}{V_0(q)} \tag{2.37}$$

being the weight-average sequence length of the bound water.

Our strategy is therefore as follows. We first solve Eq.(2.29) for the unknown q for a given concentration ϕ and temperature T, and then find θ, ν and t as functions of them. We then substitute the result into the function $\kappa(q;\phi)$ to find the spinodals.

In order to carry out complete calculations, we have to specify the statistical weight η_ζ. To do this, we employ the simplest form proposed by Zimm and Bragg[14] for the study of coil-to-helix transition of biopolymers, i.e.,

$$\eta_\zeta = \sigma\mu(T)^\zeta. \tag{2.38}$$

The front factor σ gives the statistical weight for a boundary between a helix and a coil (a hydrated sequence and a collapsed random coil in the present context), and is called *cooperativity parameter*. In the case of random adsorption where there is no interaction between the adsorbed water molecules, it is given by $\sigma = 1$ and the model reduces to our previous one[12]. Let $\Delta f_0 \equiv \epsilon - T\Delta s$ be the free energy of a hydrogen bond, and let $\Delta\epsilon$ be the interaction energy between the nearest-neighboring bound water molecules. The statistical weight $\mu(T) = \exp[-\beta(\Delta f_0 + \Delta\epsilon)]$ (called association constant) includes both hydrogen-bonding free energy and the nearest-neighbor interaction energy, and the cooperativity parameter is given by $\sigma \equiv \exp(-\beta|\Delta\epsilon|)$.

Eq.(2.29) to decide q now takes the form

$$q = \mu(T)\frac{1-\phi-\theta(q)\phi}{1+\sigma q w_0(q)}\exp[R(\theta,\phi)], \tag{2.39}$$

where μq is written as q for simplicity. The coverage θ by bound water molecules is given by

$$\theta(q) = \frac{\sigma q w_1(q)}{1+\sigma q w_{01}(q)}. \tag{2.40}$$

Here, functions w are defined by

$$w_0(x) \equiv \sum_\zeta x^{\zeta-1}, \quad \text{and} \tag{2.41}$$

$$w_1(x) \equiv \sum_\zeta \zeta x^{\zeta-1}. \tag{2.42}$$

and $w_{01}(x) \equiv w_0(x) + w_1(x)$. The average sequence length is given by $\bar{\zeta}_w = w_1(q)/w_0(q)$.

2.3 Numerical Results and Comparison with the Experiments

For numerical calculation of the phase diagrams, we fix the necessary parameters in the following way. We first assume the conventional Schultz-Flory form $\chi(T) = 1/2 - \psi\tau$ for the χ-parameter[15], where $\tau \equiv 1 - \Theta_0/T$ is the reduced temperature deviation measured from the reference theta temperature Θ_0 satisfying $\chi(\Theta_0) = 1/2$, and ψ is a material parameter of order unity. At the temperature Θ_0, the second virial coefficient of a hypothetical Flory-Huggins solution without hydrogen-bonding interaction vanishes. The association constant is then expressed

as $\mu(T) = \mu_0 \exp(|\epsilon + \Delta\epsilon|/k_B T) = \mu_0 \exp[\gamma_H(1 - \tau)]$, where μ_0 gives the entropy part of the binding free energy, and $\gamma_H \equiv |\epsilon + \Delta\epsilon|/k_B\Theta_0$ gives the binding energy measured relative to the thermal energy at the reference theta temperature. The reference temperature Θ_0 is not the true theta temperature Θ at which the second virial coefficient of the osmotic pressure vanishes. The latter lies far below Θ_0. Throughout the present numerical calculation, we fix ψ at $\psi = 1.0$, and change the amplitude μ_0, dimensionless binding energy γ_H, and the cooperative parameter σ. In particular, we are interested in the effect of the cooperativity parameter σ and see how the bottom part of the miscibility square becomes flatter with decrease in σ, or increase in cooperativity.

In order to check the accuracy of one-mode approximation, we first compare new result on the phase diagrams of randomly hydrated polymers $\sigma = 1.0$ with the old calculation[12]. Figure 2.2 plots the two spinodal lines on top of each other. Solid lines are calculated by one-mode approximation, while the broken lines are calculated by taking into consideration all possible random placement of water molecules discussed in the reference[12]. We can see that the one-mode approximation is sufficiently accurate for $n = 100$. The larger the values of DP, the better the approximation becomes.

2.3.1 Coverage of the Bound Water

Figure 2.3 shows the dehydration curves, i.e., the coverage θ of a polymer chain by hydrogen-bonded water molecules is plotted against the temperature. The cooperative parameter σ is changed from curve to curve. Dehydration of bound water takes place near the phase separation temperature, and becomes sharper with increase in the cooperativity.

Figure 2.4 shows the fraction θ of the bound water molecules plotted as functions of the temperature for three different polymer concentrations. From this figure, hydration is almost independent of polymer concentration, so we can treat hydration as single chain problem. We can find the enthalpy ΔH of dehydration. If fraction $-\Delta\theta$ is dehydrated by a small temperature rise ΔT, the absorption of heat is given by

$$\Delta H = \frac{|\epsilon + \delta\epsilon|\phi\Delta\theta}{M}. \tag{2.43}$$

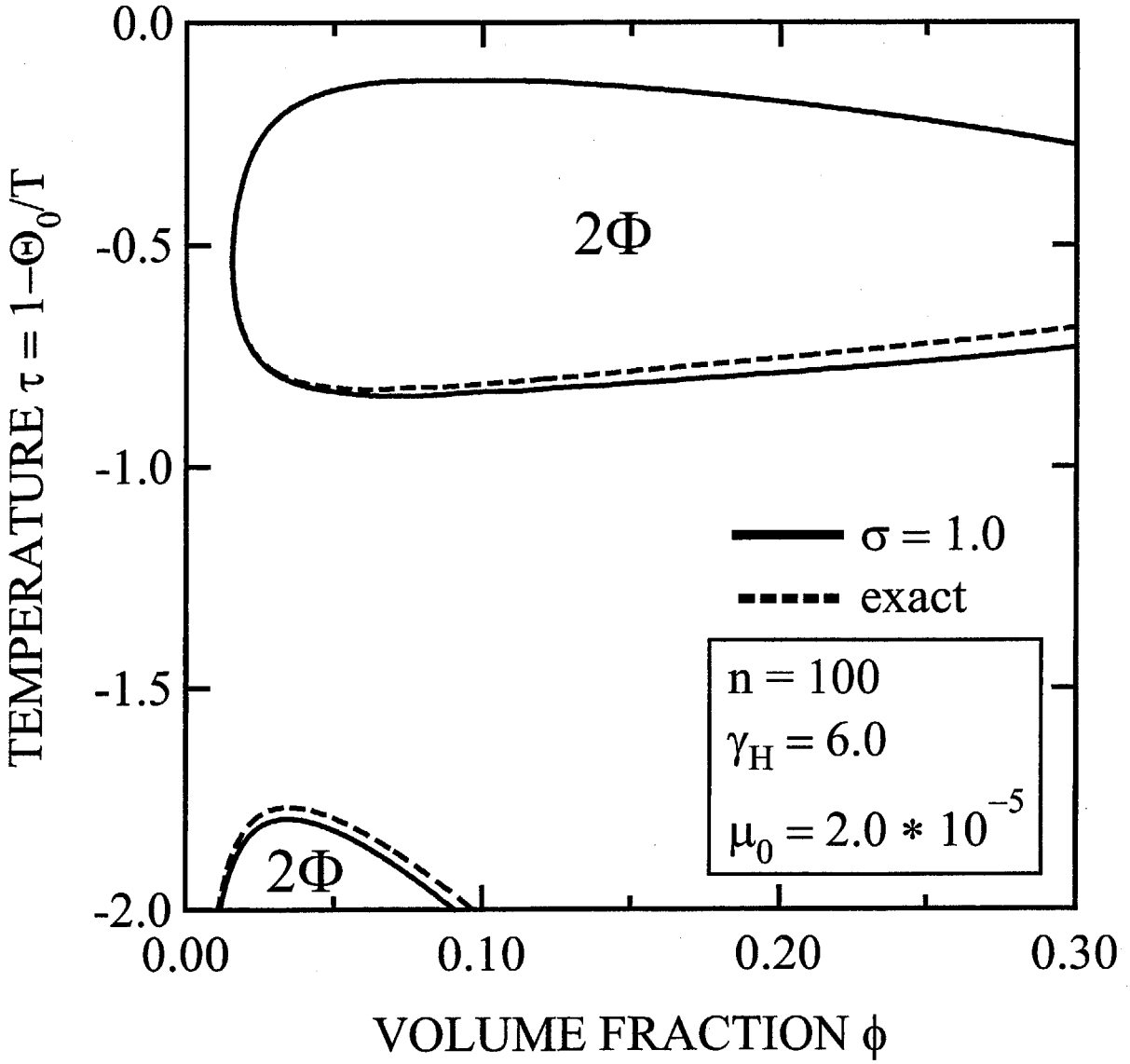

Figure 2.2: Comparison of the spinodal lines derived by the complete calculation (broken lines) and by one-mode approximation (solid lines).

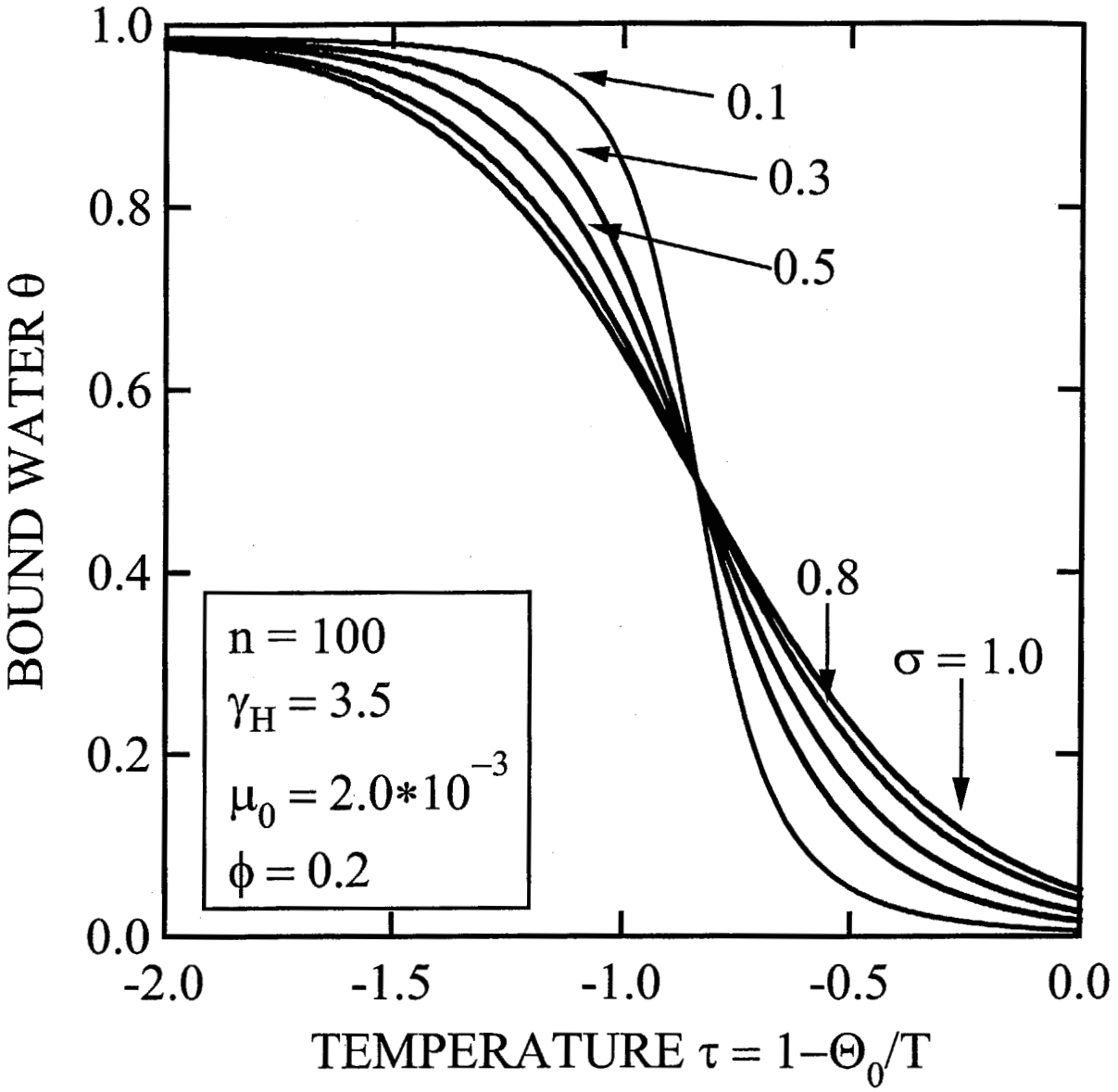

Figure 2.3: The coverage θ of a polymer chain by hydrogen-bonded water molecules plotted against the temperature. The cooperative parameter σ is changed from curve to curve. Dehydration of bound water becomes sharper with increase in the cooperativity (decrease in σ).

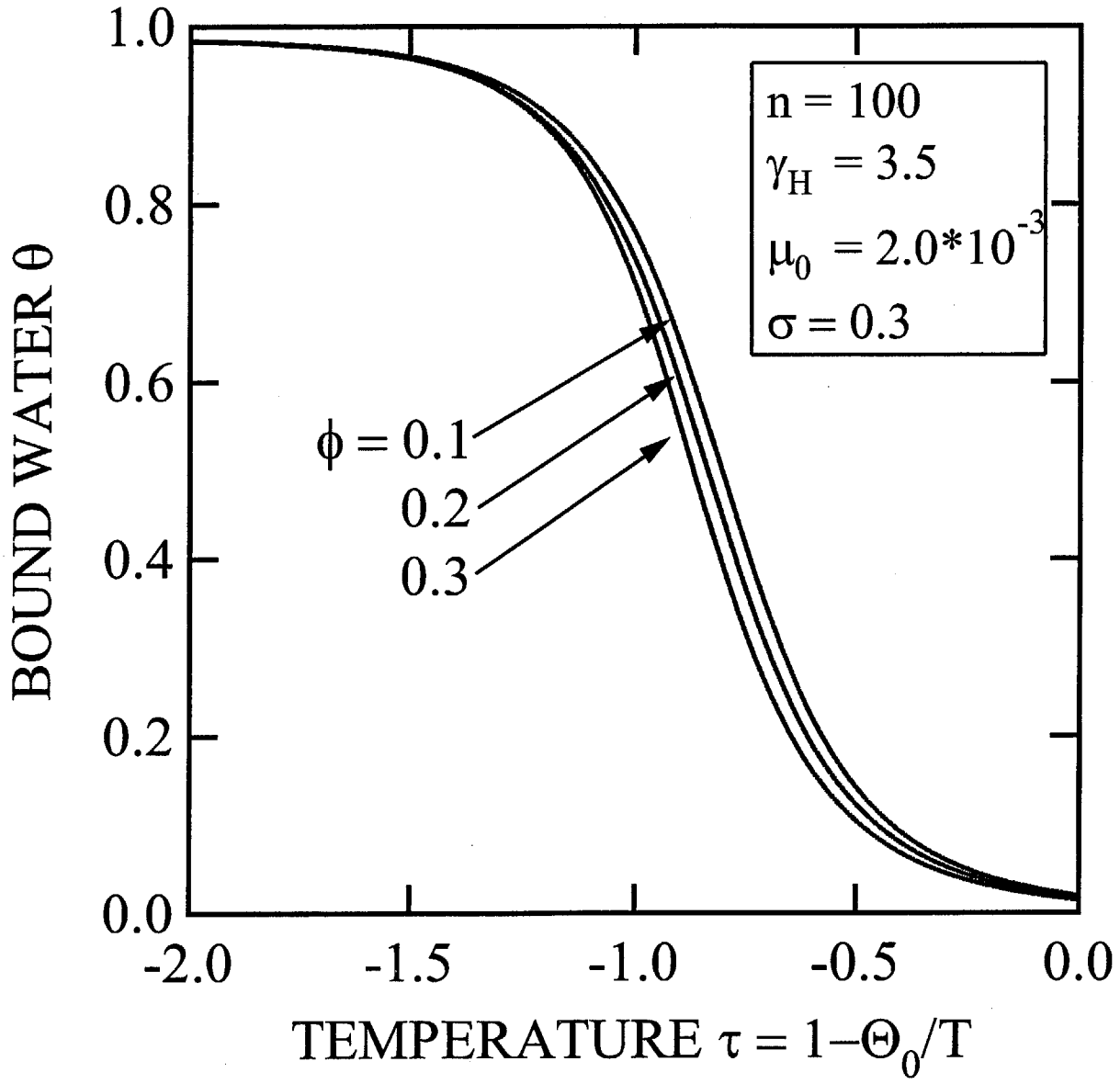

Figure 2.4: The content θ of the bound water plotted against temperature for three polymer volume fractions for n = 100.

It shows a peak at the temperature where θ changes most sharply, i.e., at the phase separation temperature. The polymer chains collapse into compact globules as soon as bound water is dehydrated.

2.3.2 Phase Diagrams

Let us move onto cooperative hydration. Figure 2.5 calculated the spinodal curves for different cooperative parameter σ with fixed other parameters. It theoretically demonstrates how the bottom part of the miscibility squares become flatter with decrease in σ. In the calculation, usual miscibility domes with UCST appear at low temperature, but these are not observable in the experiments because of the freezing of water. For the polymer concentration higher than $\phi = 0.5$, our theoretical description becomes poor because of the depletion of water molecules, i.e., the number of water molecules becomes insufficient to cover the polymers.

2.3.3 Comparison with the Experiments on the Spinodal Curves

Figure 2.6 compares theoretical calculation with experimental data[7] on the spinodal points. In the experiments, the upper part of the miscibility square cannot be observed because temperature is too high. Also, UCST phase separation seen in the theoretical calculation is not observable because of the freezing of water. The polymer molecular weight used in the experiment is $M_w = 615,500$, so that the nominal number of monomers is roughly given by $n = 5,400$. Although polymers used in the experiment are polydisperse with the index $M_w/M_n = 2.04$, we expect that this may not cause any serious problems because the dependence of binodals as well as spinodals on the polymer molecular weight becomes weaker with increase in cooperativity in hydration. Since the statistical unit used in the lattice theory must be regarded as a group of monomers, we have tried to fit the data by $n = 100$ and 1000. (Theoretical calculation does not depend so much upon the number n if it is larger than 500.) We have seen a good agreement by fixing the cooperative parameter at $\sigma = 0.3$. There is, however, a slight discrepancy in the dilute regime, i.e., theoretical curve predicts a sharper bend. Closer examination on the very dilute regime from both experimental and theoretical viewpoint is therefore necessary.

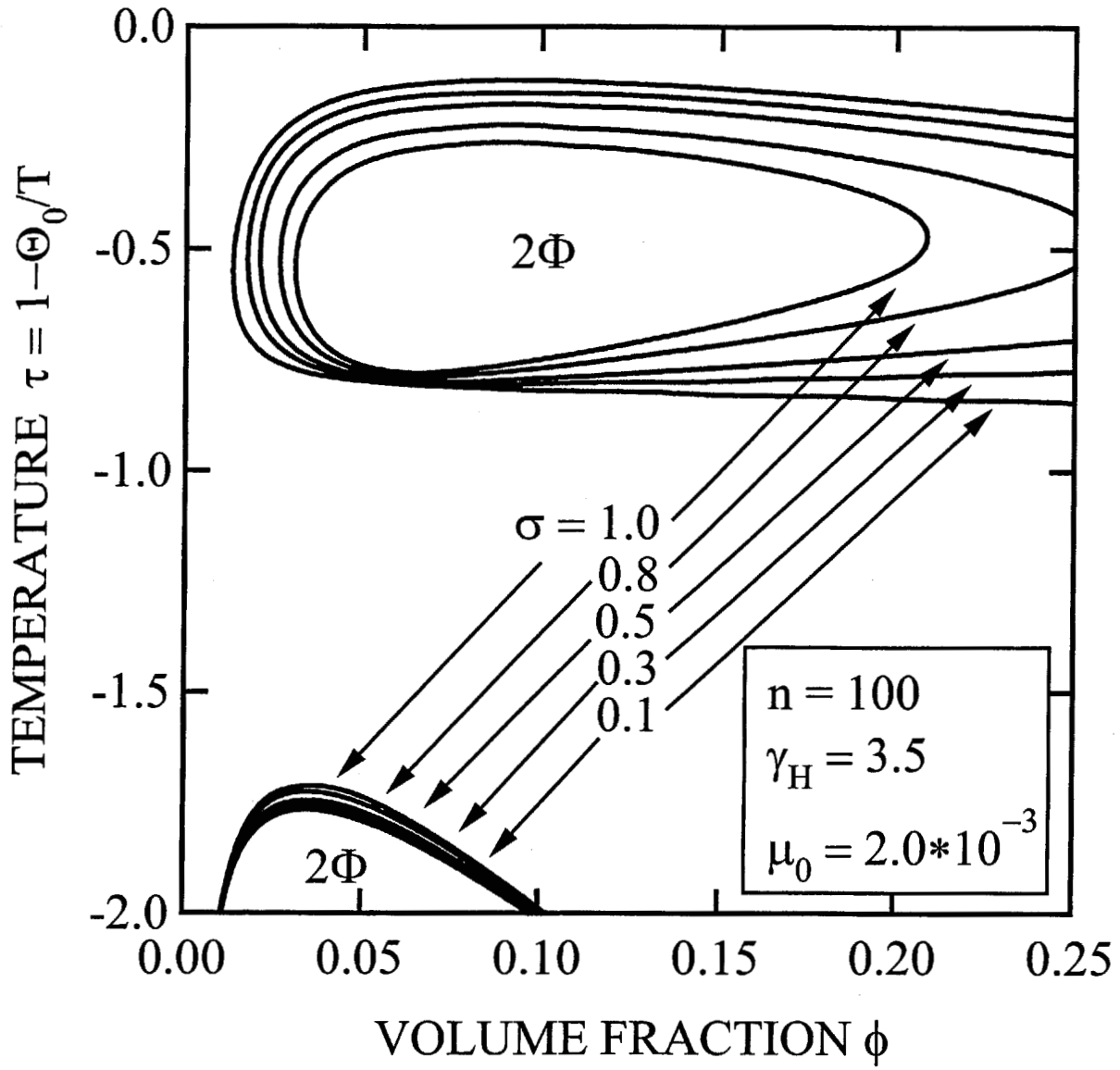

Figure 2.5: Spinodal lines calculated on the (reduced) temperature and concentration plane for different cooperative parameter σ. Other parameters are fixed at n = 100, ψ = 1.0, μ_0 = 2.0×10^{-3}, γ_H = 3.5. The bottom part of the miscibility square becomes flatter with decrease in the cooperative factor σ.

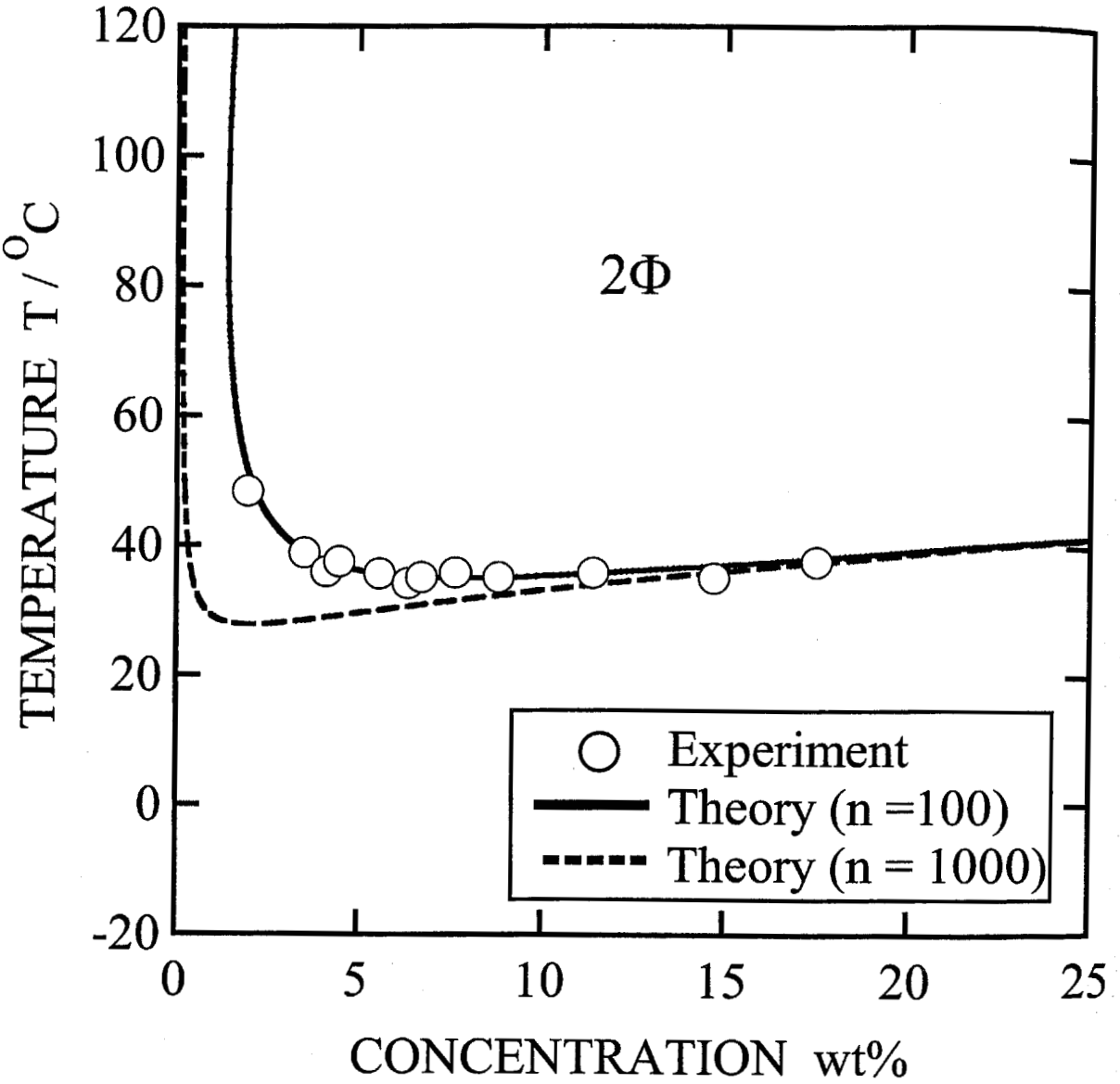

Figure 2.6: Phase diagrams of aqueous PNIPAM solution. Experimental data (○) of the spinodal curve is compared with theoretical calculation. The DP of the polymer is $n = 100$ (solid line) and $n = 1000$ (broken line). Theoretical parameters used is $\Theta_0 = 555$ and $\mu_0 = 0.002$ for $n = 100$, and $\Theta_0 = 565$ and $\mu_0 = 0.003$ for $n = 1000$. Other parameters are fixed at $\gamma_H = 3.5, \sigma = 0.3$.

2.3.4 Molecular Weight Dependence of LCST and UCST

The left panel of Figure 2.7 presents the theoretical plots of the LCST and UCST of homopolymer PEO solutions as functions of the reciprocal DP (more precisely, the reciprocal $1/n$ of the number of statistical units on a chain). The right panel displays the corresponding phase diagrams on the conventional temperature-concentration plane. DCP is the *double critical point* where the LCST and UCST merge into a single critical point, thus the loop merges with the miscibility dome at low temperatures, and turns into *hourglass*. HCP stands for the *hyper critical point* where the phase separation region of loop shape shrinks into one point. For PEO, the DCP occurs at $n = 1,800$, while HCP takes place at $n = 42$. The disappearance of the loop (HCP) was observed experimentally by Saeki et al[2] in the case of polymers of lower molecular weight.

Figure 2.8 is the same as in left panel of Figure 2.7 in the case of $\sigma = 1.0, 0.3$. For cooperative hydration with $\sigma = 0.3$, however, DCP does not appear. HCP shifts to lower DP, and is shaped like an angular square. From this figure, it is evident that cooperative hydration leads to flat LCST with almost no molecular weight dependence.

2.3.5 Osmotic Pressure

Let us now study the effect of cooperative hydration on the second virial coefficient Eq.(2.22) of the osmotic pressure within one mode approximation. The function $G(y)$ in this approximation is identical to the coverage θ of the bound water. Therefore, the value G_0 in the limit of infinite dilution is given by θ_0 which can be calculated by using the solution q_0 of Eq.(2.39) at $\phi = 0$, i.e.,

$$q_0 = \frac{\mu(T)}{1 + \sigma q_0 w_0(q_0)}. \tag{2.44}$$

The coverage is given by

$$\theta_0 = \frac{\sigma q_0 w_1(q_0)}{1 + \sigma q_0 w_{01}(q_0)}. \tag{2.45}$$

This is essentially equivalent to Zimm-Bragg's equation[14] for the single-chain problem. Figure 2.9 plots the second virial coefficient A_2 as a function of the temperature. The cooperative

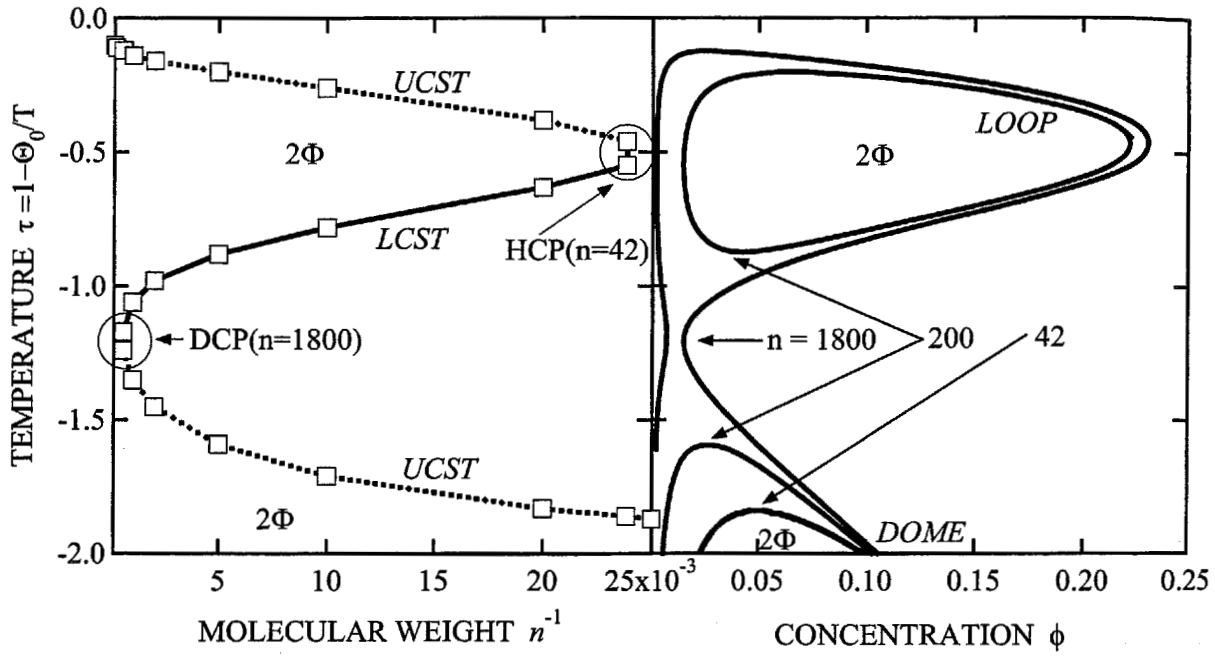

Figure 2.7: UCST lines (dotted lines) and LCST lines (solid lines) of homopolymer PEO solutions as functions of n^{-1}, the reciprocal DP (left). Phase diagrams of PEO solutions[2] on an ordinary temperature-concentration plane (right). The DP of the polymer is changed from curve to curve.

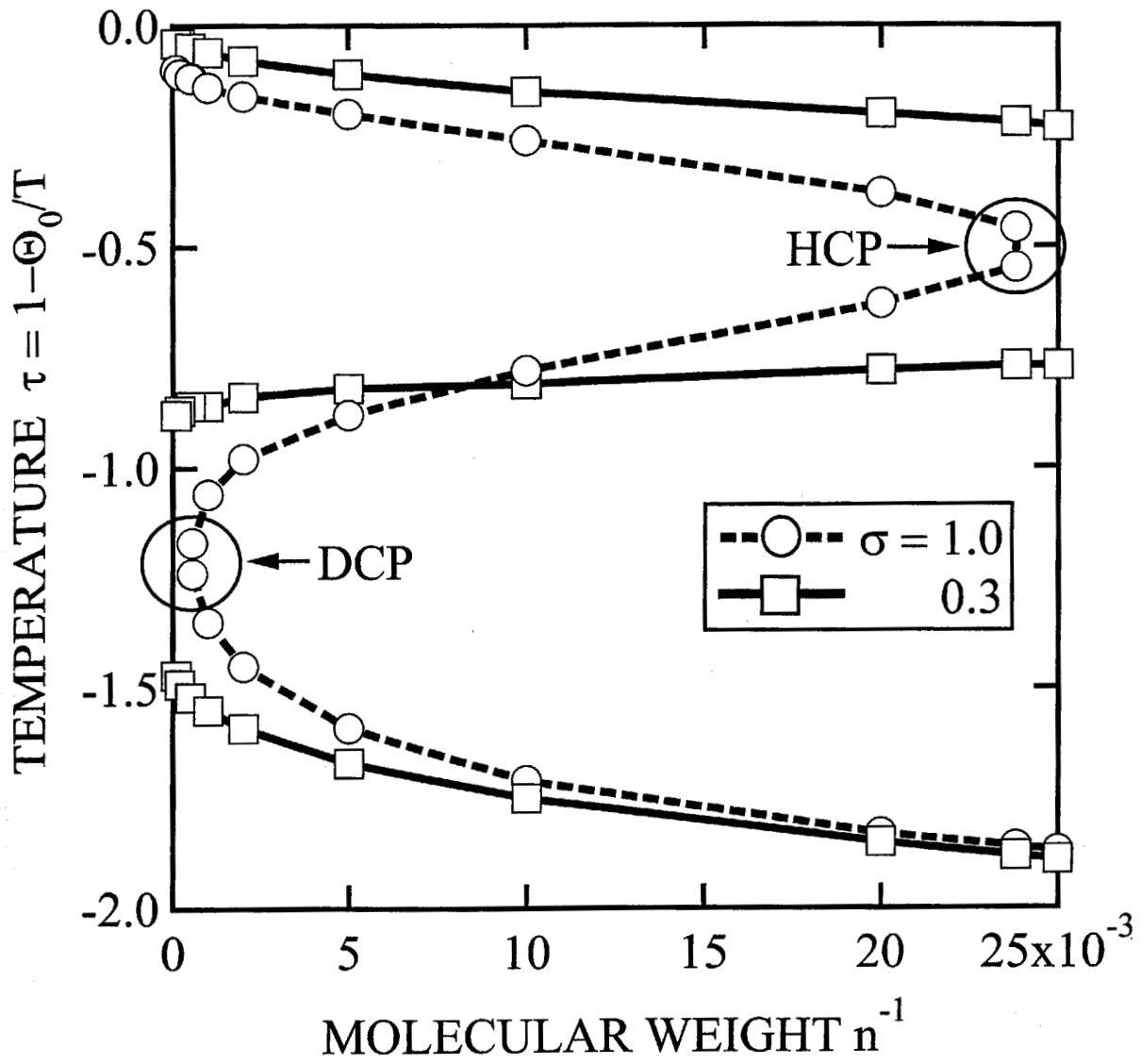

Figure 2.8: Molecular weight dependence of the LCST. The critical temperatures are plotted against the reciprocal of DP. HCP stands for hyper critical point where miscibility loop shrinks to a point. DCP stands for double critical point where LCST of the miscibility loop merges with UCST of the miscibility dome into a single point.

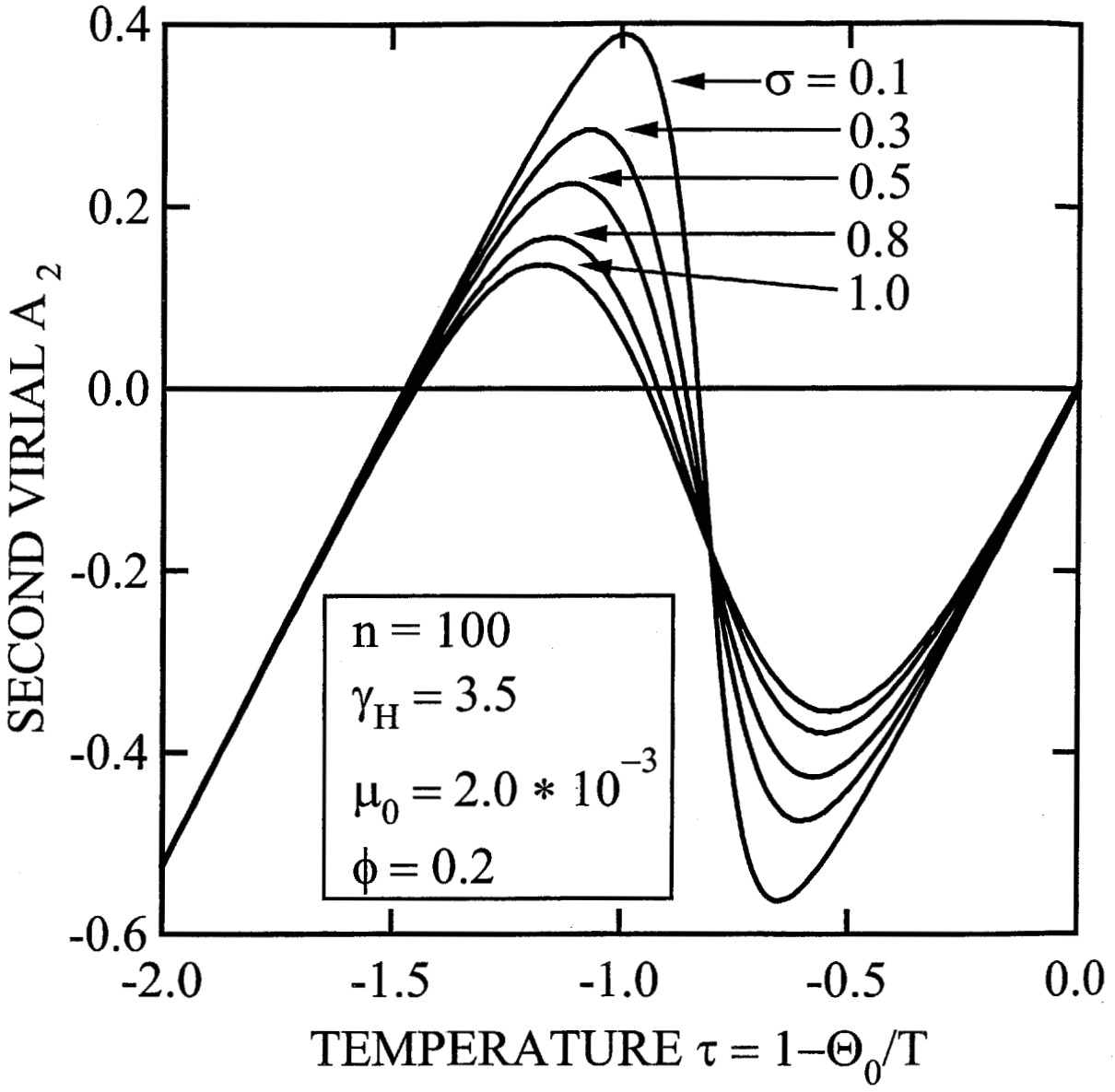

Figure 2.9: The second virial coefficient A_2 plotted against the temperature. The cooperative parameter σ is varied from curve to curve. There are in principle three theta temperatures where A_2 vanishes. The one lying in the middle temperature is relevant theta temperature to which LCST approaches in the infinite molecular weight.

parameter σ is varied from curve to curve. There are in principle three theta temperatures where A_2 vanishes. The one lying in the middle temperature is the relevant theta temperature to which LCST approaches in the infinite molecular weight. With increase in cooperativity, dehydration becomes sharper, so that the (negative) slope of A_2 becomes larger.

2.4 Conclusions and Discussion

We have theoretically studied phase separation in aqueous polymer solutions. By the calculation of phase diagrams, we have confirmed that correlation, or cooperativity, between the neighboring water molecules that are hydrogen-bonded onto the polymer chain leads to flat LCST behavior with only little molecular weight dependence. The phase separation experimentally seen in aqueous PNIPAM solutions falls onto this category, and is markedly different from PEO solutions where miscibility loops with UCST and LCST depend sensitively on the polymer molecular weight. From the temperature profile of dehydration curve, the sharpness of the single-chain coil/globule transition is also expected to originate in this cooperativity. The pearl-necklace conformation (Figure 2.1) driven by the cooperative hydration agrees with the recent measurements of concentration fluctuations in PNIPAM cross-linked gels by neutron scattering method[16]. They found necklace-like microstructure through the study of the static structure factor profile appearing after a shallow quench into the collapsed state. Comparison between solutions and gels may lead to more profound understanding of the temperature sensitivity of PNIPAM chains.

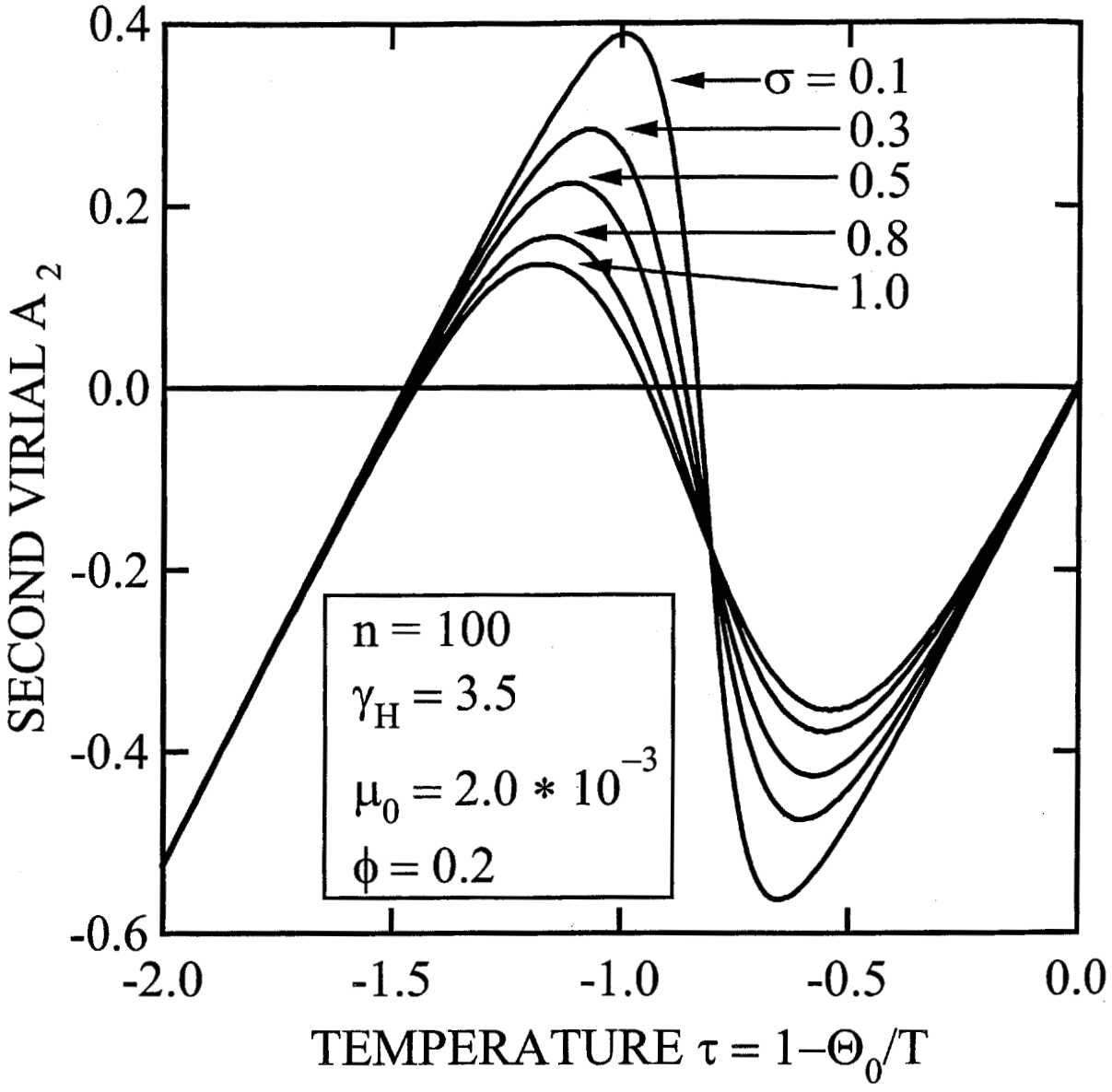

Figure 2.9: The second virial coefficient A_2 plotted against the temperature. The cooperative parameter σ is varied from curve to curve. There are in principle three theta temperatures where A_2 vanishes. The one lying in the middle temperature is relevant theta temperature to which LCST approaches in the infinite molecular weight.

parameter σ is varied from curve to curve. There are in principle three theta temperatures where A_2 vanishes. The one lying in the middle temperature is the relevant theta temperature to which LCST approaches in the infinite molecular weight. With increase in cooperativity, dehydration becomes sharper, so that the (negative) slope of A_2 becomes larger.

2.4 Conclusions and Discussion

We have theoretically studied phase separation in aqueous polymer solutions. By the calculation of phase diagrams, we have confirmed that correlation, or cooperativity, between the neighboring water molecules that are hydrogen-bonded onto the polymer chain leads to flat LCST behavior with only little molecular weight dependence. The phase separation experimentally seen in aqueous PNIPAM solutions falls onto this category, and is markedly different from PEO solutions where miscibility loops with UCST and LCST depend sensitively on the polymer molecular weight. From the temperature profile of dehydration curve, the sharpness of the single-chain coil/globule transition is also expected to originate in this cooperativity. The pearl-necklace conformation (Figure 2.1) driven by the cooperative hydration agrees with the recent measurements of concentration fluctuations in PNIPAM cross-linked gels by neutron scattering method[16]. They found necklace-like microstructure through the study of the static structure factor profile appearing after a shallow quench into the collapsed state. Comparison between solutions and gels may lead to more profound understanding of the temperature sensitivity of PNIPAM chains.

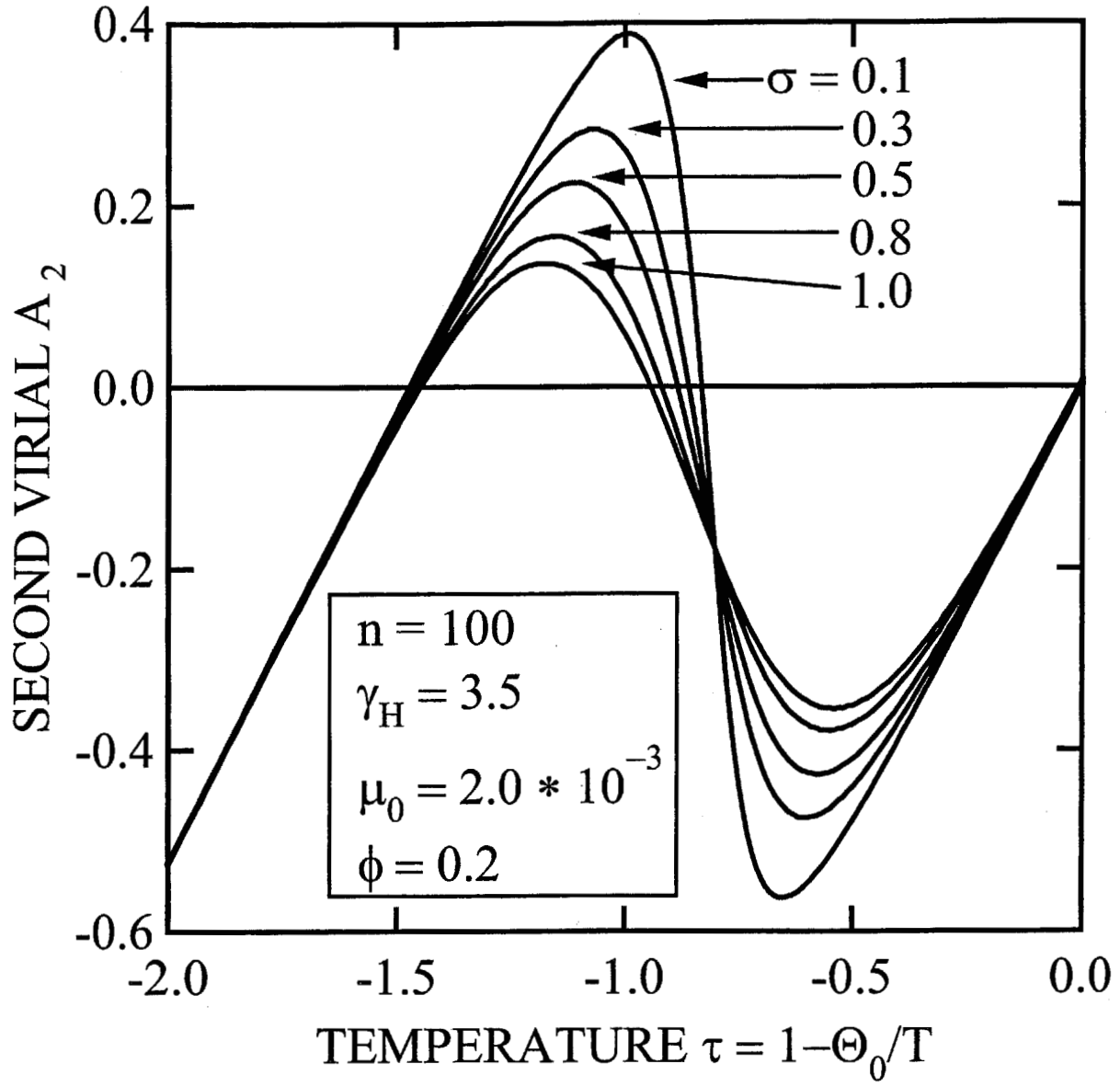

Figure 2.9: The second virial coefficient A_2 plotted against the temperature. The cooperative parameter σ is varied from curve to curve. There are in principle three theta temperatures where A_2 vanishes. The one lying in the middle temperature is relevant theta temperature to which LCST approaches in the infinite molecular weight.

parameter σ is varied from curve to curve. There are in principle three theta temperatures where A_2 vanishes. The one lying in the middle temperature is the relevant theta temperature to which LCST approaches in the infinite molecular weight. With increase in cooperativity, dehydration becomes sharper, so that the (negative) slope of A_2 becomes larger.

2.4 Conclusions and Discussion

We have theoretically studied phase separation in aqueous polymer solutions. By the calculation of phase diagrams, we have confirmed that correlation, or cooperativity, between the neighboring water molecules that are hydrogen-bonded onto the polymer chain leads to flat LCST behavior with only little molecular weight dependence. The phase separation experimentally seen in aqueous PNIPAM solutions falls onto this category, and is markedly different from PEO solutions where miscibility loops with UCST and LCST depend sensitively on the polymer molecular weight. From the temperature profile of dehydration curve, the sharpness of the single-chain coil/globule transition is also expected to originate in this cooperativity. The pearl-necklace conformation (Figure 2.1) driven by the cooperative hydration agrees with the recent measurements of concentration fluctuations in PNIPAM cross-linked gels by neutron scattering method[16]. They found necklace-like microstructure through the study of the static structure factor profile appearing after a shallow quench into the collapsed state. Comparison between solutions and gels may lead to more profound understanding of the temperature sensitivity of PNIPAM chains.

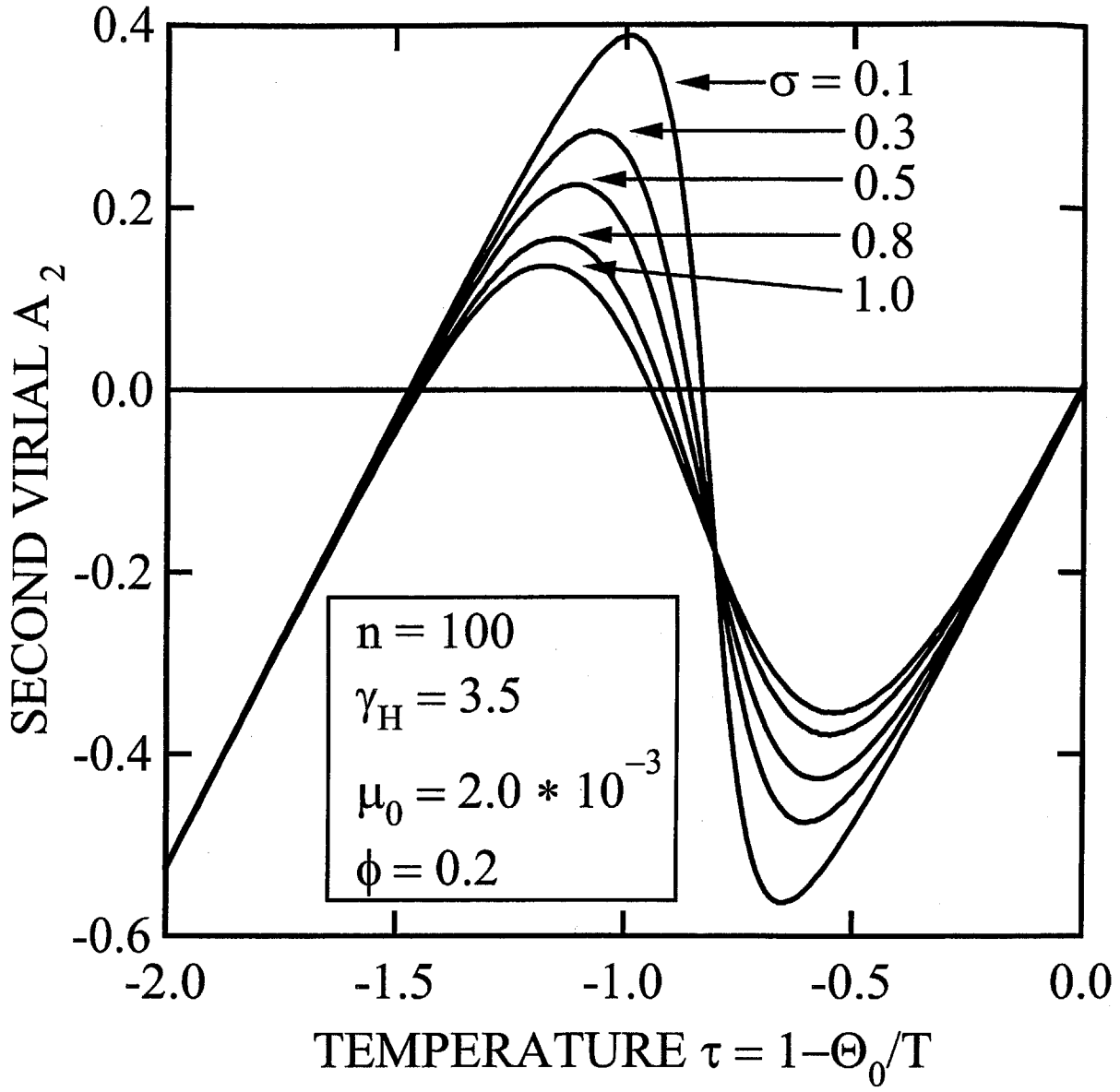

Figure 2.9: The second virial coefficient A_2 plotted against the temperature. The cooperative parameter σ is varied from curve to curve. There are in principle three theta temperatures where A_2 vanishes. The one lying in the middle temperature is relevant theta temperature to which LCST approaches in the infinite molecular weight.

parameter σ is varied from curve to curve. There are in principle three theta temperatures where A_2 vanishes. The one lying in the middle temperature is the relevant theta temperature to which LCST approaches in the infinite molecular weight. With increase in cooperativity, dehydration becomes sharper, so that the (negative) slope of A_2 becomes larger.

2.4 Conclusions and Discussion

We have theoretically studied phase separation in aqueous polymer solutions. By the calculation of phase diagrams, we have confirmed that correlation, or cooperativity, between the neighboring water molecules that are hydrogen-bonded onto the polymer chain leads to flat LCST behavior with only little molecular weight dependence. The phase separation experimentally seen in aqueous PNIPAM solutions falls onto this category, and is markedly different from PEO solutions where miscibility loops with UCST and LCST depend sensitively on the polymer molecular weight. From the temperature profile of dehydration curve, the sharpness of the single-chain coil/globule transition is also expected to originate in this cooperativity. The pearl-necklace conformation (Figure 2.1) driven by the cooperative hydration agrees with the recent measurements of concentration fluctuations in PNIPAM cross-linked gels by neutron scattering method[16]. They found necklace-like microstructure through the study of the static structure factor profile appearing after a shallow quench into the collapsed state. Comparison between solutions and gels may lead to more profound understanding of the temperature sensitivity of PNIPAM chains.

Bibliography

[1] Malcolm, G. N.; Rowlinson, J. S. *Trans. Faraday Soc.* **1953**, *53*, 921.

[2] Saeki, S.; Kuwahara, N.; Nakata, M.; Kaneko, M. *Polymer* **1976**, *17*, 685.

[3] Bae, Y. C.; Lambert, S. M.; Soane, D. S.; Prausnitz, J. M. *Macromolecules* **1991**, *24*, 4403.

[4] Bekiranov, S.; Bruinsma, R.; Pincus, P. *Phys. Rev. E* **1997**, *55*, 3072.

[5] Heskins, M.; Guillet, J. E. *J. Macromol. Sci.* **1968**, *A2*, 1441.

[6] Fujishige, S.; Kubota, K.; Ando, I. *J. Phys. Chem.* **1989**, *93*, 3311.

[7] de Azevedo, R. G.; Rebelo, L. P. N.; Ramos, A. M.; Szydlowski, J.; de Sousa, H. C.; Klein, J. *Fluid Phase Equilib.* **2001**, *185*, 189.

[8] Rebelo, L. P. N.; Visak, Z. P.; de Sousa, H. C.; Szydlowski, J.; de Azevedo, R. G.; Ramos, A. M.; Najdanovic-Visak, V.; da Ponte M. N.; Klein, J. *Macromolecules* **2002**, *35*, 1887.

[9] Milewska, A.; Szydlowski, J.; Rebelo, L. P. N. *J. Polym. Sci., Part B: Polym. Phys.* **2003**, *41*, 1219.

[10] Baulin, V. A.; Halperin, A. *Macromol. Theory Simul.* **2003**, *12*, 549.

[11] Afroze, F.; Nies, E.; Berghmans, H. *J. Mol. Struct.*, **2000**, *554*, 55.

[12] Matsuyama, A.; Tanaka, F. *Phys. Rev. Lett.* **1990**, *65*, 341.

[13] A similar combinatorial method was employed by the author to study partition functions of helical polymers whose helices are induced by hydrogen-bonded chiral side groups: Tanaka, F. *Macromolecules* **2004**, *37*, 605.

[14] Zimm, B. H.; Bragg, J. K. *J. Chem. Phys.* **1959**, *31*, 526.

[15] Schultz, A. R.; Flory, P. J. *J. Am. Chem. Soc.* **1952**, *74*, 4760.

[16] Koizumi, S.; Monkenbusch, M.; Richter, D.; Schwahn, D.; Farago, B. *J. Chem. Phys.* **2004**, *121*, 12721.

Chapter 3

Phase Separation Driven by Hydrophobic Association in Aqueous Solutions of Telechelic Associating Polymers

3.1 Introduction

The experimental study of phase behavior in hydrophobically end-capped water-soluble polymer aqueous solutions is now progressing. For example, several studies[1, 2] have shown that the LCST of aqueous telechelic Poly (ethylneoxide) (referred to as HM-PEO) solutions is much lower than the LCST of solutions of PEO samples of comparable molecular weight. The magnitude of the shift in LCST can reach 100°C. The LCST of telechelic PEOs depends on the sample molecular weight: it increases with increasing molecular weight, such that the phase separation region shrinks for telechelic polymers of larger size. This trend is opposite to that exhibited by aqueous solutions of PEO. In the case of aqueous telechelic Poly (*N*-isopropylacrylamide)s (referred to as HM-PNIPAM), the end-group induced decrease of the LCST is much weaker, on the order of 5 to 10°C[3, 4]. Moreover, the transition temperature detected by microcalorimetry, which corresponds to the coil-to-globule transition of PNIPAM, is hardly affected by the end-group substituents.

In this chapter, we discuss a study of the association and phase behavior of telechelic and semi-telechelic hydrophobically modified PEO and PNIPAM based on our previous theoretical study of water-soluble polymers. The number of hydrophobes (typically short alkyl chains) on each main chain is called the functionality f of the chain. Thus, we have $f = 1$ for one-end hydrophobized polymers, and $f = 2$ for *telechelic polymers*, i.e., polymers carrying hydrophobic chains at both ends. Hydrophobic aggregation of the chain ends triggers the formation of micelles, networks, and other self-assembled structures depending upon the temperature and concentration. We will pay special attention to telechelic polymers which interact with water differently from their homopolymer counterparts in two ways:

(1) They form micelles and networks by hydrophobic aggregation of the end chains. In the dilute region, typically solutions of concentration lower than 1 wt%, telechelic polymers form intramolecular loops, which aggregate into micelles of flower-like shape (called *flower micelles*)[1, 5, 6, 7, 8, 9, 10]. At higher concentrations, the chains start to form bridges between micelles, resulting in the formation of networks with micellar junctions.

(2) The hydrophobic end-chains interact directly with water, so that they drive the solutions towards liquid-liquid phase separation.

Mechanism (1) results in an apparent increase of the polymer molecular weight, compared to the homopolymers. Hence the mixing entropy decreases, inducing the polymers to demix in water. We will call this demixing enhancement tendency an "*association-induced phase separation*" as in the literature (referred to as TS)[11, 12]. The hydrophobe number density and the polymer volume fraction ϕ are important parameters controlling this mechanism.

Mechanism (2) leads to phase separation between the end groups and water through direct hydrophobic interaction[13]. The tendency towards phase separation increases as the number of end-groups per unit volume becomes larger. Thus, for the same volume fraction ϕ, shorter telechelic polymers tend to phase separate more readily than longer ones.

We present here a unified model of the LCST phase separation of aqueous hydrophobically-modified telechelic polymer solutions which takes into account the nature of the water-main chain interactions through a hydration cooperativity parameter σ.

In aqueous solutions of hydrophobic polymers, chain association interferes with hydration with consequences on the macroscopic scale. If hydration is so strong that there are many bound water molecules near the hydrophobes, association must compete with hydration. In such a case, gelation is possible only after dehydration takes place by raising the temperature (high-temperature gelation). High-temperature gelation with LCST phase separation in solutions with such competing hydration and association phenomena has already been theoretically derived[14]. For telechelic polymers, however, hydration takes place along the main chain, so that it is only indirectly affected by end-chain association, except for the chain sections very close to the chain end. Dehydration and chain collapse start near the core of the flower micelles in the form of heterogeneous nucleation. In other words, hydration is decoupled from association. The solutions with such coexisting hydration and association turn into gels on cooling (low-temperature gelation) with LCST phase separation. We study here the phase diagrams of

the telechelic polymer/water systems under the assumption of coexisting hydration and association. The theoretically derived phase diagrams will be compared to experimentally established phase diagrams of telechelic PNIPAM/water and telechelic PEO/water systems.

3.2 Statistical-Mechanical Theory of Associating Polymer Solutions

3.2.1 Model Aqueous Solutions of Associating Polymers

Let us consider a model solution consisting of N telechelic polymer chains having a main chain of degree of polymerization (DP) n and two end groups of DP n^*. The total DP of the polymer chains is $n_t \equiv n+2n^*$. The chains are mixed with a number N_0 of water molecules. We start with the lattice-theoretical description of polymer solutions[15, 16], and divide the system volume V into cells of size a, each of which can accommodate either a water molecule or a statistical repeat unit of the polymer chain. We assume incompressibility of the solution, so that the total number $\Omega \equiv V/a^3$ of cells is given by $\Omega = N_0 + n_t N$. To describe the hydration of the chains by water, we follow the convention of previous chapter, and let $\mathbf{i} \equiv \{i_1, i_2, \cdots\}$ be the index specifying the polymer chain carrying the number i_ζ of water molecule sequences that consist of a run of ζ consecutive hydrogen-bonded water molecule, and let $N(\mathbf{i})$ be the number of such polymer-water complexes of type $\mathbf{i}$ (see Figure 3.1). In particular, we have $\mathbf{i}_0 \equiv (0, 0, \cdots)$ for a bare polymer chain devoid of bound water. The total number of water molecules on a chain specified by $\mathbf{i}$ is given by $\sum \zeta i_\zeta$, and the DP of a complex is given by $n(\mathbf{i}) \equiv n[1 + \theta(\mathbf{i})] + 2n^*$, where

$$\theta(\mathbf{i}) \equiv \sum_{\zeta=1}^{n} \frac{\zeta i_\zeta}{n} \tag{3.1}$$

is the coverage by the bound water molecules relative to the total DP of a polymer.

In thermal equilibrium, the population distribution of connected clusters formed by the end-chain association in solution is fixed by the equilibrium conditions. Following the notation used by Fukui and Yamabe[17], we define a cluster as $(\mathbf{j}; \mathbf{m})$ if it consists of j_k junctions of multiplicity k ($k = 1, 2, 3, ...$) and $\mathbf{m}(\mathbf{i})$ molecules of the hydration type $\mathbf{i}$. The bold letters

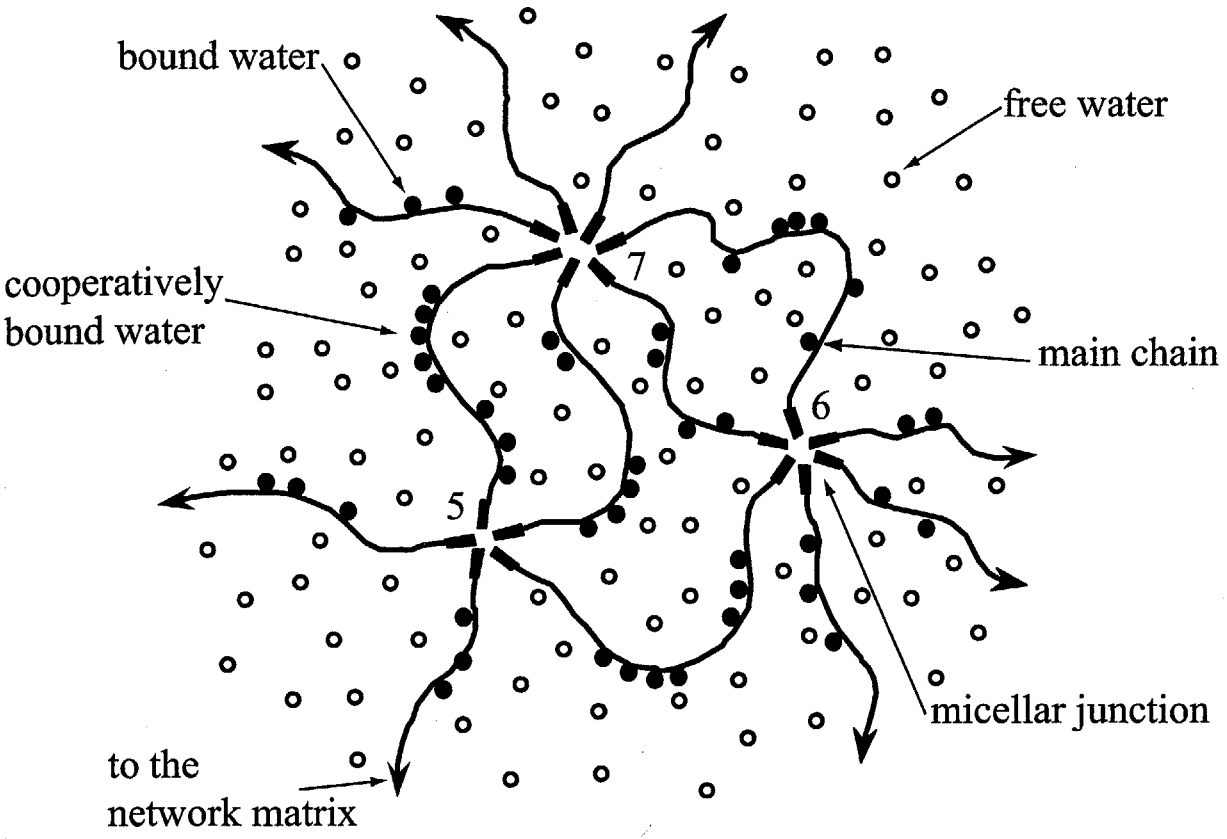

Figure 3.1: Pictorial representation of a telechelic polymer network made up of hydrated polymer chains. The polymer chains are cross-linked by the micellar junctions formed by hydrophobic association of the end-chains. In the case of cooperative hydration, sequences of bound water molecules are formed along the polymer chains. Chain association and hydration are expected to be independent except in the region near the junctions. The multiplicity k is indicated by the figure near a junction.

$\mathbf{j} \equiv \{j_1, j_2, j_3, ...\}$ and $\mathbf{m} \equiv \{m(\mathbf{i})\}$ denote the sets of indices. The multiplicity is here given by the number of hydrophobes in a micelle. A $(\mathbf{j}; \mathbf{m})$ cluster is a connected cluster consisting of the number $m(\mathbf{i})$ of hydrated chains of type $\mathbf{i}$. An isolated molecule of the type $\mathbf{i}$, for instance, is indicated by the labels $\mathbf{j_0} \equiv \{f, 0, 0, ...\}$ (with $f = 2$ for a telechelic chain), and $\mathbf{m_0(i)} \equiv$ 1(for the type specified by $\mathbf{i}$), $\equiv$ 0(for others).

Let $N(\mathbf{j}; \mathbf{m})$ be the number of $(\mathbf{j}; \mathbf{m})$-clusters in the system. Their number density is given by $\nu(\mathbf{j}; \mathbf{m}) = N(\mathbf{j}; \mathbf{m})/\Omega$, and their volume fraction is given by

$$\phi(\mathbf{j}; \mathbf{m}) = \tilde{n}(\mathbf{m})\nu(\mathbf{j}; \mathbf{m}), \tag{3.2}$$

where

$$\tilde{n}(\mathbf{m}) \equiv \sum_{\mathbf{i}} n(\mathbf{i})m(\mathbf{i}) \tag{3.3}$$

and $n(\mathbf{i}) \equiv n(1 + \theta(\mathbf{i}) + 2n^*/n)$ is the total DP of a polymer-water complex of type $\mathbf{i}$. It is approximately given by $n(\mathbf{i}) \simeq n(1 + \theta(\mathbf{i}))$ for a polymer in which the main chain is much longer than the end groups. This gives the volume fraction of the clusters including the bound water. The total volume fraction of the polymer-water complexes is then given by $\sum_{\mathbf{j},\mathbf{m}} \phi(\mathbf{j}; \mathbf{m})$.

In the postgel regime where hydrated gel networks exist, one needs to consider in addition the number, $N(\mathbf{i})$, of polymer chains of type $\mathbf{i}$ involved in network formation. Their number density is given by $\nu^G(\mathbf{i}) = N^G(\mathbf{i})/\Omega$, and their volume fraction by $\phi^G(\mathbf{i}) = n(\mathbf{i})\nu^G(\mathbf{i})$.

The total number of polymer chains in solution is

$$N = \sum_{\mathbf{j},\mathbf{m}} \left[\sum_{\mathbf{i}} m(\mathbf{i}) \right] N(\mathbf{j}; \mathbf{m}) + \sum_{\mathbf{i}} N^G(\mathbf{i}). \tag{3.4}$$

For instance, polymer chains of hydration type $\mathbf{i}$ that remain unassociated in solution is given by $N(\mathbf{j_0}; \mathbf{m_0(i)})$. Similarly, the number of bound water molecules is

$$N_{\mathrm{bw}} = \sum_{\mathbf{j},\mathbf{m}} \left[\sum_{\mathbf{i}} n\theta(\mathbf{i})m(\mathbf{i}) \right] N(\mathbf{j}; \mathbf{m}) + \sum_{\mathbf{i}} n\theta(\mathbf{i})N^G(\mathbf{i}), \tag{3.5}$$

and the number of free water molecules is

$$N_{\mathrm{fw}} = (1 - \phi)\Omega - N_{\mathrm{bw}}. \tag{3.6}$$

The total volume $\Omega \equiv N_0 + nN$ of the solution is now given by

$$\Omega = \sum_{\mathbf{j},\mathbf{m}} \tilde{n}(\mathbf{m}) N(\mathbf{j};\mathbf{m}) + \sum_{\mathbf{i}} n(\mathbf{i}) N^G(\mathbf{i}) + N_{\mathrm{fw}}. \tag{3.7}$$

Before introducing the free energy of the solution, let us consider the number of contacts between polymers and water. Since the volume fraction of the main chain is $\phi_c = (n/n_t)\phi$, and that of the end chain is $\phi_e = (2n^*/n_t)\phi$, the number of main chain-water contacts (mw) is $\phi_c(1-\phi)$, and the number of end chain-water contacts (ew) is $\phi_e(1-\phi)$. We introduce the conventional χ parameter for each contact type (mw and ew), and find that the enthalpy of polymer-water interaction per lattice cell is given by $\tilde{\chi}(T)\phi(1-\phi)$, where

$$\tilde{\chi}(T) \equiv \frac{n}{n_t}\chi_{\mathrm{mw}}(T) + \frac{2n^*}{n_t}\chi_{\mathrm{ew}}(T). \tag{3.8}$$

χ_{mw} corresponds to χ in chapter 2. In the case of linear alkyl chains in water near room temperature, a detailed study[13] of hydrophobic interaction has shown that

$$n^*\chi_{\mathrm{ew}}(T) = 2.102\, n_{\mathrm{CH_3}} + 0.884\, n_{\mathrm{CH_2}}/k_BT \text{ [kcal/mol]}. \tag{3.9}$$

In particular, for the octadecyl group for which $n_{\mathrm{CH_3}} = 1, n_{\mathrm{CH_2}} = 17$, we find

$$n^*\chi_{\mathrm{ew}}(T) = 2.102 + 0.884 \times 17/k_BT. \tag{3.10}$$

It is approximately 28.5 kcal/mol at room temperature. When we can neglect the length n^* of the end chain compared to n, the length of the main chain, the effective contact interaction parameter is given as

$$\tilde{\chi}(T) \equiv \chi_{\mathrm{mw}}(T) + \frac{\chi_1(T)}{n}, \tag{3.11}$$

where $\chi_1 \equiv 2n^*\chi_{\mathrm{ew}}$ is the effective interaction parameter between the end chain and water. The direct interaction between hydrophobic groups and water gives an $O(1/n)$ correction, and is stronger for shorter chains.

3.2.2 Free Energy of the Associating Polymer Solutions

The free energy of the model solution has three contributions:

$$\Delta F = \Delta F_{\rm mix} + \Delta F_{\rm hyd} + \Delta F_{\rm assoc}. \tag{3.12}$$

The free energy of mixing is given by

$$\beta \Delta F_{\rm mix} = N_{\rm fw} \ln \phi_{\rm fw} + \sum_{\mathbf{j},\mathbf{m}} N(\mathbf{j};\mathbf{m}) \ln \phi(\mathbf{j};\mathbf{m}) + \bar{\chi} \Omega \phi (1-\phi) \tag{3.13}$$

by applying the Flory-Huggins mixing entropy for polydisperse polymer solutions[16]. The free energy of hydration is given by

$$\beta F_{\rm hyd} = \sum_{\mathbf{j},\mathbf{m}} \left[\sum_{\mathbf{i}} \beta \Delta A(\mathbf{i}) m(\mathbf{i}) \right] N(\mathbf{j};\mathbf{m}) + \sum_{\mathbf{i}} \beta \Delta A(\mathbf{i}) N^G(\mathbf{i}), \tag{3.14}$$

where $\Delta A(\mathbf{i}) \equiv A(\mathbf{i}) - A(\mathbf{i_0})$ is the free energy of hydration to form a complex of type $\mathbf{i}$ starting from a bare polymer of reference conformation $\mathbf{i_0} \equiv \{0, 0, \cdots\}$. The free energy of hydrophobic association is given by[11, 12]

$$\beta F_{\rm assoc} = \sum_{\mathbf{j},m} \Delta(\mathbf{j};\mathbf{m}) N(\mathbf{j};\mathbf{m}) + \sum_{\mathbf{i}} \delta_{\mathbf{i}}(\phi) N^G(\mathbf{i}), \tag{3.15}$$

where $\Delta(\mathbf{j};\mathbf{m}) \equiv \beta[\mu^\circ(\mathbf{j};\mathbf{m}) - \sum_{\mathbf{i}} \mu^\circ(\mathbf{j}_0;\mathbf{m}_0(\mathbf{i}))m(\mathbf{i})]$ is the free energy change upon formation of a cluster of type $(\mathbf{j};\mathbf{m})$ from separated chains of type $\mathbf{i}$, and where $\delta_{\mathbf{i}}(\phi)$ is the dimensionless free energy gain when a polymer chain of type $\mathbf{i}$ is connected to the network. The terms that include the number $N^G(\mathbf{i})$ of polymer chains of the type $\mathbf{i}$ in the gel network need to be introduced only in the postgel regime.

We next derive the chemical potential for the free water and the associated complex by differentiating the free energy given above with respect to their number. We find

$$\beta \Delta \mu_{\rm fw} = 1 + \ln \phi_{\rm fw} - \nu^S + \bar{\chi} \phi^2 - d^G(\phi)\phi \tag{3.16}$$

for the free water, and for the associated complex of the type $(\mathbf{j};\mathbf{m})$

$$\begin{aligned} \frac{\beta \Delta \mu(\mathbf{j};\mathbf{m})}{\tilde{n}(\mathbf{m})} &= \frac{1}{\tilde{n}(\mathbf{m})} \left[1 + \Delta(\mathbf{j};\mathbf{m}) + \beta \sum_{\mathbf{i}} \Delta A(\mathbf{i}) m(\mathbf{i}) + \ln \phi(\mathbf{j};\mathbf{m}) \right] \\ &- \nu^S + \bar{\chi}[\phi^2 + r(\mathbf{m})(1-2\phi)] + d^G(\phi)[r(\mathbf{m}) - \phi], \end{aligned} \tag{3.17}$$

where

$$\nu^S \equiv \nu_{\rm fw} + \sum_{\mathbf{j},\mathbf{m}} \nu(\mathbf{j};\mathbf{m}) \tag{3.18}$$

is the total number of molecules and clusters that possess center of mass translational degree of freedom, and

$$r(\mathbf{m}) \equiv \frac{(n+2n^*)\sum_{\mathbf{i}} m(\mathbf{i})}{\sum_{\mathbf{i}} n(\mathbf{i})m(\mathbf{i})} \tag{3.19}$$

the volume of the polymer parts measured relative to the total volume of a cluster of type $\mathbf{m}$. In particular, $r(\mathbf{m}_0(\mathbf{i})) \simeq 1/[1+\theta(\mathbf{i})]$ for a hydrated but unassociated polymer chain. The terms in the chemical potentials including

$$d^G(\phi) \equiv \sum_{\mathbf{i}} \delta_{\mathbf{i}}'(\phi)\nu^G(\mathbf{i}) \tag{3.20}$$

are relevant only in the postgel regime. Finally, we have for a chain in the gel network

$$\beta\frac{\Delta\mu^G(\mathbf{i})}{n(\mathbf{i})} = \frac{\delta_{\mathbf{i}}(\phi)}{n(\mathbf{i})} - \nu^S + \bar{\chi}[\phi^2 + r(\mathbf{m}_0(\mathbf{i}))(1-2\phi)] + d^G(\phi)[r(\mathbf{m}_0(\mathbf{i})) - \phi]. \tag{3.21}$$

3.2.3 Equilibrium Conditions and Other Solution Properties

In order to study equilibrium solution properties, we first impose association-dissociation equilibrium conditions on the formation of hydrophobic clusters as well as on the hydration. For the cluster formation by end-chain association, the chemical potentials should satisfy the condition

$$\Delta\mu(\mathbf{j};\mathbf{m}) = \sum_{\mathbf{i}} \Delta\mu(\mathbf{j}_0;\mathbf{m}_0(\mathbf{i}))m(\mathbf{i}). \tag{3.22}$$

Similarly, for hydration we have the condition

$$\Delta\mu(\mathbf{j}_0;\mathbf{m}_0(\mathbf{i})) = \Delta\mu(\mathbf{j}_0;\mathbf{m}_0(\mathbf{i}_0)) + n\theta(\mathbf{i})\Delta\mu_{\rm fw}. \tag{3.23}$$

Finally, for a chain of arbitrary type $\mathbf{i}$, the equilibrium between the free state and the network-bound state gives the relation

$$\Delta\mu(\mathbf{j}_0;\mathbf{m}_0(\mathbf{i})) = \Delta\mu^G(\mathbf{i}). \tag{3.24}$$

The first association equilibrium (3.22) gives the volume fraction of clusters in the form

$$\phi(\mathbf{j};\mathbf{m}) = \exp\left[\sum_{\mathbf{i}} m(\mathbf{i}) - 1 - \Delta(\mathbf{j};\mathbf{m})\right]\prod_{\mathbf{i}} \phi(\mathbf{j}_0;\mathbf{m}_0(\mathbf{i}))^{m(\mathbf{i})}. \tag{3.25}$$

The hydration equilibrium (3.23) gives

$$\phi(\mathbf{j}_0; \mathbf{m}_0(\mathbf{i})) = \exp[n\theta(\mathbf{i}) - \beta\Delta A(\mathbf{i})]\phi(\mathbf{j}_0; \mathbf{m}_0(\mathbf{i}_0))\phi_{\mathrm{fw}}^{n\theta(\mathbf{i})} \tag{3.26}$$

for the volume fraction of the unassociated chains of the type **i**. This leads to the distribution function for the number density $\nu(\mathbf{j}_0; \mathbf{m}_0(\mathbf{i}))$ of the polymer chains as

$$\nu(\mathbf{j}_0; \mathbf{m}_0(\mathbf{i})) = K_{\mathrm{H}}(\mathbf{i})\nu(\mathbf{j}_0; \mathbf{m}_0(\mathbf{i}_0))\phi_{\mathrm{fw}}^{n\theta(\mathbf{i})}, \tag{3.27}$$

where K_{H} is the equilibrium constant for hydration and is expressed by the Eq.(2.8). Upon substitution of (3.26) into (3.25), we find

$$\nu(\mathbf{j}; \mathbf{m}) = K(\mathbf{j}; \mathbf{m}) \prod_{\mathbf{i}} \left[K_{\mathrm{H}}(\mathbf{i})\nu_\lambda \phi_{\mathrm{fw}}^{n\theta(\mathbf{i})}\right]^{m(\mathbf{i})}, \tag{3.28}$$

where we have introduced the symbol $\nu_\lambda \equiv \nu(\mathbf{j}_0; \mathbf{m}_0(\mathbf{i}_0))$ for the number density of unassociated bare polymers (called lambda chain) in the solution, and

$$K(\mathbf{j}; \mathbf{m}) \equiv \frac{n^{\sum m(\mathbf{i})}}{\tilde{n}(\mathbf{m})} \prod_{\mathbf{i}} [1 + \theta(\mathbf{i})]^{m(\mathbf{i})} \exp\left[\sum_{\mathbf{i}} m(\mathbf{i}) - 1 - \Delta(\mathbf{j}; \mathbf{m})\right] \tag{3.29}$$

is the equilibrium constant for the reversible formation of connected clusters of type $(\mathbf{j}; \mathbf{m})$.

In the postgel regime, we have an additional equilibrium condition (3.24) for the association of a free chain to the gel network. We are led to the result

$$\ln \phi(\mathbf{j}_0; \mathbf{m}_0(\mathbf{i})) = \delta_{\mathbf{i}}(\phi) - 1 - \beta\Delta A(\mathbf{i}). \tag{3.30}$$

The dimensionless binding free energy $\delta_{\mathbf{i}}$ is therefore related to the volume fraction of the unassociated polymers. After taking the difference between **i** and $\mathbf{i}_0$, and substituting the relation

$$\frac{\phi(\mathbf{j}_0; \mathbf{m}_0(\mathbf{i}))}{\phi(\mathbf{j}_0; \mathbf{m}_0(\mathbf{i}_0))} = \exp[n\theta(\mathbf{i}) - \beta\Delta A(\mathbf{i})]\phi_{\mathrm{fw}}^{n\theta(\mathbf{i})} \tag{3.31}$$

into the result, we find

$$\delta_{\mathbf{i}}(\phi) = 1 + n\theta(\mathbf{i}) + \ln \phi_\lambda + n\theta(\mathbf{i}) \ln \phi_{\mathrm{fw}}. \tag{3.32}$$

The free energy per lattice cell of the solution

$$f(\phi, T) \equiv \beta\frac{\Delta F}{\Omega} = \beta\Delta\mu_{\mathrm{fw}}(1 - \phi) + \beta\Delta\mu_\lambda\frac{\phi}{n} \tag{3.33}$$

can now be decomposed into the ordinary Flory-Huggins mixing free energy $f_{\rm FH}$ and the free energy $f_{\rm AW}$ of association-hydration as $f = f_{\rm FH} + f_{\rm AW}$, where

$$f_{\rm FH} \equiv (1-\phi)\ln(1-\phi) + \frac{\phi}{n}\ln\phi + \bar{\chi}\phi(1-\phi), \tag{3.34}$$

and

$$f_{\rm AW} \equiv \frac{\phi}{n}\ln\left(\frac{\phi_\lambda}{\phi}\right) + (1-\phi)\ln\left(\frac{\phi_{\rm fw}}{1-\phi}\right) + \Delta\nu \tag{3.35}$$

with

$$\Delta\nu \equiv 1 - \phi + \frac{\phi}{n} - \nu^S \tag{3.36}$$

being the loss in the degree of center of mass translational motion as a result of intermolecular association.

By using the mass conservation laws for polymer and water, let us find next the two fundamental volume fractions ϕ_λ and $\phi_{\rm fw}$ as functions of the volume fraction ϕ of the polymers fixed in the sample preparation. Because the number $\nu^S(\mathbf{i})$ of chains of hydration type $\mathbf{i}$ in the sol part is given by

$$\nu^S(\mathbf{i}) = \sum_{\mathbf{j},\mathbf{m}} m(\mathbf{i})\nu(\mathbf{j};\mathbf{m}), \tag{3.37}$$

and this number is given by $\nu^G(\mathbf{i})$ in the gel parts, we find

$$\phi = n\sum_{\mathbf{i}}\left[\nu^S(\mathbf{i}) + \nu^G(\mathbf{i})\right]. \tag{3.38}$$

Similarly, we have

$$1 - \phi = \phi_{\rm fw} + n\sum_{\mathbf{i}}\theta(\mathbf{i})\left[\nu^S(\mathbf{i}) + \nu^G(\mathbf{i})\right] \tag{3.39}$$

for water. The chemical potentials of these two components, lambda chains and free water, are then given by

$$\beta\Delta\mu_\lambda = \frac{1+\ln\phi_\lambda}{n} - \nu^S + \bar{\chi}(1-\phi)^2 + d^G(\phi)(1-\phi), \tag{3.40}$$

$$\beta\Delta\mu_{\rm fw} = 1 + \ln\phi_{\rm fw} - \nu^S + \bar{\chi}\phi^2 - d^G(\phi)\phi. \tag{3.41}$$

The osmotic pressure π can be found from the thermodynamic relation $\pi a^3 = -\Delta\mu_{\rm fw}$.

3.2.4 Spinodal Condition

The spinodal condition is derived by differentiating the osmotic pressure once more with respect to the concentration. It can also be found by taking the derivative of the difference $\Delta\mu_\lambda - \Delta\mu_{\rm fw}$ between the chemical potential of the lambda chains and that of the free water. We find

$$\frac{\kappa_\lambda(\phi)}{n\phi} + \frac{\kappa_{\rm fw}(\phi)}{1-\phi} - 2\bar{\chi} = 0, \tag{3.42}$$

for the spinodal, where the relations

$$\kappa_\lambda(\phi) \equiv \frac{\partial}{\partial \ln \phi}\left[1 + \left(\sum_{\mathbf{i}} n\nu^G(\mathbf{i})\right)\frac{\partial}{\partial\phi}\right]\ln\phi_\lambda, \tag{3.43}$$

$$\kappa_{\rm fw}(\phi) \equiv \frac{\partial}{\partial \ln \phi}\left[1 + \left(\sum_{\mathbf{i}} n\theta(\mathbf{i})\nu^G(\mathbf{i})\right)\frac{\partial}{\partial\phi}\right]\ln\phi_{\rm fw}, \tag{3.44}$$

describe the effects of end-chain association and of hydration, respectively. The volume fraction $\phi_{\rm fw}$ of free water is assumed to be a function of the total polymer volume fraction ϕ and it is substituted into these κ-functions.

3.2.5 Tree Statistics for End-Chain Association

To study gelation by end-chain association, we employ the conventional tree statistics for multiple association developed by Fukui-Yamabe[17], and also by TS. The multiplicity of a junction in the present situation is given by the aggregation number of the micelle. Under the tree assumption, there are two fundamental geometrical relations

$$\sum_{\mathbf{i}} m(\mathbf{i}) = \sum_{k\geq 1}(k-1)j_k + 1, \tag{3.45}$$

$$\sum_{k\geq 1} j_k = (f-1)\sum_{\mathbf{i}} m(\mathbf{i}) + 1 \tag{3.46}$$

for the number of polymer chains and junctions, where f is the functionality of the primary chain. ($f = 2$ for telechelic chains.)

The multiplicity of junctions is in principle determined by the equilibrium requirement for a given associative interaction. In the case of hydrophobic interaction, the chain length of

the hydrophobe, the strength of water-hydrophobe interaction, and the geometric form of the aggregate determine the association constant $\lambda(T)$ and the multiplicity of junctions.

Let p_k be the probability for a hydrophobe (end chain) to be associated into a micelle of multiplicity k, and let α be the extent of association, i.e., the probability for an arbitrarily chosen hydrophobe to be associated. Then, $p_1 = 1 - \alpha$ gives the probability for a hydrophobe to remain unassociated. In accordance with TS, we assume association-dissociation equilibrium condition for the hydrophobes forming micelles of multiplicity k, so that we have

$$p_k = K_k \psi^{k-1} p_1^k, \tag{3.47}$$

where K_k is the equilibrium constant, and $\psi \equiv f\phi/n_t$ is the total number density of hydrophobes. We may write, as in TS, the equilibrium constant in the form

$$K_k = [\lambda(T)]^{k-1} \gamma_k \tag{3.48}$$

by separating the binding free energy of a micelle into a bulk part $\Delta g_k^0 = (k-1)\Delta g_{\mathrm{AS}}$ and a surface part. The association constant $\lambda(T)$ comes from the bulk part through the relation

$$\lambda(T) = \exp(-\beta \Delta g_{\mathrm{AS}}). \tag{3.49}$$

Under these assumptions, the extent of association can be written as

$$p_1 = 1 - \alpha = \frac{1}{u(z)} \tag{3.50}$$

in terms of the junction function $u(z)$ defined by

$$u(z) \equiv \sum_{k \geq 1} \gamma_k z^{k-1}, \tag{3.51}$$

where the parameter $z \equiv \lambda(T)\psi p_1$ is the total number density of hydrophobes that remain unassociated. The number density of unassociated polymer chains of hydration type $\mathbf{i}$ is given by

$$\nu(\mathbf{j_0}; \mathbf{m_0(i)}) = p_1^f \nu^S(\mathbf{i}) \tag{3.52}$$

by definition. Upon substitution of Eqs.(3.50) and (3.51) for p_1, we find

$$\sum_{\mathbf{i}} \nu^S(\mathbf{i}) = u(z)^f \nu_\lambda \sum_{\mathbf{i}} K_{\mathrm{H}}(\mathbf{i}) \phi_{\mathrm{fw}}^{n\theta(\mathbf{i})} = u(z)^f \nu_\lambda g_0(\phi_{\mathrm{fw}}), \tag{3.53}$$

where the $g_0(y)$ is defined by (2.11).

The mass conservation law (3.38) for the polymer is then expressed as

$$\phi = u(z)^f \phi_\lambda g_0(\phi_{\mathrm{fw}}) + \phi^G. \tag{3.54}$$

Similarly, the conservation law (3.39) for water is transformd into

$$1 - \phi = \phi_{\mathrm{fw}} + u(z)^f \phi_\lambda g_1(\phi_{\mathrm{fw}}) + \phi_{\mathrm{bw}}^G, \tag{3.55}$$

where ϕ_{bw}^G is the volume fraction of the water molecules that are bound to the gel network. g_1 is defined by (2.12). In the pregel regime where there is no gel network, we may simply set $\phi^G = \phi_{\mathrm{bw}}^G = 0$. By solving Eq.(3.54) with respect to ϕ_λ, and substituting the result into Eq.(3.55), we find

$$1 - \phi = \phi_{\mathrm{fw}} + \phi G(\phi_{\mathrm{fw}}). \tag{3.56}$$

where $G(y)$ is defined by Eq.(2.14).

To summarize, we have the following set of equations

$$\lambda(T)\psi = zu(z), \tag{3.57}$$

$$\phi = u(z)^f \phi_\lambda g_0(\phi_{\mathrm{fw}}), \tag{3.58}$$

$$1 - \phi = \phi_{\mathrm{fw}} + \phi G(\phi_{\mathrm{fw}}). \tag{3.59}$$

These should be solved for the unknowns z, ϕ_λ and ϕ_{fw} as functions of the polymer volume fraction ϕ and the temperature T. If there is no hydration, we have $g_0(z) = g_1(z) = 1$. The equations reduce to those studied in TS for thermoreversible gelation with multiple association. If there is no hydrophobic association, on the contrary, we have $\lambda(T) = 0$ ($z = 0$) and $u(z) = 1$. The equations reduce to those studied in chapter 2. Hence, we here have unified theory.

The number density of molecules and clusters that possess translational degree of freedom reduces by the amount

$$\Delta\nu(\phi) = \phi G(\phi_{\rm fw}) + \frac{1}{\lambda}\int_0^z zu'(z)dz \tag{3.60}$$

due to association and hydration.

After taking the derivatives of the mass conservation laws, we find that the κ-functions in the spinodal condition (3.42) take the form

$$\kappa_\lambda(\phi) = 1 + f\left[\frac{\partial \ln z}{\partial \ln \phi} - 1\right], \tag{3.61}$$

$$\kappa_{\rm fw}(\phi) = \frac{[1 + G(\phi_{\rm fw})]^2(1-\phi)}{\phi_{\rm fw}[1 + \phi G'(\phi_{\rm fw})]}. \tag{3.62}$$

in the pregel regime.

The κ-function for a lambda chain can be described in terms of the average multiplicity of micellar junctions. For this, we first take the logarithmic derivative of Eq.(3.57), and find

$$\frac{\partial \ln z}{\partial \ln \phi} = \frac{1}{1 + zu'(z)/u(z)}. \tag{3.63}$$

The denominator gives the average multiplicity

$$\mu_{\rm w} \equiv \sum_{k\geq 1} kp_k = 1 + \frac{zu'(z)}{u(z)}, \tag{3.64}$$

and hence we have

$$\kappa_\lambda(\phi) = \frac{1 - (f-1)(\mu_{\rm w} - 1)}{\mu_{\rm w}}. \tag{3.65}$$

Because the gel point in multiple tree statistics is given by the divergence condition[11, 17] of the weight-average multiplicity

$$(f-1)(\mu_{\rm w} - 1) = 1, \tag{3.66}$$

we find that κ_λ vanishes at the gel point. This is due to the vanishing of the translational motion of the largest cluster when it grows to macroscopic dimensions.

At this stage, we realize that we can study monofunctional polymers ($f = 1$) and telechelic polymers ($f = 2$) (and also their mixtures) from the unified point of view described above.

Important examples of the monofunctional case are amphiphilic diblock copolymers made up of a hydrophilic block and a hydrophobic block, such as PEO-PPO diblock copolymer, PEO-PNIPAM diblock copolymer[18], etc. Another common example is that of the nonionic surfactants C_iO_j made up of a short alkyl chain and an ethyleneoxide chain[19, 20]. The LCST phase separation depends sensitively on the number of ethyleneoxide units[20]. The phase separation and mixing law of the end chains in the mixtures of telechelic PEO and semi telechelic hydrophobic PEO have been studied in detail in the literature[21]

As for the postgel regime, there have been several different theoretical methods to treat the reaction in the sol and gel parts. One such method assumes tree structures for the gel network as well as for the sol (Stockmayer's picture)[22], while the other theory permits cycle formation within the network (Flory's treatment)[23]. The difference between the two methods was examined later by Ziff and Stell[24] from the kinetic viewpoint, leading to a third method which bridges the two original methods. The specific form of the binding free energy $\delta_i(\phi)$ depends on which method one chooses to treat the postgel regime. In this study, we avoid this complex problem and employ the simplest treatment of Stockmayer[22].

3.2.6 Cooperative Hydration

We employ the same model of section 2.4 in chapter 2 as the model of hydration.

The κ_{fw} function in our spinodal condition (3.42) takes the form

$$\kappa_{fw}(q;\phi) = \frac{1+(1-\theta)QR}{1+(1-\theta)QR^2}(1+\theta)^2(1+R), \tag{3.67}$$

where

$$Q(q) \equiv \theta(q) - [1-\theta(q)]\bar{\zeta}_w(q) \tag{3.68}$$

with

$$\bar{\zeta}_w(q) \equiv \frac{V_1(q)}{V_0(q)} \tag{3.69}$$

being the weight average length of a sequence of bound water molecules.

q is a parameter defined by the equation

$$q = \mu(T)\frac{[1-\phi-\theta(q)\phi]e^{R(q,\phi)}}{1+\sigma q w_0(q)}. \tag{3.70}$$

The coverage θ by bound water molecules is given by

$$\theta(q) = \frac{\sigma q w_1(q)}{1+\sigma q w_{01}(q)}. \tag{3.71}$$

Here, the functions w are defined by

$$w_0(x) \equiv \sum_{\zeta=1}^{n} x^{\zeta-1}, \quad \text{and} \quad w_1(x) \equiv \sum_{\zeta=1}^{n} \zeta x^{\zeta-1} \tag{3.72}$$

and $w_{01}(x) \equiv w_0(x) + w_1(x)$. The average sequence length is given by $\bar{\zeta}_w = w_1(q)/w_0(q)$.

3.3 Numerical Results and Comparison with the Experiments

For numerical calculation of the phase diagrams, we set the necessary parameters in the following way. We first assume the conventional Schultz-Flory form[25] $\chi_{mw}(T) = 1/2 - \psi\tau$ for the χ-parameter between monomer units of the main chains and water, where $\tau \equiv 1 - \Theta_0/T$ is the reduced temperature deviation measured from the reference theta temperature Θ_0 satisfying the condition $\chi_{mw}(\Theta_0) = 1/2$, and ψ is a material parameter of order unity. For the interaction between the end chains and water, we have $\chi_1 \simeq 2 \times 28.5$ [kcal/mol]$/k_BT$. To have the sol/gel transition lines in the observed concentration range near 2%, we tried two fixed values of $\chi_1(T) = 3.0$ and 10.0. The association constant of the hydrophobic aggregation of the end-chains is then given by $\lambda(T) \equiv \exp(-\Delta g_{AS}/k_BT) = \lambda_0 \exp(\Delta\epsilon/k_BT) = \lambda_0 \exp[\gamma(1-\tau)]$ in terms of the reduced temperature, where $\gamma \equiv \Delta\epsilon/k_B\Theta_0$ is the association energy in a unit of thermal energy at the reference temperature. We varied the numerical values of λ_0 and γ to assess fits to the observed downward shift of the LCST.

Similarly, the association constant $\mu(T)$for hydration is referred at section 3 in chapter 2. It is expressed as $\mu(T) = \mu_0 \exp(|\epsilon_H + \Delta\epsilon_H|/k_BT) = \mu_0 \exp[\gamma_H(1-\tau)]$. Throughout the present numerical calculation, we fix ψ at $\psi = 1.0$, and change the amplitude λ_0, μ_0, the dimensionless

binding energy γ, γ_H, and the cooperative parameter σ. In particular, we monitor how changes in the value of σ affect the LCST line. The parameters related to the strength of hydration, such as μ_0, γ_H were taken from Ref.[26] for PEO, and chapter 2[27] for PNIPAM. These parameters led to good fits of the experimental data in the case of the two homopolymers.

3.3.1 Sol/Gel Transition Curve

Before we discuss about phase separation, let us discuss the sol/gel transition by the hydrophobic interaction at both ends of polymer. Figure 3.2 shows the sol/gel transition curve of telechelic polymer on the temperature-concentration plane. The sol/gel transition curve shifts higher concentration when the DPs increase. This is because the higher DP, the lower density of functional groups, thus interaction between hydrophobic groups is weaker.

3.3.2 Phase Diagrams

In Figure 3.3 we compare the phase diagrams of aqueous solutions of telechelic associating polymers undergoing random hydration (left figure with $\sigma = 1.0$) or cooperative hydration (right figure with $\sigma = 0.3$). The spinodal lines (solid lines) and the sol/gel transition lines (broken lines) are shown over a wide concentration range up to 25 wt%. The molecular weights of the polymers vary from $n = 50$ to 1000. The phase separation region (unstable region) shrinks, i.e., the LCST moves upwards and the UCST moves downwards with increasing molecular weight for solutions of polymer concentrations higher than 2 wt%. For the solutions of concentration lower than 2 wt%, however, the opposite trend is observed; the shorter the polymer chains, the higher the spinodal temperature. In such low concentration region, intermolecular end-chain association is so limited that the average molecular weight of the aggregates of shorter chains remains smaller than that of longer chains. Hence, the tendency for phase separation is larger for longer chains as in homopolymer solutions. With increasing concentration, however, association develops to an extent such that the average molecular weight of the associated shorter chains exceeds that of the longer chains. As a result, shorter chains show a more pronounced tendency for phase separation. Such an inversion of the molecular weight effect

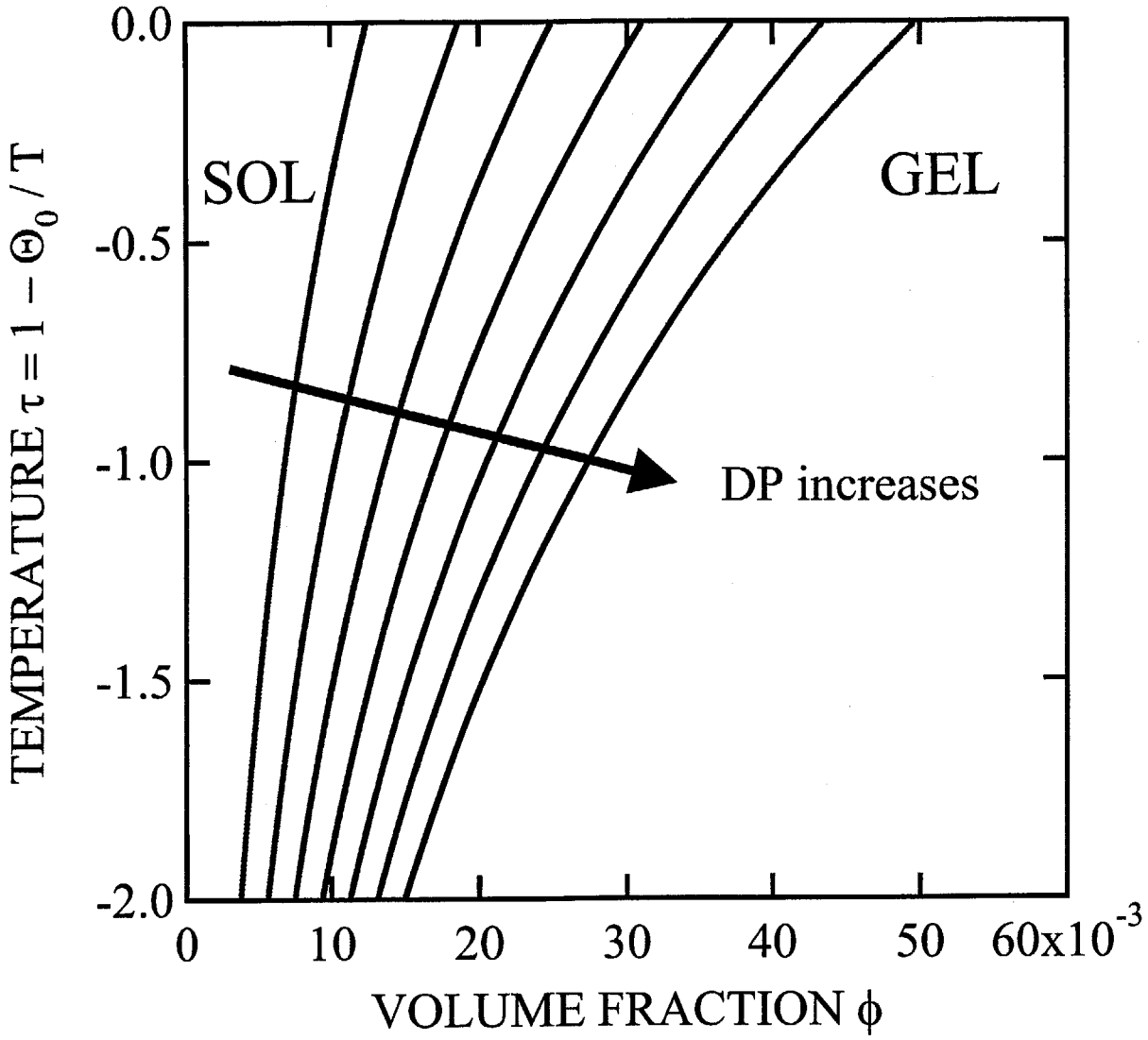

Figure 3.2: The sol/gel transition curve on the temperature-concentration plane. The DPs n is changed from curve to curve.

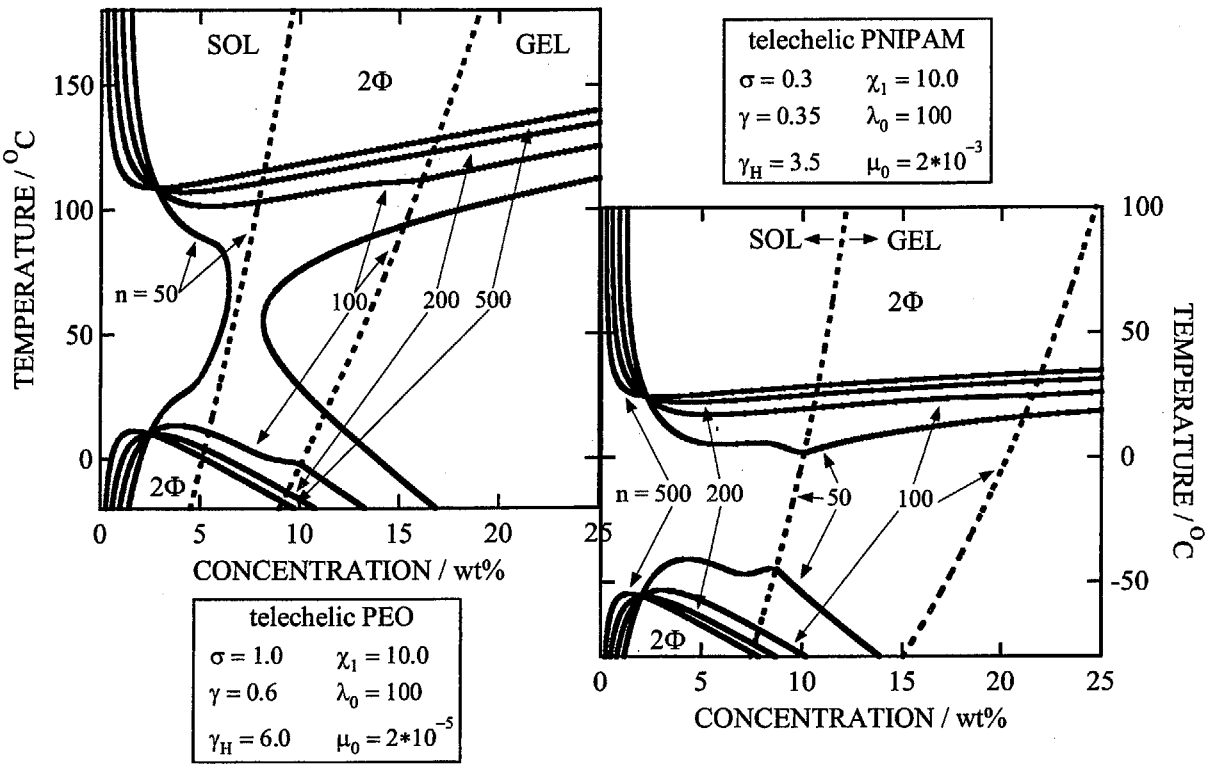

Figure 3.3: Comparison of the phase diagrams of telechelic associating polymers with random hydration (σ = 1.0, left) and with cooperative hydration (σ = 0.3, right) over a wide concentration range. Spinodal lines (solid lines) and sol/gel transition lines (broken lines) are shown. The various curves correspond to polymers of different molecular weights.

takes place at the point on the phase plane where LCST curves for different molecular weight cross each other.

In the case of solutions of polymers undergoing random hydration, the LCST and UCST merge for polymers having a molecular weight between $n = 50$ and 100, and the phase separation region turns into hourglass shape. In cooperative hydration, the LCST curves are very flat up to high polymer concentration with only weak molecular weight dependence.

In the left panel of Figure 3.4, we present the low concentration region, up to 5 wt%, of the phase diagram of the telechelic polymer/water system for which $\sigma = 1.0$ for polymers of four different molecular weights. Note that, as a result of end-chain association, the LCST lines shift downwards, and the UCST lines shift upwards, along the sol/gel transition line. The right panel of Figure 3.4 shows the same phase diagram region, but for a telechelic polymer/water system for which $\sigma = 0.3$. The spinodal curves for polymers of different molecular weight cross, and solutions of concentrations beyond the crossover point exhibit an inversion of the molecular-weight dependence of their LCST curves. Since the critical micelle concentration is reported to be extremely small ($c < 10^{-3}$wt%), the spinodal curves for solutions of telechelic polymer concentration lower than 1wt% are expected to be substantially modified due to the formation of flower micelles. Within our tree approximation, the LCST is identical to the crossing point of the spinodal curve and the sol/gel transition curve.

3.3.3 Comparison with the Experiments on the Telechelic PEO and the Telechelic PNIPAM

Experimental cloud points of telechelic PNIPAM with $M_w = 37,000$g/mol recorded for solutions of various concentrations are presented in Figure 3.5 together with the theoretical spinodal line[3, 4]. Because their spinodal lines are expected to lie above the binodal lines (cloud points), the comparison is only qualitative. The discrepancy between the binodal and spinodal becomes larger at lower concentrations, so that the fitting in the very dilute region should not be taken as a comparison.

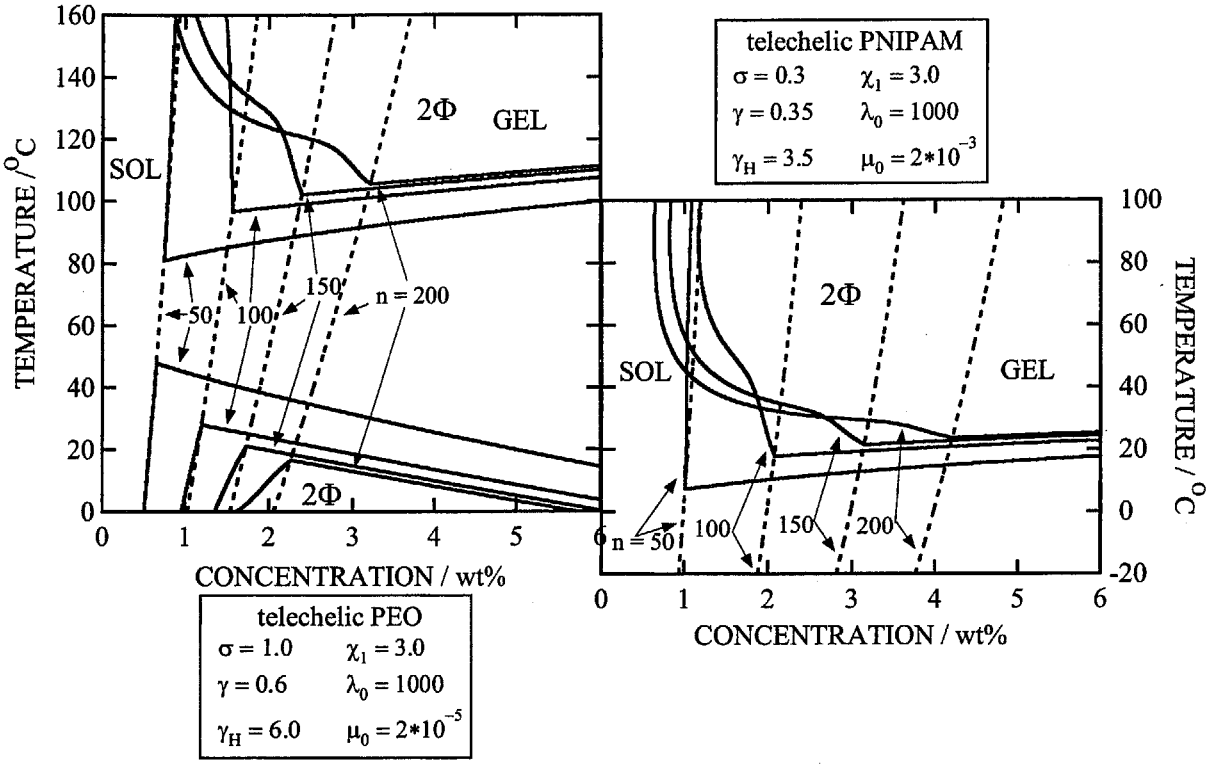

Figure 3.4: (Left) Detailed representation of the phase diagram in the low concentration regime for random hydration with σ = 1.0. The various curves correspond to polymers of different molecular weight. The LCST and UCST lines come closer to each other as the molecular weight of the polymers decreases due to end-chain association. The lines eventually merge, and the phase separation region turns into an hourglass shape. (Right) Same as the left figure, but with σ = 0.3. The LCST remains flat almost independent of the polymer molecular weight regardless of end-chain association.

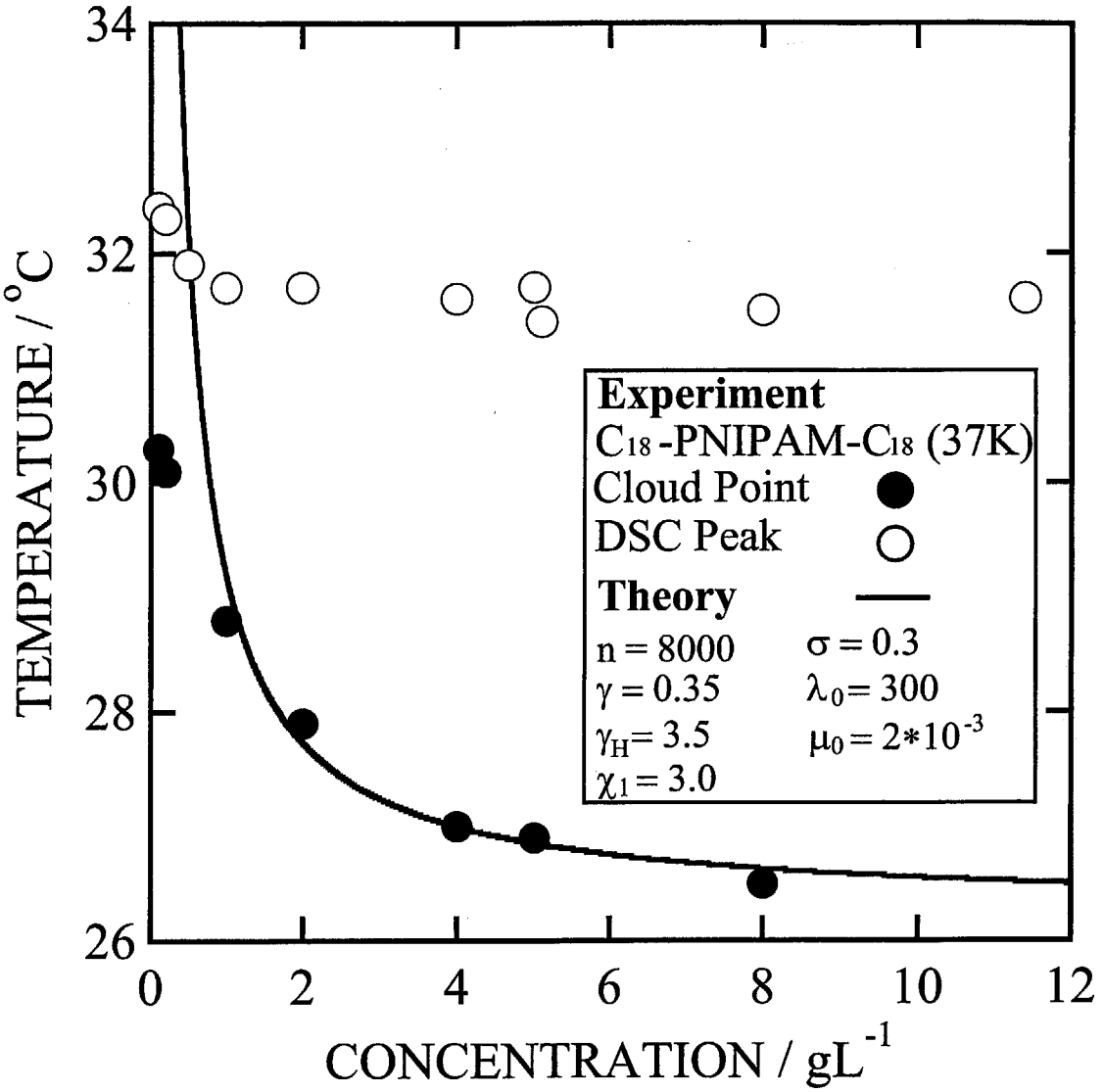

Figure 3.5: Experimental cloud points (black circles) and theoretical spinodal curve (solid line) of aqueous solutions of a telechelic PNIPAM (M_w = 37,000 g/mol). The coil-to-globule transition temperatures detected by DSC are also plotted (open circles). The cloud points (onset of phase separation) lie below the coil-to-globule transition temperature due to hydrophobic association. The latter temperature is almost independent of the polymer concentration because the transition is essentially related to the intramolecular conformation of each chain.

3.3.4 Molecular Weight Dependence of LCST and UCST

The LCST-UCST diagrams of aqueous solutions of PEO and telechelic PEO (σ = 1.0) are presented in Figure 3.6. For chains shorter than $n \simeq 200$, the average molecular weight of the aggregates becomes larger than that of the longer chains, and hence, the LCST decreases and the UCST increases. The two temperatures eventually merge into a DCP at a molecular weight indicated by a circle in the figure, and disappear for solutions of low DP polymers. This nonmonotonic variation of the critical points as a function of DP is a characteristic feature of associating polymer solutions. A phase separation of the hourglass type was observed in solutions of short telechelic PEO[2].

The LCST-UCST diagrams of aqueous solutions of PNIPAM and telechelic PNIPAM are presented in Figure 3.7 as a function of n^{-1}, the reciprocal DP, for the cooperative hydration of PNIPAM with σ = 0.3. We note that for chains shorter than $n \simeq 200$, the LCST decreases and the UCST follows the same trends as those of solutions of telechelic PEO, but the magnitude of the LCST downward shift and the UCST upward shift are lower for HM-PNIPAMs compared to HM-PEOs. Also, the variation of the LCST values with n^{-1} is much more gradual (upper dotted line) in the case of HM-PNIPAM. Thus, if the hydration of the polymer is cooperative, the LCST phase separation takes place within a very narrow temperature range lower than the collapse transition temperature, the latter being practically independent of the concentration because the collapse transition is caused by a sudden dehydration of each chain. A DCP cannot be seen in the diagrams calculated using the parameters shown in the right panel of Figure 3.4 .

3.4 Conclusions and Discussion

We have presented a theoretical framework to assess the interplay between hydration and hydrophobic association in the phase behavior of aqueous solutions of telechelic PEO and of telechelic PNIPAM. In solutions of low polymer concentration, polymers form self-loops, and loops associate into micelles of flower shape. With increasing polymer concentration, some loops turn into bridge chains connecting neighboring flowers, and the solution eventually turns

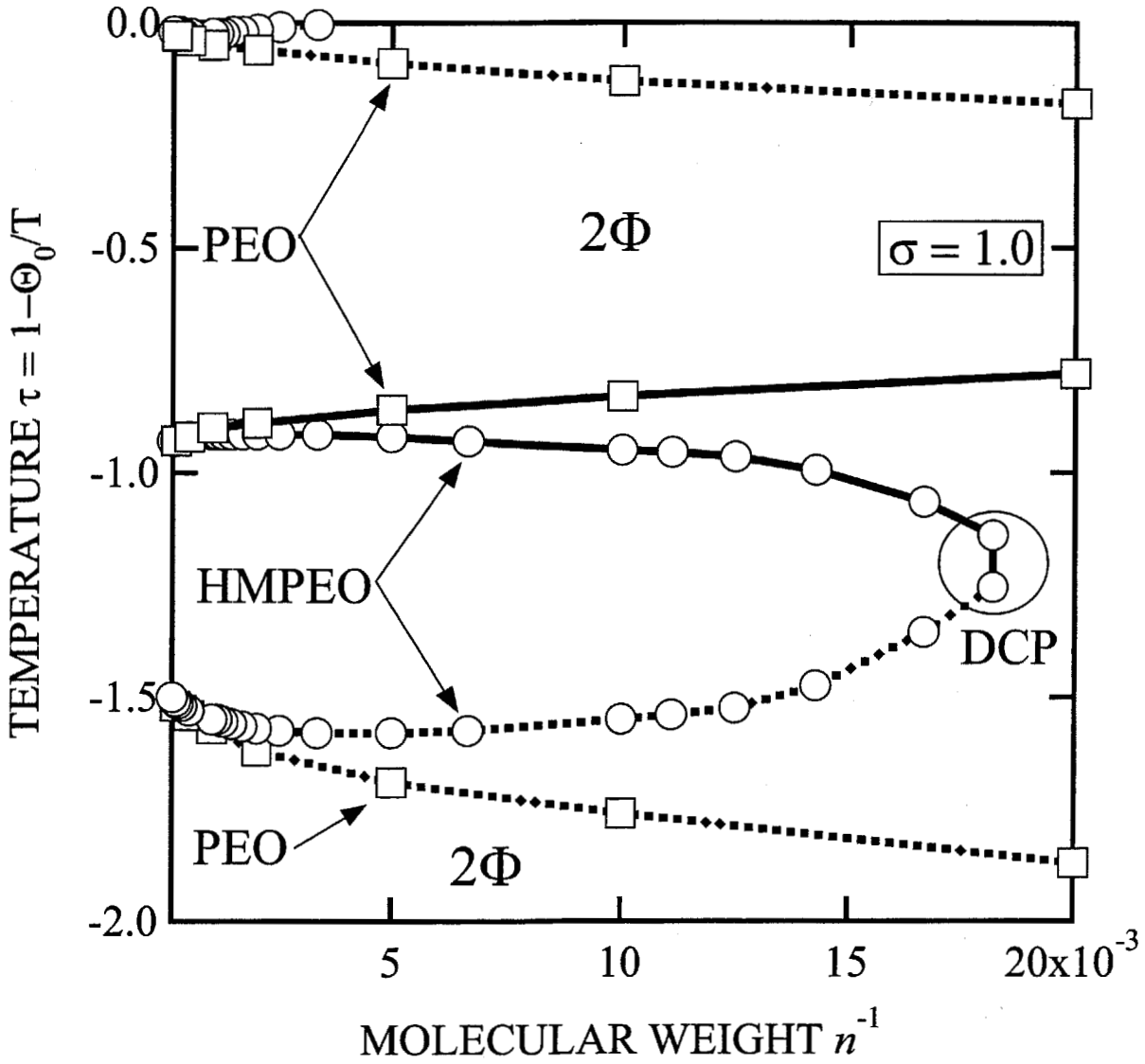

Figure 3.6: LCST-UCST diagram for aqueous solutions of PEO and telechelic PEO (HM-PEO) represented as a function of the reciprocal DP. Hydrophobic modification of the polymers triggers an inversion of the molecular weight dependence of the critical points; shorter chains tend to phase separate more easily than longer chains (dotted lines). DCP appears for solutions of polymers of low molecular weights.

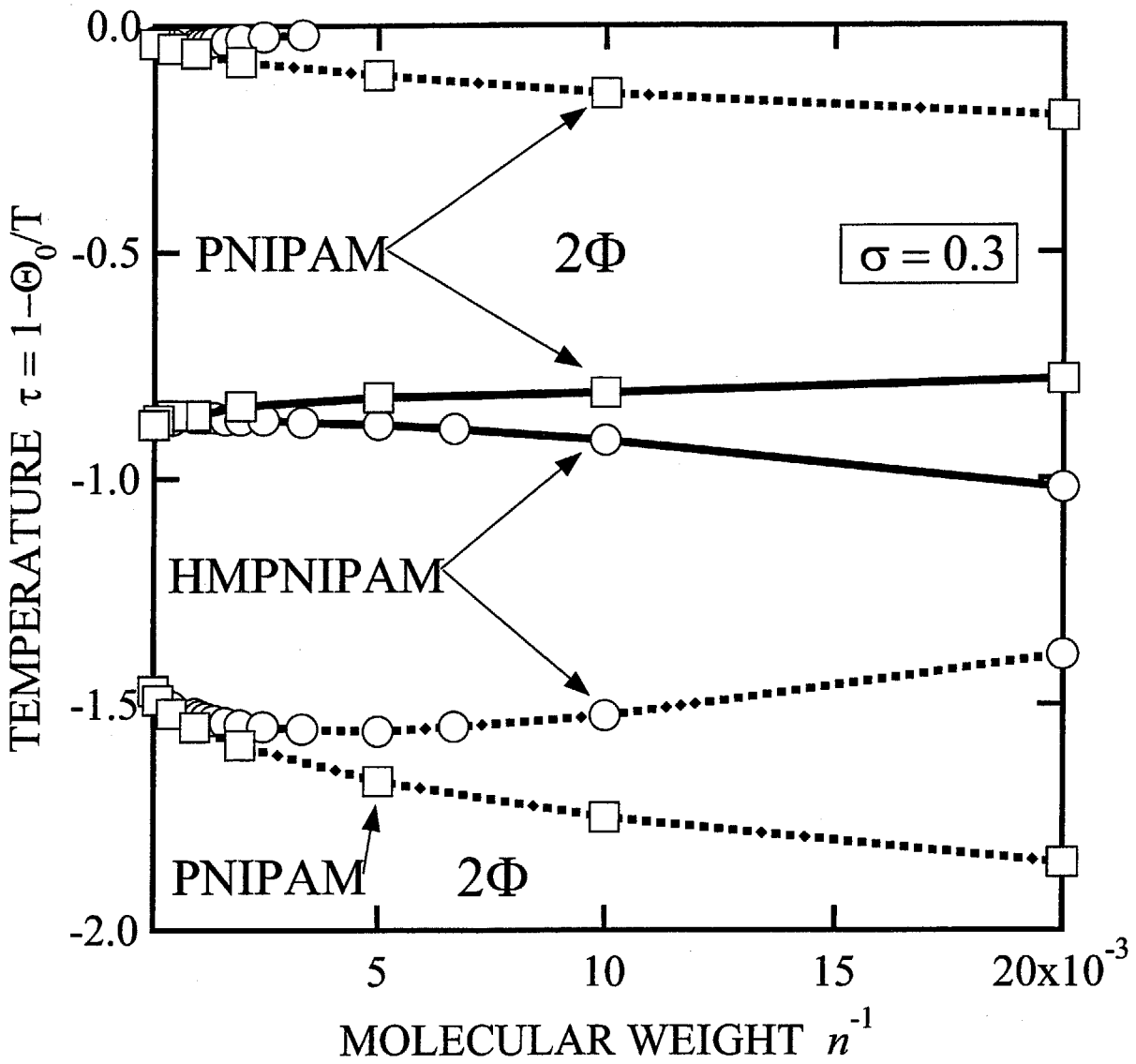

Figure 3.7: The LCST-UCST diagrams of aqueous solutions of PNIPAM and telechelic PNIPAM (σ = 0.3) are presented. LCST changes only gradually as a function of n^{-1}. DCP cannot be seen for solutions of polymers of molecular weights in the range of the graph.

into a connected network. In this study, we focused on network formation at and above the overlap concentration, and hence neglected the effect of flower micelles on the phase separation and gelation of a solution. This deficiency of the present theory may be remedied by introducing loops in equilibrium with open chains as species different from polymers, as was treated in our preceding paper[29].

In solutions of the telechelic polymers studied here, hydration (hydrogen bonding) and association (hydrophobic aggregation) are not strongly competitive, but almost decoupled from each other except for the chain parts near the end groups. In our model, we have neglected the interference between hydration and end-chain association. There is, however, experimental evidence that the dehydration starts at the core of the flower micelles, and this dehydration is followed by chain collapse, in the case of PNIPAM[30]. Upon heating a polymer solution above the phase transition temperature, end-chain association triggers dehydration and the networks start to shrink from the core of the micellar junctions. Such interference between (de)hydration and chain association remains an open problem with regard to aqueous polymer solutions.

Bibliography

[1] Alami, E.; Almgren, M.; Brown, W. *Macromolecules* **1996**, *29*, 5026.

[2] Alami, E.; Rawiso, M.; Isel, F.; Beinert, G.; Binana-Limbele, W.; François, J. *Adv. Chem. Series* (American Chemical Society, Washington DC, 1996), Vol. 248, p. 343.

[3] Kujawa, P.; Segui, F.; Shaban, S.; Diab, C.; Okada, Y.; Tanaka, F.; Winnik, F. M. *Macromolecules* **2006**, *39*, 341.

[4] Kujawa, P.; Tanaka, F.; Winnik, F. M. *Macromolecules* **2006**, *39*, 3048.

[5] Annable, T.; Buscall, R.; Ettelaie, R.; Whittlestone, D. *J. Rheol.* **1993**, *37*, 695.

[6] Annable, T.; Buscall, R.; Ettelaie, R.; Shepherd, P.; Whittlestone, D. *Langmuir* **1994**, *10*, 1060.

[7] Rao, B.; Uemura, Y.; Dyke, L.; Macdonald, P. M. *Macromolecules* **1995**, *28*, 531.

[8] Alami, E.; Almgren, M.; Brown, W.; Francois, J. *Macromolecules* **1996**, *29*, 2229.

[9] Xu, B.; Yekta, A.; Winnik, M. A. *Langmuir* **1997**, *13*, 6903.

[10] Tam, K. C.; Jenkins, R. D.; Winnik, M. A.; Bassett, D. R. *Macromolecules* **1998**. *31*, 4149.

[11] Tanaka, F.; Stockmayer, W. H. *Macromolecules* **1994**, *27*, 3943.

[12] Tanaka, F. in *Molecular Gels*, edited by Weiss, G.; Terech, P. (Kluwer Academic Pub., London, 2004), Chapter.1.

[13] Tanford, C. *The Hydrophobic Effects* (John Wiley & Sons, Inc., New York, 1980).

[14] Tanaka, F.; Ishida, M. *J. Chem. Soc. Faraday Trans.* **1995**, *91*, 2663.

[15] Flory, P. J. *J. Chem. Phys.* **1942**, *10*, 51.

[16] Flory, P. J. *Principles of Polymer Chemistry*, (Cornell University Press, Ithaca, NY 1953), Chapter.XII.

[17] Fukui, K.; Yamabe, T. *Bull. Chem. Soc. Japan* **1967**, *40*, 2052.

[18] Motokawa, R.; Morishita, K.; Koizumi, S.; Nakahira, T.; Annaka, M. *Macromolecules* **2005**, *38*, 5748.

[19] Degiorgio, V. Chapter.V in *Physics of Amphiphiles: Micelles, Vesicles and Microemulsions*, edited by Dergiogio, V.; Corti, M. (North-Holland Phys. Pub., Amsterdam 1985).

[20] Shirai, S.; Einaga, Y. *Polym. J.* **2005**, *37*, 913.

[21] Lafleche, F.; Durand, D.; Nicolai, T. *Macromolecules* **2003**, *36*, 1331.

[22] Stockmayer, W. H. *J. Chem. Phys.* **1943**, *11*, 45; **1944**, *12*, 125.

[23] Flory, P. J. *J. Am. Chem. Soc.* **1941**, *63*, 3091; 3096.

[24] Ziff, R. M.; Stell, G. *J. Chem. Phys.* **1980**, *73*, 3492.

[25] Schultz, A. R.; Flory, P. J. *J. Am. Chem. Soc.* **1952**, *74*, 4760.

[26] Matsuyama, A.; Tanaka, F. *Phys. Rev. Lett.* **1990**, *65*, 341.

[27] Okada, Y.; Tanaka, F. *Macromolecules* **2005**, *38*, 4465.

[28] Saeki, S.; Kuwahara, N.; Nakata, M.; Kaneko, M. *Polymer* **1976**, *17*, 685.

[29] Tanaka, F.; Koga, T. *Comp. Theor. Polym. Sci.* **2000**, *10*, 259.

[30] Motokawa, R.; Koizumi, S.; Winnik, F. M.; Tanaka F. in preparation (2007).

Chapter 4

Pressure-Controlled Thermoreversible Gelation and Phase Separation in Polycondensation Systems

4.1 Introduction

In polycondensation reactions, such as polyesterification from carboxylic acids and alcohols, polyamidation from carboxylic acids and amines, water molecules split during the reaction are immediately removed to prevent backward reaction and to reach high conversion with high molecular weight linear polymers[1, 2]. The condensation reaction is basically reversible, and hence, backward reaction takes place when there is excess water. Consider, for instance, a condensation reaction of the type

$$-\mathrm{A} + \mathrm{B}- \rightleftarrows -\mathrm{AB}- + \mathrm{H_2O}, \tag{4.1}$$

where A and B are functional groups. If we assume a complete reaction equilibrium, we have the condition

$$\frac{[-\mathrm{AB}-][\mathrm{H_2O}]}{[-\mathrm{A}](1-\alpha_A)[\mathrm{B}-](1-\alpha_B)} = \lambda(T), \tag{4.2}$$

where [-AB-] is the molar concentration of the A-B bonds, [H_2O] the molar concentration of water, α_A and α_B the conversion of A and B functional groups, and $\lambda(T)$ the equilibrium constant. For an equimolar reaction where [−A] = [B−] holds, we have the same conversion $\alpha_A = \alpha_B$, which we write as α. From the equilibrium condition (4.2), the conversion α is approximately given by $\alpha \simeq 1 - 1/\sqrt{h}$, and the average degree $< x >$ of polymerization, both number- and weight-average, is given by $< x > \simeq 1/\sqrt{h}$, where

$$h \equiv \frac{[\mathrm{H_2O}]}{\lambda(T)\psi} \tag{4.3}$$

is an important dimensionless parameter to measure the effect of water[1, 2]. Here, ψ is the molar concentration of the functional groups. Hence, the concentration of water must be small, or the reaction equilibrium constant must be large, in order to obtain long chains. The parameter h can be changed at will through experimental manipulation. Reaction is usually processed in an open vessel, and water vapour is removed by the flow of inert gasses.

In contrast, in polycondensation of multifunctional monomers, reaction easily reaches the gel point because the conversion at the gel point is roughly estimated to be

$$\alpha \simeq \frac{1}{f-1}, \tag{4.4}$$

where f is the functionality of the monomer, i.e., the number of functional groups carried by a monomer[1, 3, 4]. For example, it is 0.33 for tetrafunctional monomers. In such polycondensation reaction of multifunctional monomers, the water molecules should not necessarily be removed from the reaction bath, but instead, the system can be brought to the gel point by controlling the vapour pressure of water. In fact, in some extreme cases as seen in polycondensation of tetraethoxysilane (TEOS) in water and alcohol, gelation can be observed even in a closed vessel[5]. The purpose of the present paper is to theoretically study thermodynamics of multifunctional polycondensation, and to find the condition to bring the system to the gel point by changing the vapour pressure of water with or without phase separation. In the previous chapter, we theoretically studied phase separation and gelation in hydrophobically modified polymer solutions. We can regard hydrophobic aggregation as reversible reaction in the same way as polycondensation reaction. Thus, we can construct the suitable theory for pressure-controlled in polycondensation systems as we develop the previous theory.

In the conventional statistical theories of polycondensation[1, 3, 4], the effect of eliminant molecules have not been explicitly taken into consideration. The molecular weight distribution, its averages, and the condition for gelation were studied as functions of the conversion α under the condition of simple bond formation between functional groups. In a series of our preceding studies[6, 7, 8], we have studied thermoreversible gelation of reactive solutions with the temperature and concentration as controllable parameters. In polycondensing systems in open vessels, the concentration of solute molecules is, however, not a controllable parameter because of the evaporation of water molecules. The main purpose of the present study is to find the condition for the gel point in terms of the vapour pressure, and to study the physico chemical nature of sol/gel transition interfering with the phase separation.

The formation of cross-links with simultaneous solvent evaporation is the main processes that govern quality of a majority of protective organic coating films. Thereby, the amount of evaporated solvent and increase in the conversion of reactive groups are interdependent. Formation of polymer films by simultaneous cross-linking and solvent evaporation was studied by combining the polymer-solvent mixing free energy with the elastic free energy of the networks

due to swelling[9]. The motivation of the present study is basically the same as this literature, but we focus more on the interference between phase separation and thermoreversible gelation at reaction equilibrium, and attempt to find conditions for reaching the gel point without phase separation. We expect this problem to be important for the formation of homogeneous films. The kinetic processes with time-dependent reaction will be studied in the chapter 5.

4.2 Theoretical Fundamentals on Vapour Pressure of Reacting Solutions

4.2.1 Definitions of the Model Solutions

Consider polycondensing functional molecules A dissolved in water. Let f be the number of functional groups (for example -OH) on an A molecule, and let n be the volume of an A molecule measured relative to the molecular volume a^3 of the solvent molecule (H_2O). The present theory treats only the extreme limit of complete hydrolysis. We mix the number N of primary A molecules (referred to as A) with the number N_0 of the solvent molecules, both in the standard reference state. The initial volume of the solution is $V_0 = (N_0 + nN)a^3$. As reaction proceeds, the volume of the solution changes if the solvent is allowed to evaporate. Let V be the volume of the solution at equilibrium under the given temperature T. In what follows, we study our reactive solutions on the basis of the lattice theory of polymer solution[10, 11, 12], so that the volume is measured in terms of the total number Ω of the lattice cells. Hence we have $\Omega_0 = N_0 + nN$ for the initial volume, and $\Omega = V/a^3$ for the volume at final equilibrium. For reaction in a closed vessel, we have a condition $\Omega = \Omega_0$, but, for reaction under a controlled pressure, the solvent molecules move between the solution phase and the gas phase, and hence the volume of the solution changes (Figure 4.1). The volume fraction ϕ of the polymers in the pressure-controlled system changes as a function of the pressure and the temperature, and is different from that of the initial solution $\Phi \equiv nN/\Omega_0$.

We assume the reaction equilibrium

$$l\mathrm{A} \rightleftarrows \mathrm{A}_l + \Delta n_l \mathrm{H_2O} \tag{4.5}$$

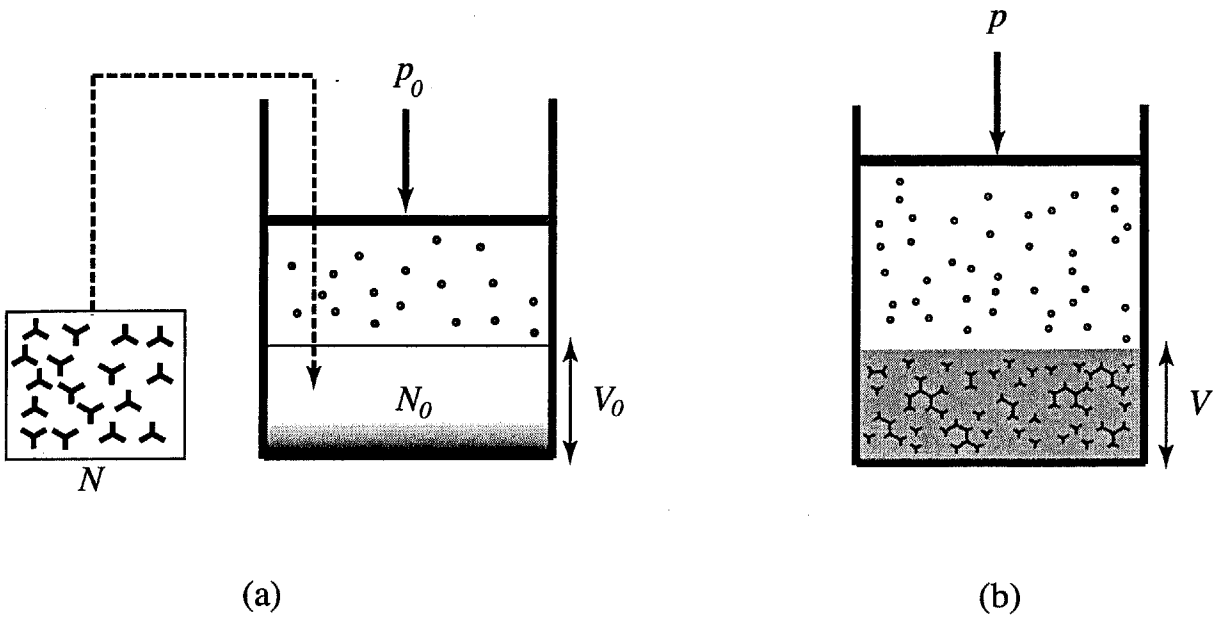

Figure 4.1: (a) Preparation of the polycondensing solution with the initial volume V_0 and vapour pressure p_0 immediately after mixing. (b) The final equilibrium state with a solution phase of volume V and a gas phase at pressure p.

for polycondensation of A molecules, where Δn_l is the number of water molecules produced when an l-mer is formed from l primary molecules by reaction. The volume n_l of the l-mer is then given by

$$n_l = ln - \Delta n_l. \tag{4.6}$$

The number Δn_l may change from the minimum $l-1$ (tree form) to $fl/2$ (complete reaction), but here we simply consider tree forms only and neglect internal loops. We then employ the classical theory of gelation[1, 3, 4]. The effect of cycle formation within polymers can be taken into consideration step by step by the usual spanning-tree procedure[13], but here we confine tree statistics. We then have $\Delta n_l = l - 1$ and

$$n_l = ln - (l-1). \tag{4.7}$$

As reaction proceeds, the average molecular weight of the connected clusters grows, and eventually becomes infinite at the gel point. Let N_l be the number of the l-mers, and let N^G be the number of A molecules in the gel network, if it exists, in the final equilibrium. The volume of the solution is then given by

$$\Omega = N_0 + \sum_{l\geq 1}(l-1)N_l + \Delta n^G N^G + \sum_{l\geq 1} n_l N_l + n^G N^G, \tag{4.8}$$

where n^G is the effective volume of an A molecule in the gel network and Δn^G is the number of cross-links on it. The first three terms gives the total number

$$N_{\mathrm{w}} \equiv N_0 + \sum_{l\geq 1}(l-1)N_l + \Delta n^G N^G \tag{4.9}$$

of water molecules in the solution. The volume fraction of the polymer in the sol part is given by

$$\phi^S = \sum_{l\geq 1} \frac{n_l N_l}{\Omega}, \tag{4.10}$$

and that in the gel part is

$$\phi^G = \frac{n^G N^G}{\Omega}. \tag{4.11}$$

The total volume fraction of the polymer is given by $\phi = \phi^S + \phi^G$, and the volume fraction of water is

$$\phi_w \equiv \frac{N_w}{\Omega} = 1 - \phi. \tag{4.12}$$

The gel fraction w is defined by the ratio ϕ^G/ϕ. The number of water molecules moved from the solution to the gas phase is given by

$$\Delta N_0 = \Omega_0(1 - \Phi) - \Omega(1 - \phi). \tag{4.13}$$

The total number of A molecules remains constant.

4.2.2 Free Energy of the Reactive Solutions

We apply lattice theory of associating solutions[6, 7, 8] to the present polycondensation system, and start from the free energy

$$\beta\Delta F = N_w \ln(1 - \phi) + \sum_{l\geq 1} N_l \ln \phi_l + \chi(T)\Omega\phi(1 - \phi) + \sum_{l\geq 1} \Delta_l N_l + \delta(\phi)N^G, \tag{4.14}$$

where $\beta \equiv 1/k_BT$, $\chi(T)$ is Flory's interaction parameter, and

$$\Delta_l \equiv \beta(\mu_l^\circ - l\mu_1^\circ) \tag{4.15}$$

is the free energy change in forming an l-mer from the number l of separated primary molecules in the standard reference state. The volume fraction of the l-mers is given by

$$\phi_l \equiv \frac{n_l N_l}{\Omega}, \tag{4.16}$$

and its number density is given by

$$\nu_l \equiv \frac{N_l}{\Omega}. \tag{4.17}$$

The last term in (4.14) describes the free energy of the gel network in the postgel regime, where $\delta(\phi)$ is the free energy change per A molecule when it is connected to the gel. This term is necessary as soon as the gel point is passed (in the postgel regime), because the macroscopic number of molecules (finite fraction w of the total number of molecules) belong to the gel part. However,

how the postgel free energy has to be approximated adequately is not a simple problem, and has been a matter of vivid controversies. Earlier papers by Veytsman[14], by Panayiotou *et al.*[15], neglected the gel fraction and studied the hydrogen-bonding gelling polymers without the last term in the free energy. Later, Semenov and Rubinstein[16] studied gelation of polyfunctional molecules without taking into consideration the free energy of the gel fraction, and came to the conclusion such that there is no singularity associated with physical quantities. Erukhimovich *et al.*[17] considered the effect of excessive loop formation, and reached the conclusion that the sol/gel transition is a first order phase transition. We showed[18] that there are several possible ways to treat the free energy from the gel fraction and, for theoretical study without ambiguity, we need at least one unknown parameter specifying the relative probability of occurrence of intra- and intermolecular reactions in the gel network.

Quite recently, we studied the thermodynamic nature of the sol/gel transition with strong analogy to Bose-Einstein condensation[19]. If we assume that the binding free energy $\delta(\phi)$ depends on the concentration, it corresponds to the smoothed potential model of a Bose-Einstein liquid studied in the literature[20]. If it is a constant, it corresponds to the energy spectrum with a constant gap[20]. We will, however, not discuss this subtle point here, and confine the present study to the pregel regime and the gel point. Hence, in what follows, we assume $N^G = 0$ and discard the last term in the free energy.

We can find the chemical potential for each component by taking derivatives of the free energy with respect to the corresponding number of molecules. We find

$$\beta\Delta\mu_{\rm w} = \phi + \ln(1-\phi) - \nu + \chi\phi^2 \tag{4.18}$$

for the water, and

$$\beta\Delta\mu_l = 1 + \Delta_l + \ln\phi_l - n_l(1-\phi+\nu) + \chi n_l(1-\phi)^2 \tag{4.19}$$

for an l-mer, where

$$\nu \equiv \sum_{l\geq 1} \nu_l \tag{4.20}$$

is the number of monomers and clusters that possess center of mass translational degree of freedom[6, 7, 8].

4.2.3 Equilibrium Polycondensation

In the final equilibrium state, the reaction (4.5) reaches a chemical equilibrium, so that we have the condition

$$l\Delta\mu_1 = \Delta\mu_l + (l-1)\Delta\mu_{\rm w}. \tag{4.21}$$

Substituting the chemical potentials into this equilibrium condition, we find that the volume fraction of the l-mers is given by

$$\phi_l = \frac{K_l(\phi){\phi_1}^l}{{\phi_{\rm w}}^{l-1}}, \tag{4.22}$$

where

$$K_l(\phi) \equiv \exp\left[-\Delta_l + (l-1)\chi(T)(1-2\phi)\right] \tag{4.23}$$

is the equilibrium constant of the reaction, and ϕ_1 is the volume fraction of the primary molecules that remain unreacted. In contrast to the simple association without production of the solvent molecules, the equilibrium constant depends on the concentration through the interaction term with χ-parameter. Such concentration dependence appears from the change in the number of monomer-solvent contacts during the reaction. It renormalizes the free energy of reaction Δ_l, and leads to many interesting new features. We can now rewrite (4.22) as

$$\eta(\phi)\phi_l = K_l^\circ[\eta(\phi)\phi_1]^l, \tag{4.24}$$

where $K_l^\circ \equiv \exp(-\Delta_l)$ is the "bare" (superscript $\circ$) equilibrium constant, and

$$\eta(\phi) \equiv \frac{e^{\chi(1-2\phi)}}{1-\phi} \tag{4.25}$$

is a new important factor due to water production (denominator) and to the change in the mixing enthalpy (numerator). We often encounter the same factor when we consider adsorption of molecules onto an attractive surface on which the nearest neighboring molecules interact with each other when adsorbed[21]. It leads to an Ising model type phase transition. Here, we have a new phase transition driven by the combination of water production and the contact interaction between water and the functional molecules. The conversion of functional groups becomes a

nonmonotonic function of the concentration below a certain critical temperature, so that we can find three possible values of the concentration for a given value of the conversion.

The part due to the change in the number of molecular contact can be seen as follows. Consider the mixing enthalpy

$$\frac{\Delta_{\rm mix}H}{k_BT} \equiv \chi(T)N_{\rm w}\sum_{l\geq 1}\frac{n_lN_l}{\Omega} \tag{4.26}$$

in the free energy (4.14), and find its change when an $(l+m)$-mer is produced as a result of the reaction between an l-mer and an m-mer. The number N_l and N_m both decrease by 1, and the number N_{l+m} increases by 1, resulting in the volume change $n_{l+m} - n_l - n_m$. The number $N_{\rm w}$ of water increases by 1. This gives the change $\Delta_{\rm mix}H/k_BT = -\chi(1-2\phi)$ per single bond, and hence the reaction free energy is renormalized from Δ_l to $\Delta_l - (l-1)\chi(1-2\phi)$ due to the contact interaction.

In order to find the bare part of the equilibrium constant, we now split the reaction free energy into three part : combinatorial, conformational and bonding term as $\Delta_l = \Delta_l^{\rm comb} + \Delta_l^{\rm conf} + \Delta_l^{\rm bond}$. To find the combinatorial part, all clusters are assumed to take tree forms. Cycle formation within a cluster is neglected. We consider the entropy change on combining l identical f-functional molecules to form a single Cayley tree. The classical tree statistics [4] gives $\Delta S_l^{\rm comb} = k_B \ln[f^l\omega_l]$, where

$$\omega_l \equiv \frac{(fl-l)!}{l!(fl-2l+2)!} \tag{4.27}$$

is Stockmayer's combinatorial factor. The free energy is given by $\Delta_l^{\rm comb} = -\Delta S_l^{\rm comb}/k_B$.

For the conformational free energy, we employ the lattice theoretical entropy of disorientation [12],

$$S_{\rm dis}(n) = k_B \ln\left[\frac{n\zeta(\zeta-1)^{n-2}}{\sigma e^{n-1}}\right] \tag{4.28}$$

for a chain consisting of n statistical units, where ζ is the lattice coordination number, σ the symmetry number of the chain. We then find

$$\Delta S_l^{\rm conf} = S_{\rm dis}(ln) - lS_{\rm dis}(n) = k_B \ln\left[\left\{\frac{\sigma(\zeta-1)^2}{\zeta en}\right\}^{l-1} l\right], \tag{4.29}$$

with most probably $\sigma = 1$.

Finally, the free energy of bonding is given by

$$\Delta_l^{\text{bond}} = (l-1)\beta\Delta f_0, \tag{4.30}$$

because there are $l-1$ bonds in a tree of l molecules, where Δf_0 is the free energy change on forming a bond.

Combining all results together, we find

$$K_l^\circ = \frac{fn_l}{n}\omega_l\left[\frac{f\lambda(T)}{n}\right]^{l-1} \tag{4.31}$$

for the equilibrium constant, where

$$\lambda(T) \equiv \frac{\sigma(\zeta-1)^2}{\zeta e}\exp(-\beta\Delta f_0) \tag{4.32}$$

is the association constant.

Collecting all results together, we find that the number ν_l of l-mers in a unit volume of the solution obeys the distribution law

$$\lambda(T)\eta(\phi)\nu_l = \omega_l x^l, \tag{4.33}$$

where

$$x \equiv \frac{f\lambda(T)}{n}\eta(\phi)\phi_1 \tag{4.34}$$

is the number of functional groups on the A molecules that remain unreacted, with the renormalization factor $\eta(\phi)$ arising from solvent production during reaction. The volume fraction of the l-mers is then given by

$$\phi_l = n_l\nu_l \tag{4.35}$$

with $n_l = ln - l + 1$.

4.2.4 Reactivity and the Average Molecular Weight

Let us first consider the pregel regime where there is no infinite cluster. We take the sum of (4.33) over all sizes l, and find that the total number ν of monomers and clusters is given by

$$\lambda(T)\eta(\phi)\nu = S_0(x). \tag{4.36}$$

Similarly, the total volume fraction ϕ of the clusters at final equilibrium is given by

$$\lambda(T)\eta(\phi)\phi = (n-1)S_1(x) + S_0(x). \tag{4.37}$$

These are written in terms of the moments of Stockmayer's distribution function defined by

$$S_k(x) \equiv \sum_{l=1}^{\infty} l^k \omega_l x^l \quad (k = 0, 1, 2 \cdots). \tag{4.38}$$

If we define a parameter α by the equation

$$x \equiv \alpha(1-\alpha)^{f-2}, \tag{4.39}$$

we can express these moments explicitly in terms of α. For instance,

$$S_0(x) = \frac{\alpha(1 - f\alpha/2)}{f(1-\alpha)^2}, \tag{4.40}$$

$$S_1(x) = \frac{\alpha}{f(1-\alpha)^2}, \tag{4.41}$$

$$S_2(x) = \frac{\alpha(1+\alpha)}{f[1-(f-1)\alpha](1-\alpha)^2}. \tag{4.42}$$

To see the physical meaning of α, let us calculate the probability for a randomly chosen functional group to be associated. Since an l-mer carries the total of fl groups, among which $2(l-1)$ are associated, the probability of association (extent of reaction) is given by

$$\frac{2[S_1(x) - S_0(x)]}{fS_1(x)} \tag{4.43}$$

by using the number distribution function (4.33). This agrees with α, and hence, we find that α in fact gives the conversion, or the extent of reaction.

By using α, Eq.(4.37) can be written as

$$\lambda(T)\eta(\phi)\phi = \frac{\alpha(1 - f_1\alpha/2)}{f_1(1-\alpha)^2}, \tag{4.44}$$

where $f_1 \equiv f/n$ is the number of functional groups per monomer unit on a primary molecule. This condition connects the conversion with the polymer volume fraction. Similarly, the number of clusters is given by

$$\nu = \frac{(1 - f\alpha/2)\phi}{n(1 - f_1\alpha/2)}. \tag{4.45}$$

Since an l-mer contains the number l of A molecules, the total number of A molecules in the solution is given by $\Omega \sum l\nu_l$, which must be equal to the number $N = \Phi\Omega_0/n$ of A molecules mixed when the solution is prepared. Hence we have

$$\frac{\Omega}{\Omega_0} = \left(n - 1 + \frac{n}{\bar{l}_n}\right)\frac{\Phi}{n\phi}, \tag{4.46}$$

where

$$\bar{l}_n \equiv \frac{\sum l\nu_l}{\sum \nu_l} \tag{4.47}$$

is the nominal number-average molecular weight of the clusters. Similarly, we define

$$\bar{l}_w \equiv \frac{\sum l^2\nu_l}{\sum l\nu_l}, \tag{4.48}$$

for the nominal weight average molecular weight. These are different from the true ones

$$< n_l >_n \equiv \frac{\sum n_l\nu_l}{\sum \nu_l}, \tag{4.49}$$

$$< n_l >_w \equiv \frac{\sum n_l^2\nu_l}{\sum n_l\nu_l}, \tag{4.50}$$

which are observed in the experiments. Since we have $\bar{l}_n = 1/(1 - f\alpha/2)$ and $\bar{l}_w = (1 + \alpha)/[1 - (f - 1)\alpha]$ in terms of the conversion, we find

$$\frac{\Omega}{\Omega_0} = \left(1 - \frac{f_1\alpha}{2}\right)\frac{\Phi}{\phi}. \tag{4.51}$$

The total number (4.13) of evaporated solvent molecules is given by

$$\frac{\Delta N_0}{N_0} = 1 - \frac{(1 - f_1\alpha/2)\Phi(1 - \phi)}{\phi(1 - \Phi)}. \tag{4.52}$$

For a closed system, we have a constant volume of the solution $\Omega = \Omega_0$, and hence

$$\phi = \left(1 - \frac{f_1\alpha}{2}\right)\Phi. \tag{4.53}$$

As reaction proceeds, the volume fraction of the A molecules monotonically decreases due to the solvent production.

4.2.5 Vapour Pressure, Gel Point, and Spinodal Condition

Let us study Eq.(4.44), which connects the conversion with the volume fraction. It is rewritten in the form

$$\lambda(T)e^{\chi(T)(1-2\phi)}\frac{f\phi}{n(1-f_1\alpha/2)} = \frac{\alpha(1-\phi)}{(1-\alpha)^2}. \tag{4.54}$$

This must be compared with conventional Eq.(4.2) under equilibrium condition found in the literature. Obviously, $[H_2O] = 1 - \phi$ is the number density of water molecules, but there are two differences. The first one is the volume change due to reaction. The effective volume of A molecules is reduced from n to $n(1 - f_1\alpha/2)$. The second one is the interaction between A molecules and water. It gives rise to the exponential factor, and renormalizes the reaction free energy from $\beta\Delta f_0$ to $\beta\Delta f_0 - \chi(T)(1 - 2\phi)$. The latter leads to a nonmonotonic conversion, or reverse reaction when molecular interaction $\chi(T)$ is strong compared with reaction Δf_0. By solving Eq.(4.54) with respect to the conversion, we find it explicitly as

$$\alpha = \frac{1 + c(\phi) - \sqrt{1 + (2 - f_1)c(\phi)}}{f_1 + c(\phi)}, \tag{4.55}$$

where

$$c(\phi) \equiv 2\lambda(T)f_1\eta(\phi)\phi \tag{4.56}$$

is the scaled concentration of the functional groups.

Let us next consider reactive solutions whose vapour pressure is controlled. The vapour pressure is given by the chemical potential of water in the solution under equilibrium condition. We then find

$$\ln\frac{p}{p_0} = \beta\Delta\mu_w. \tag{4.57}$$

From Eq.(4.18), together with ν of Eq.(4.45), we have

$$\ln \frac{p}{p_0} = \ln(1-\phi) + \frac{(1-1/n)\phi}{1-f_1\alpha/2} + \chi\phi^2. \tag{4.58}$$

In usual polymer solutions without reaction, the concentration ϕ is a controllable parameter. It is fixed at the preparatory stage. But for reactive solutions treated here, the concentration is not directly controllable. Instead, we take the vapour pressure as a controlling parameter, and try to find how to bring the solution to the gel point without phase separation. We therefore solve Eq.(4.58) with respect to the conversion and the concentration for a given pressure and temperature, with the help of the equilibrium condition (4.54).

The gel point can be found from the conventional condition for the weight-average molecular weight $< n_l >_w$ to become infinite. It is a percolation point where the largest cluster grows to macroscopic dimensions and spans the entire solution. Simple calculation gives $\alpha = 1/(f-1) \equiv \alpha^*$ as in the classical Flory-Stockmayer theory. We then find from Eq.(4.54) that the concentration ϕ^* of the solution at the gel point is given by the condition

$$\lambda(T) f_1 \eta(\phi^*)\phi^* = \frac{(f-1)[1-f_1/2(f-1)]}{(f-2)^2}. \tag{4.59}$$

This equation must be compared with our previous result $\lambda(T)f_1\phi^* = (f-1)/(f-2)^2$ for simple pairwise association of polyfunctional molecules without solvent production during reaction[6]. The effect of solvent evaporation appears mainly in the factor $\eta(\phi^*)$. Since it is a nonmonotonic function of ϕ^* when $\chi > 2$, the gel phase turns back to a sol phase as the concentration increases at low temperatures (reentrant sol phase).

To study phase separation, let us derive the spinodal condition in the pregel regime. From the chemical potential (4.18) for water, and (4.19) with $l = 1$ for a solute molecule, we find the difference between the two components is given by

$$\beta\left(\frac{\Delta\mu_1}{n} - \Delta\mu_w\right) = \frac{1}{n}\ln\phi_1 - \ln(1-\phi) + \chi(1-2\phi). \tag{4.60}$$

By taking the derivative, we find that the spinodal condition is given by

$$\frac{\kappa(\phi)}{n\phi} + \frac{1}{1-\phi} - 2\chi = 0, \tag{4.61}$$

where a new function κ is defined by

$$\kappa(\phi) \equiv \frac{\partial \ln \phi_1}{\partial \ln \phi}. \tag{4.62}$$

It is explicitly given by

$$\kappa(\phi) = 1 + \frac{f\phi}{1 + (1 - f_1)\alpha}\left[\frac{1}{1-\phi} - 2\chi\phi\right]\left[\frac{1 + (f-1)\alpha}{2n} - 1\right]. \tag{4.63}$$

In the phase diagrams presented below, we calculated the sol/gel transition lines and spinodal lines in the pregel regime. The spinodal lines lying inside the gel region (lines connecting the point A and B) on the phase plane are drawn by thin lines, or broken lines, only for guiding the reader's eyes.

4.3 Numerical Results

For numerical calculation of the temperature-pressure phase diagrams, we fix the necessary parameters in the following way. We first assume the conventional Schultz-Flory form $\chi(T) = 1/2 - \psi\tau$ for the χ-parameter[22], where $\tau \equiv 1 - \Theta/T$ is the reduced temperature deviation measured from the reference theta temperature Θ satisfying the condition $\chi(\Theta) = 1/2$, and ψ is a material parameter of order unity. At the temperature Θ, the second virial coefficient of a hypothetical Flory-Huggins solution without chemical reaction vanishes. The equilibrium constant is then expressed as $\lambda(T) = \lambda_0 \exp(|\epsilon|/k_B T) = \lambda_0 \exp[\gamma(1-\tau)]$, where λ_0 gives the entropy part of the standard reaction free energy, and $\gamma \equiv |\epsilon|/k_B\Theta$ the reaction enthalpy in the unit of the thermal energy at the reference temperature. The reference temperature Θ is not the true theta temperature where the second virial coefficient $A_2(T)$ of the osmotic pressure vanishes. The latter lies far below Θ, because A_2 is renormalized to

$$A_2(T) = \frac{1}{2} - \chi(T) - \frac{(1 - 1/n)\lambda(T) f_1^2}{2} \tag{4.64}$$

by reaction. Throughout the present numerical calculation, we fix at $\psi = 1.0$, $\lambda_0 = 1.0$, and changes the reaction enthalpy γ. For $\gamma > 1.0$, i.e., the reaction enthalpy is larger than the thermal

energy at the reference temperature, we call the solution "strongly reactive", and for $\gamma << 1.0$ we call "weakly reactive". The functionality and the molecular weight of the primary molecules are fixed at $f = 4$ and $n = 5$ as a typical example in attempting to apply the present study to pressure controlled sol/gel transition in polycondensation of silicic acid $Si(OH)_4$ in water.

4.3.1 Athermal Solutions

We first study the simplest case of athermal solutions where there is no solvent-solute interaction. We have $\chi \equiv 0$. The only parameter we change in the calculation is the association constant $\lambda(T)$, or the free energy Δf_0 of the reaction. Even in such an ideal case, we can use a certain appropriate reference temperature Θ, and measure the temperature by the dimensionless parameter $\tau \equiv 1 - \Theta/T$. The strength of the reaction is given by the dimensionless enthalpy γ.

Figure 4.2 shows the concentration of the solution as a function of the vapour pressure, although the latter is taken as the vertical axis. The temperature is changed from curve to curve in the range $-4.0 \leq \tau \leq 1.0$. The concentration monotonically increases with decreasing pressure, i.e., by removing solvent vapour, due to the promotion of forward reaction. The conversion is plotted against the polymer concentration in Figure 4.3. They are monotonically increasing functions of the concentration. We first find the equilibrium concentration for a given pressure from Figure 4.2, and then find the conversion under the pressure from Figure 4.3. The conversion is uniquely found for a given pressure. By cooling the solution, the equilibrium conversion becomes larger, so that the population of the reacted functional groups relative to the total number of groups increases. This temperature effect is opposite to the reaction rate, which is accelarated by heating. The latter is decided by the height of free energy barrier lying between reacted and unreacted state of a functional group. It is modified by pH, catalysts, etc. In contrast, the equilibrium conversion is larger when the reaction free energy $|\Delta f_0|$ is larger compared to the thermal energy $k_B T$. Study of reaction rate is beyond the scope of the present paper.

Figure 4.4 shows the sol/gel transition line on the temperature-pressure plane as a phase diagram for 3 different enthalpy of reaction. They are found by the condition (4.59). Under a

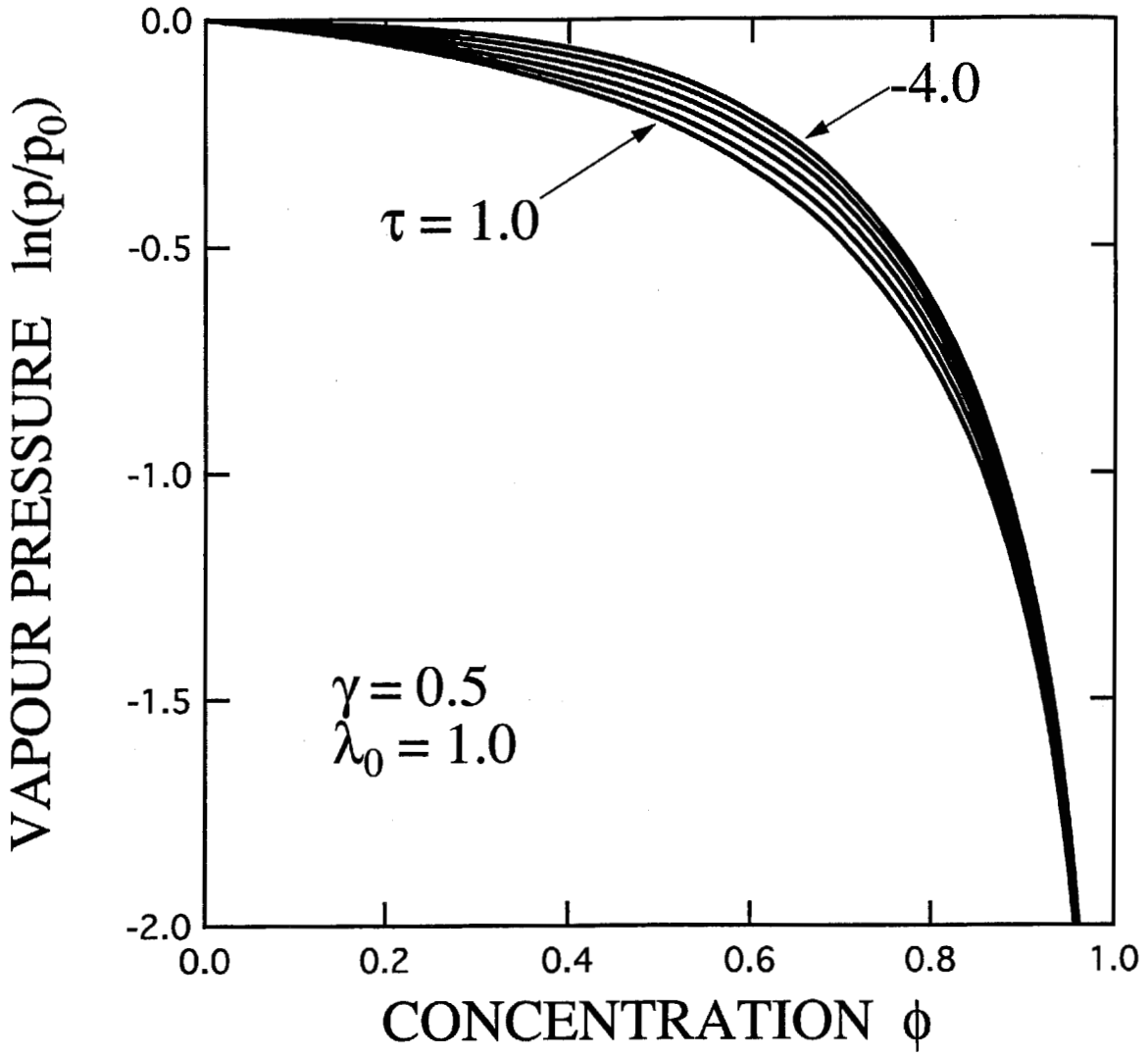

Figure 4.2: Polymer concentration (horizontal axis) plotted as a function of the vapour pressure (vertical axis) of the athermal solvent.

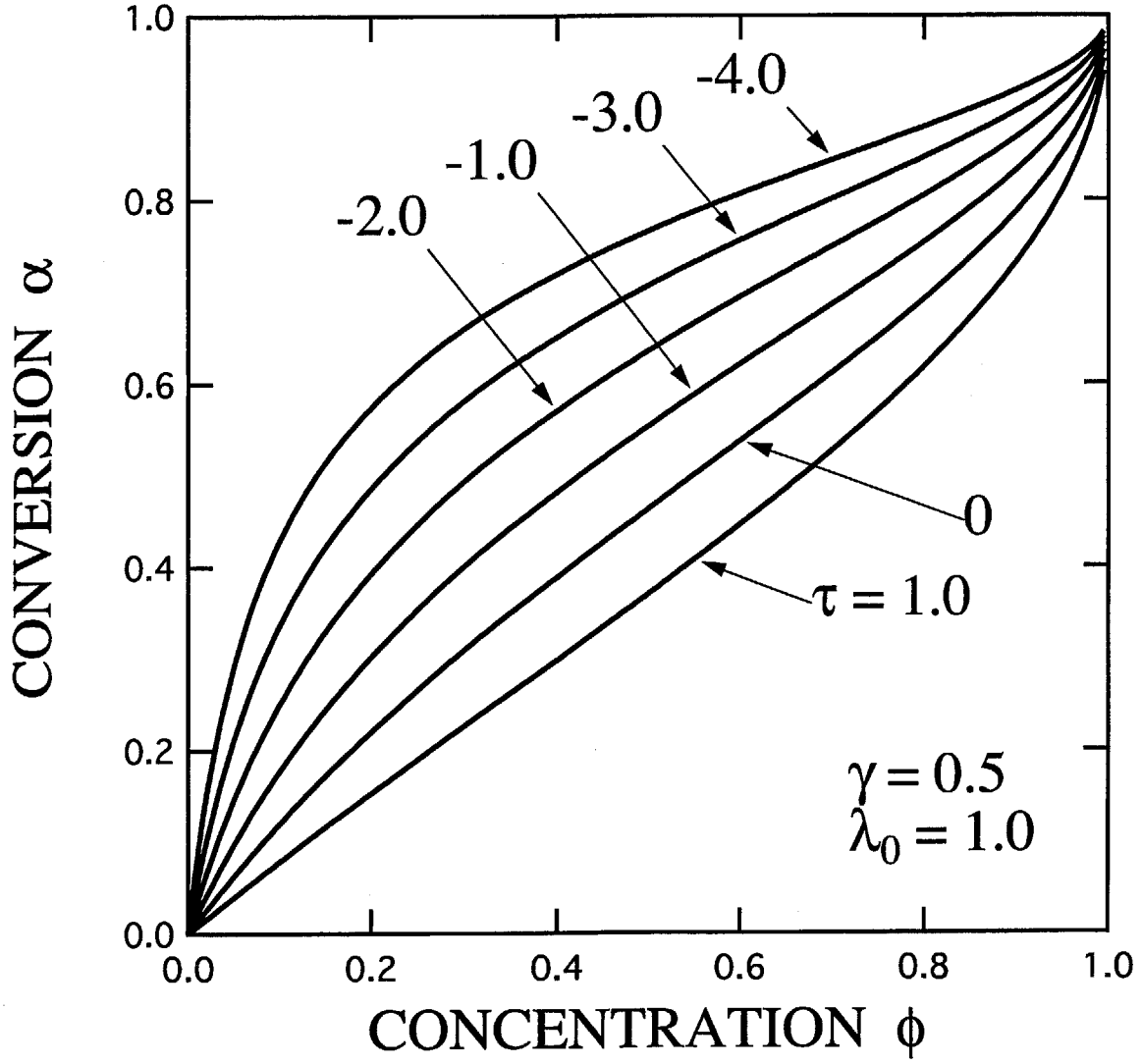

Figure 4.3: The conversion of the functional groups plotted against the polymer concentration produced in the solution.

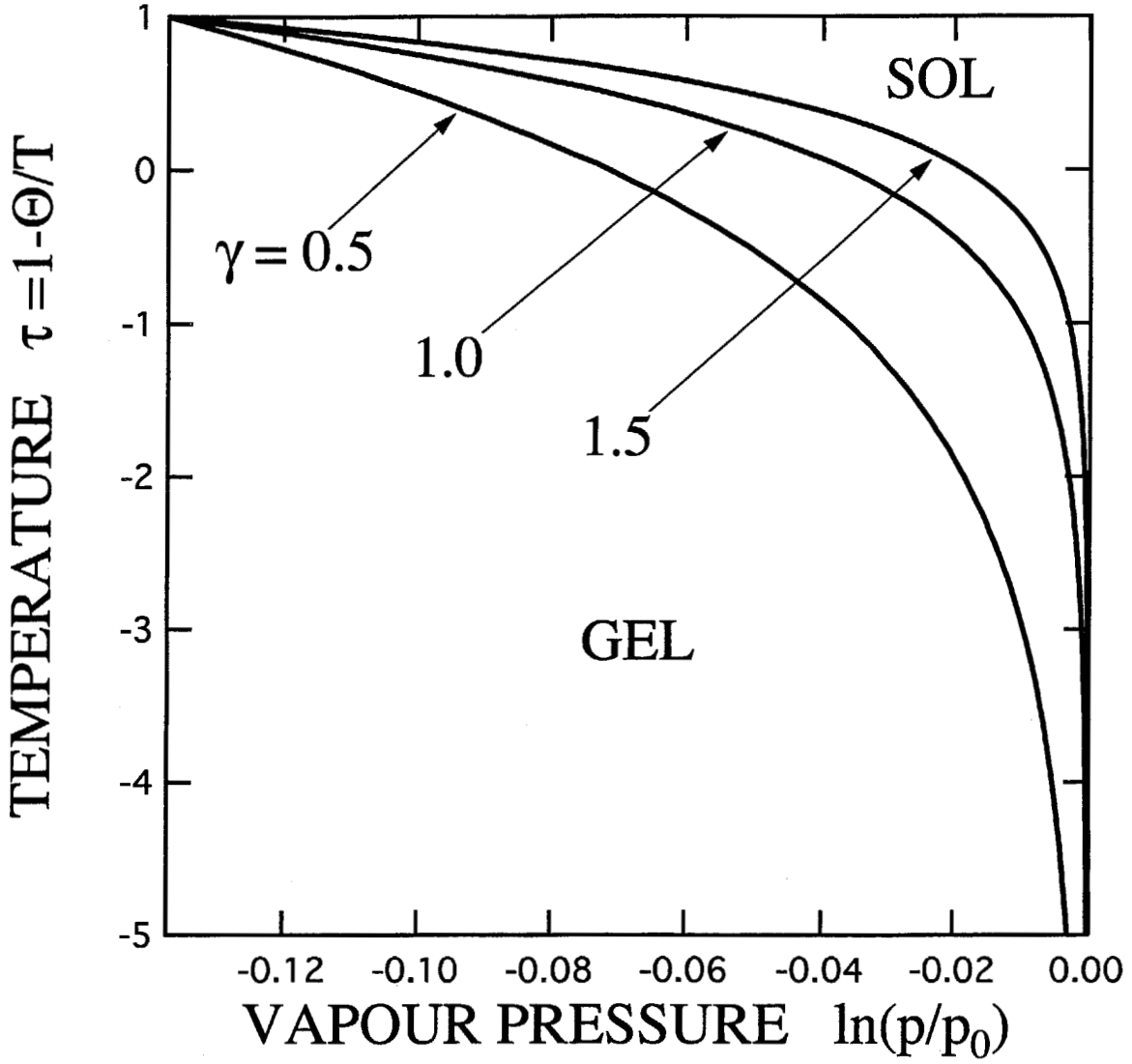

Figure 4.4: The sol/gel transition lines drawn on the temperature-pressure phase plane. The enthalpy of reaction is changed from curve to curve.

fixed temperature, for instance $\tau = -1.0$, we move from right to left as the pressure is lowered and hit the sol/gel line at $\ln(p/p_0) = -0.04$ for a weakly reactive solution $\gamma = 0.5$. Thus, we can control the sol/gel transition by pressure drop. We can also stay on the transition line by keeping the pressure. Figure 4.5 shows the same result shown on the temperature-concentration phase plane as usual. This phase diagram is, however, not useful because the concentration in the reaction bath cannot be controlled.

4.3.2 Strong Reaction

We next study solutions with finite interaction parameter. Reaction competes with phase separation. In the case of strong reaction where reaction enthalpy is larger than the mixing enthalpy, and hence the parameter γ is large, the conversion increases sharply with the concentration. Figure 4.6 shows the concentration as a function of the vapour pressure. At high temperatures it is a monotonic function. On cooling, however, the tendency for phase separation becomes stronger. As a result, the vapour pressure becomes larger than that of the pure solvent, and shows a maximum at a certain concentration as in the usual phase-separating polymer solutions[12], for instance, in the case of $\gamma = 1.0$ in Figure 4.6. Given a pressure higher than that of the pure solvent at low temperatures, there are two concentrations giving the same pressure. If the pressure is gradually increased in the experiment by keeping equilibrium condition, the lower concentration is realized. It easily reaches $\simeq 0.5$ under $\ln(p/p_0) \simeq 1.0$ for $\tau = -2.0$. Figure 4.7 shows the corresponding conversion as a function of the concentration. It reaches as high as 0.8 as is shown. There is a reverse reaction in the region $\phi = 0.6 \sim 0.8$ at low temperatures, but it is not strong.

In Figure 4.8 we show for $\gamma = 1.0$ the vapour pressure surface (thin grey lines), as a function of the reduced temperature τ and the polymer concentration, on which the sol/gel transition line (thin black line) and the spinodal line (thick black line) are drawn. (The broken line indicates the spinodal line in the postgel regime for guiding the eyes of readers.) The surface is called Bakhuis-Rooseboom space diagram in the literature[23]. We can obtain the pressure-

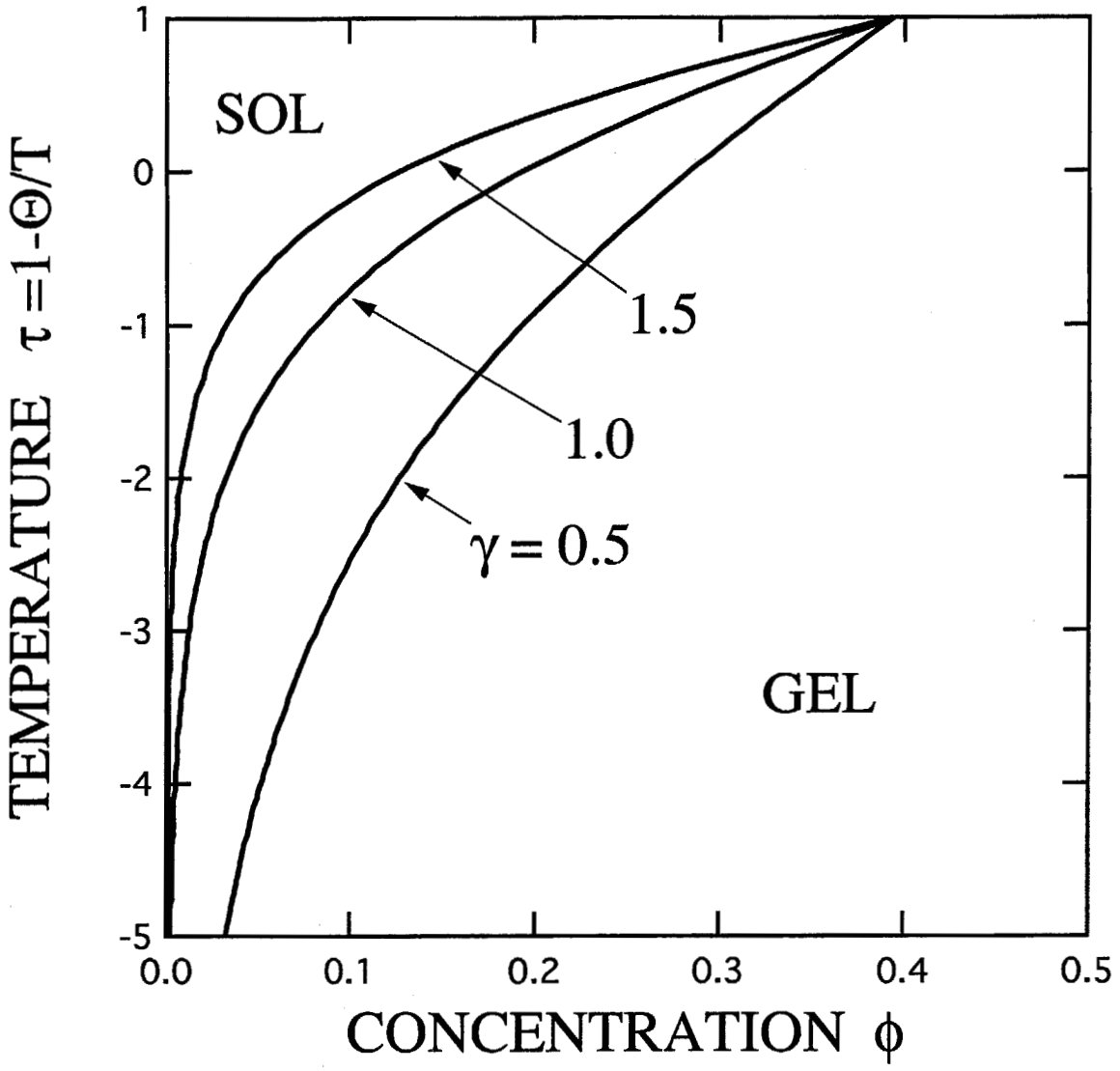

Figure 4.5: The sol/gel transition lines drawn on the usual temperature-concentration plane. The reaction enthalpy is changed from curve to curve.

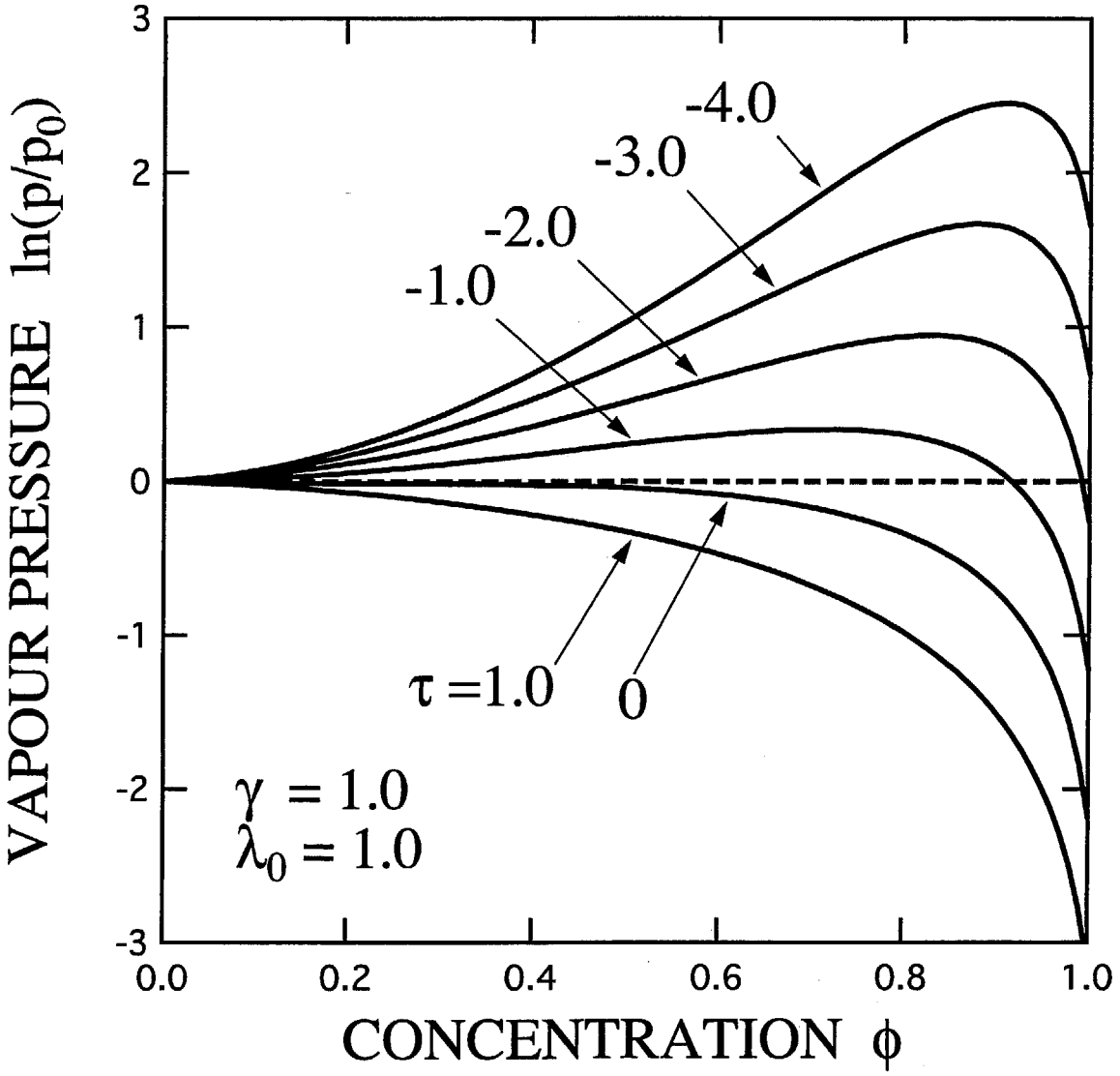

Figure 4.6: Polymer concentration (horizontal axis) plotted as a function of the vapour pressure (vertical axis) of the solvent for strong reaction of $\gamma = 1.0$.

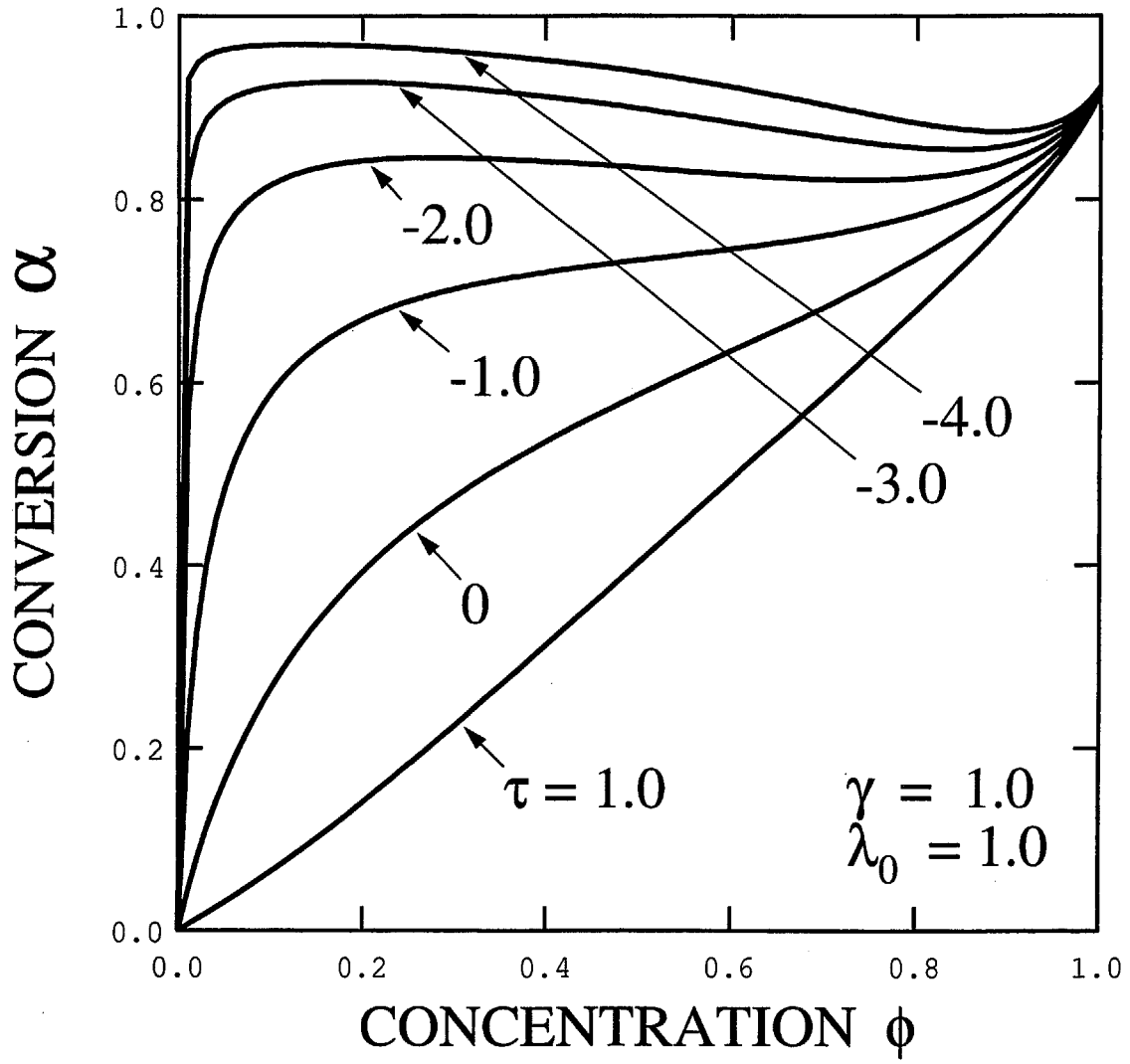

Figure 4.7: The conversion of the functional groups plotted against the polymer concentration produced in the solution. At low temperatures, they are not monotonically increasing functions of the concentration due to the backward reaction.

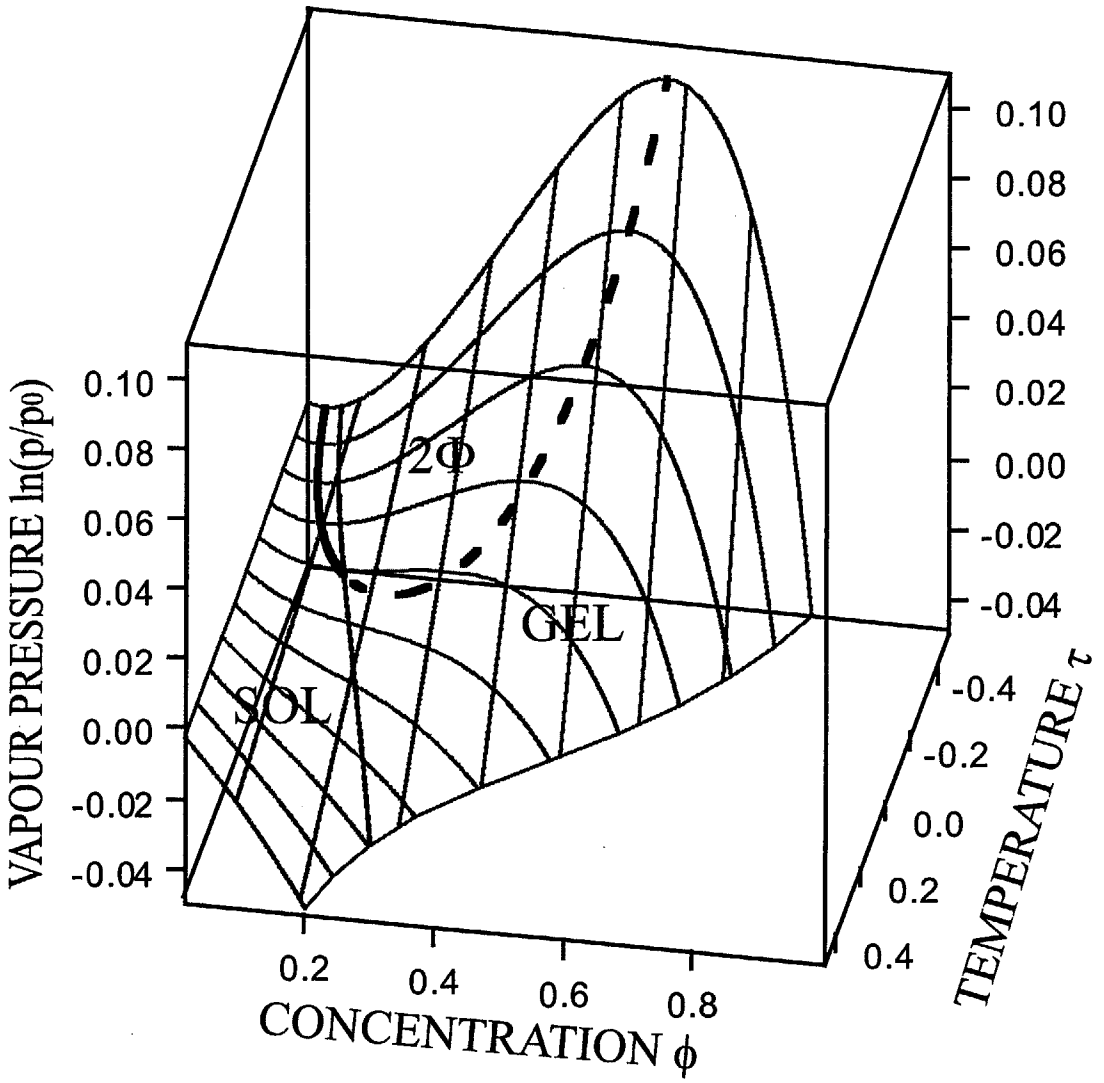

Figure 4.8: Three-dimensional diagram in the temperature-concentration-pressure space (Bakhuis-Rooseboom diagram) with the sol/gel transition curve (thin black line) and the spinodal lines (thick black line) for strong reaction of $\gamma = 1.0$. The vapour pressure of the solution is shown as the surface indicated by the grey thin lines. The broken line for the spinodal inside the gel region is just to guide reader's eyes. The area on the surface indicated by 2Φ is the unstable region.

concentration phase diagram and the temperature-concentration phase diagram by simply projecting this surface onto the corresponding plane.

The phase diagram projected onto the temperature-pressure plane is shown for three values of γ in Figure 4.9. Solid lines show the sol/gel transition lines. The broken lines show the stability limit (spinodal line) inside which the solution becomes thermodynamically unstable. The part connecting the point A and B lying inside the postgel regime is shown only for guiding the eyes of readers. Its precise location depends on how the reaction inside the gel network is treated, but nevertheless the overall structure of the spinodal boundary remains the same irrespective of the treatment. The reaction enthalpy γ is changed from curve to curve within the strong reaction regime. It has a spike at a certain temperature, like a "spinning" tool as etymological origin of spinodal line. If the solvent water is evaporated on a substrate plane below such a spike point temperature, the solution is phase separated, so that homogeneous coating of the substrate is impossible. In Figure 4.10, the phase diagram is mapped onto the usual temperature-concentration plane. The sol/gel transition line crosses the two-phase region indicated by the symbol 2Φ. Gelation is interfered with phase separation. The phase behavior of coexisting thermoreversible gelation and phase separation has been explored in the series of study[6, 7, 8]. For the present reactive solutions, however, the concentration is not an independent variable, but is decided by the vapour pressure.

4.3.3 Weak Reaction

Figure 4.11 ~ 4.15 show the results for weak reaction. The reaction enthalpy γ relative to the thermal energy is assumed to take the value within the range $\gamma = 0.05 \sim 0.15$. In such weak reaction, the van der Waals type contact interaction factor $-\chi(1 - 2\phi)$ due to the change in the number of monomer-water contact is more important than the reaction enthalpy, in particular, at low temperatures. By giving pressure, the condensation reaction is easily pushed back to reduce the number of contact. The tendency to phase separation becomes stronger with lowering the temperature. As a result, a very interesting reentrant sol phase appears at high pressure, which interferes with the phase separation.

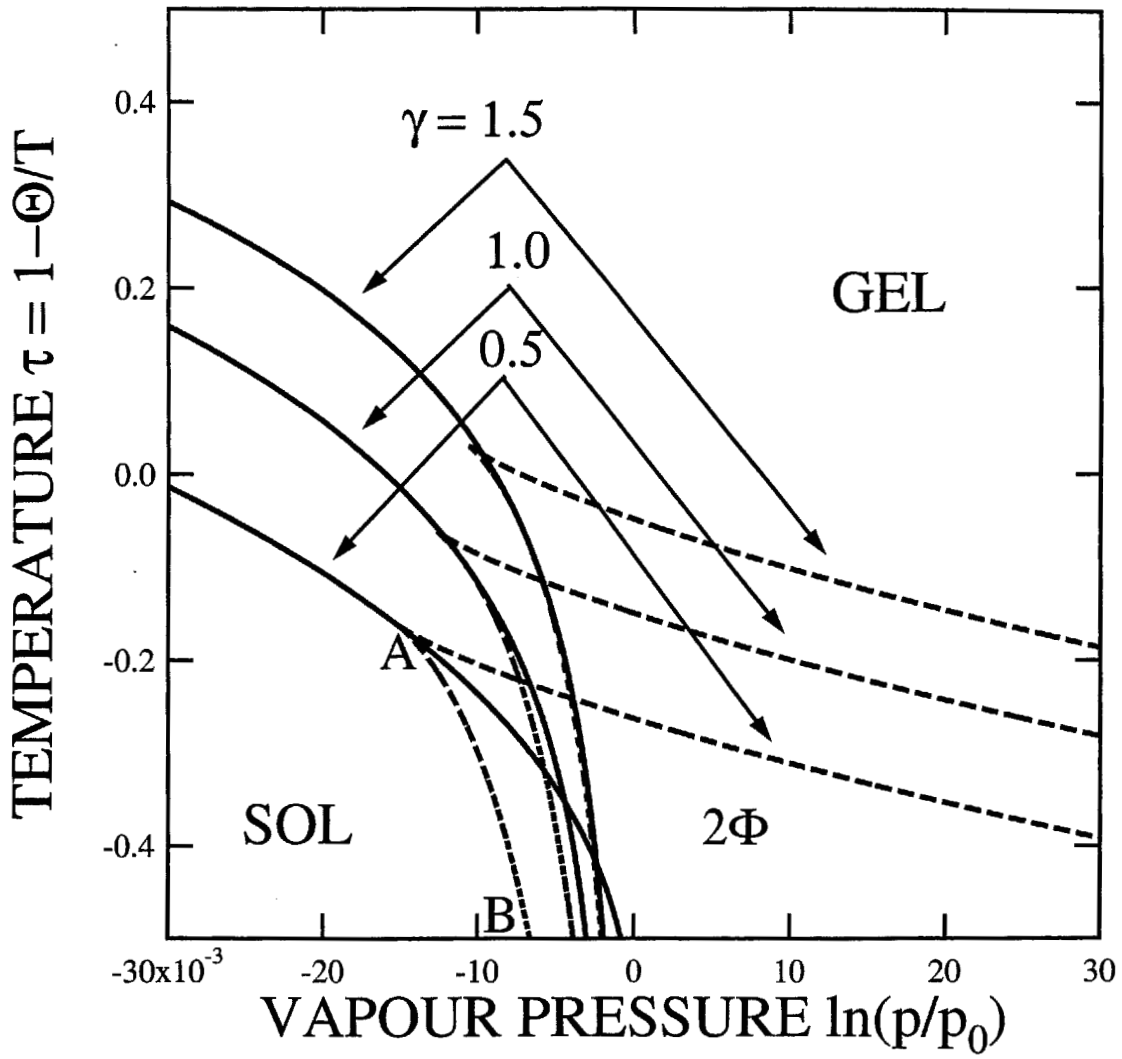

Figure 4.9: The sol/gel transition lines (solid lines) together with the spinodal lines (broken lines) drawn on the temperature-pressure phase plane in the case of strong reaction. The enthalpy of reaction is changed from curve to curve. The two curves (sol/gel and spinodal) cross each other at the spike point of the spinodal region indicated by 2Φ. The reaction enthalpy is changed from curve to curve.

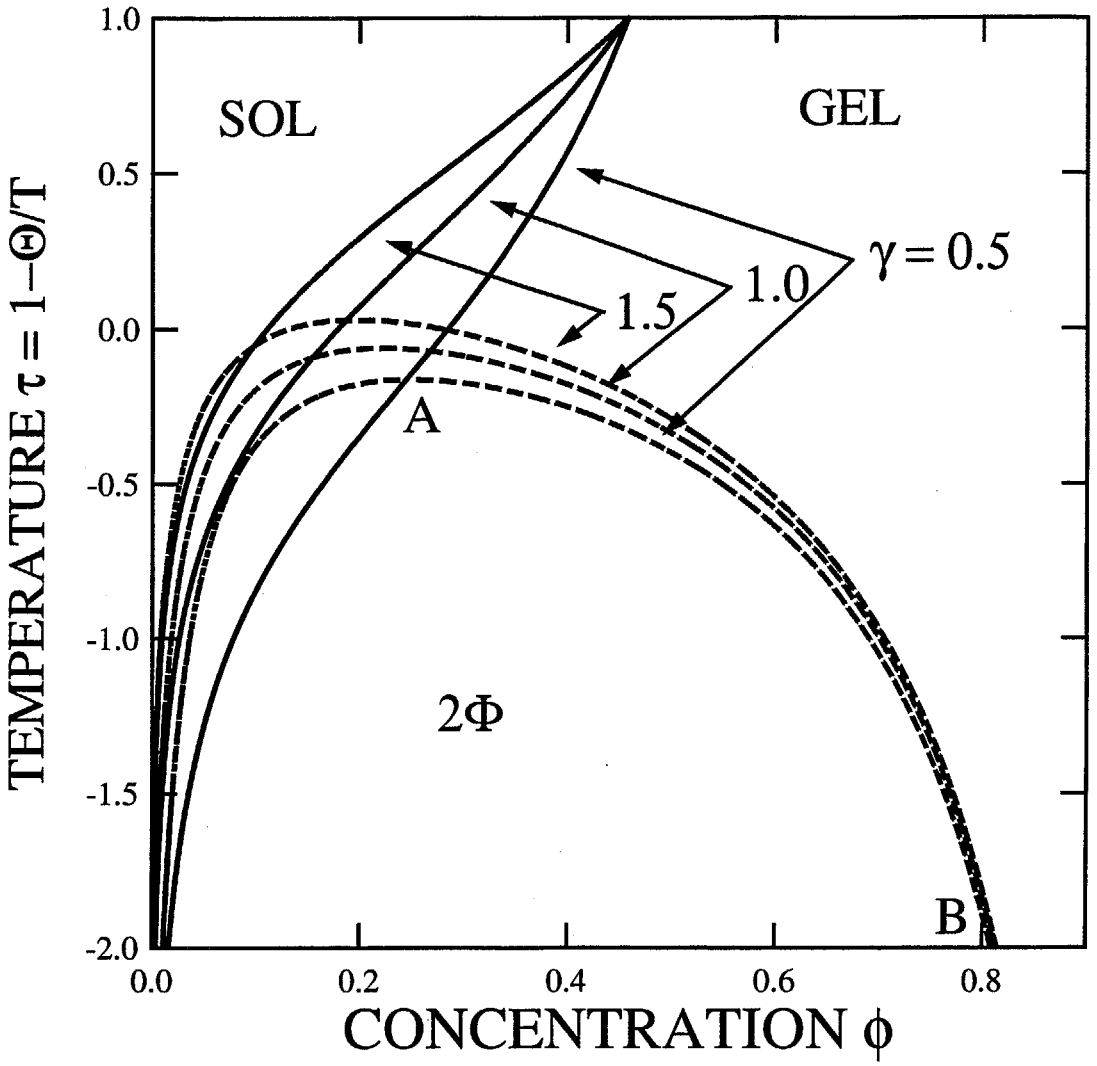

Figure 4.10: The sol/gel transition lines (solid lines) together with the spinodal lines (broken lines) drawn on the usual temperature-concentration plane. The two curves cross each other at the top of the spinodal region. The reaction enthalpy is changed from curve to curve.

Figure 4.11 shows the polymer concentration (horizontal axis) plotted as a function of the vapour pressure (vertical axis) of water as before. At low temperatures, the vapour pressure shows a positive shift, reaches a maximum and the sharply decreases. Such peaks indicate strongly repulsive interaction between polymers and solvent molecules in the solution. It eventually leads to a phase separation. Figure 4.12 shows the conversion of the functional groups plotted against the concentration of polymers produced in the solution. At low temperatures, we notice a strong tendency to low conversion after passing a maximum with increase in the polymer concentration, or by giving high pressure. For instance, for the lowest temperature $\tau = -4.0$ in our calculation, the conversion is pushed back as low as 0.25, which is lower than the gel point 0.33. The solution, thus, goes back to sol phase.

Figure 4.13 shows Bakhuis-Roosboom space diagram for the case of weak reaction. We can readily see the appearance of the reentrant sol phase at low temperature with high vapour pressure.

Projecting onto the temperature-pressure phase plane, we have similar sol/gel transition curves and the spinodal curves to those in the strong reaction case as shown in Figure 4.14, but there is a large difference at high pressure. (Three curves near the spinodal spike fall nearly on top of each other in this axis scale, so that their difference cannot be seen clearly in this figure.) There appears a closed loop type sol region as we can see in the figure, whose position depends upon the reaction enthalpy. These are the reentrant sol phases. Figure 4.15 shows more clearly these reentrant sol phases on the usual temperature-concentration phase plane. We see two groups of sol/gel transition lines: one with the same shape as in the strong reaction at low concentrations (sol/gel transition), the other with dome shape at high concentrations (gel/sol transition). Such new cooperative phenomena between gelation (connection of molecules by chemical bonds) and phase separation (coexisting two different phases) by changing the vapour pressure indicate potential applications of the pressure controlled sol/gel transformation in polycondensing systems.

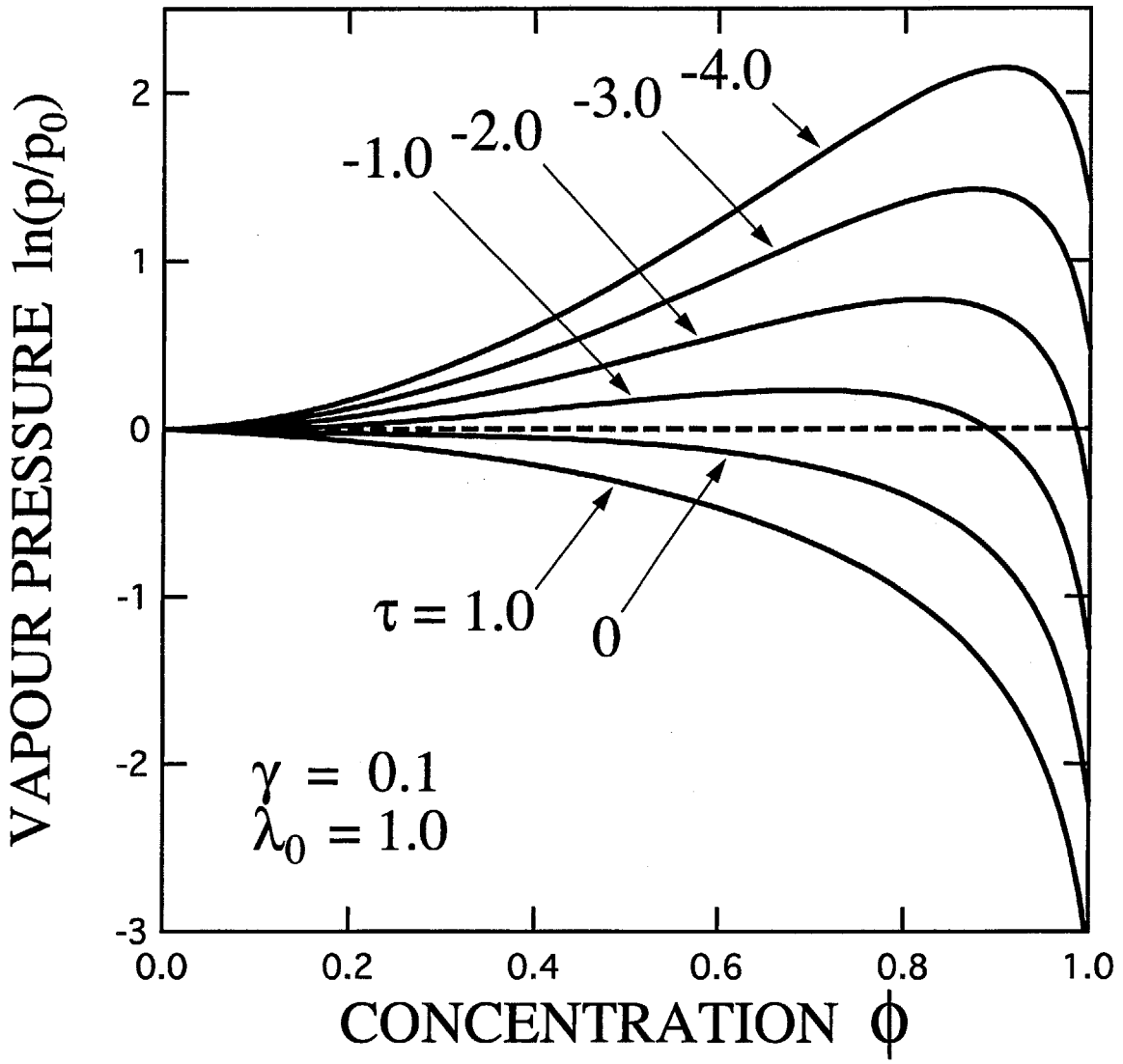

Figure 4.11: Polymer concentration (horizontal axis) plotted as a function of the vapour pressure (vertical axis) of the solvent for weak reaction of $\gamma = 0.1$.

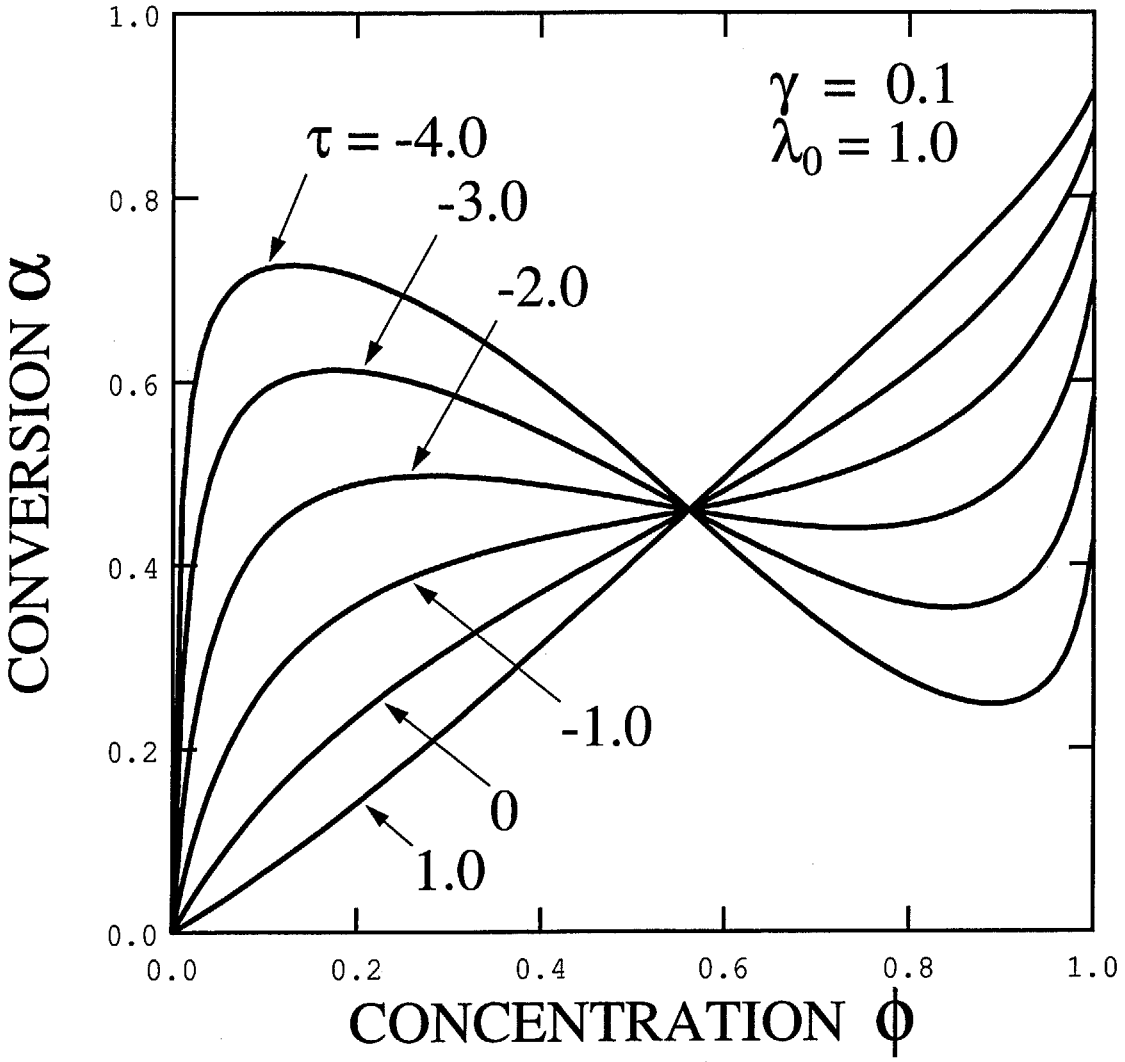

Figure 4.12: The conversion of the functional groups plotted against the produced polymer concentration in the case of weak reaction.

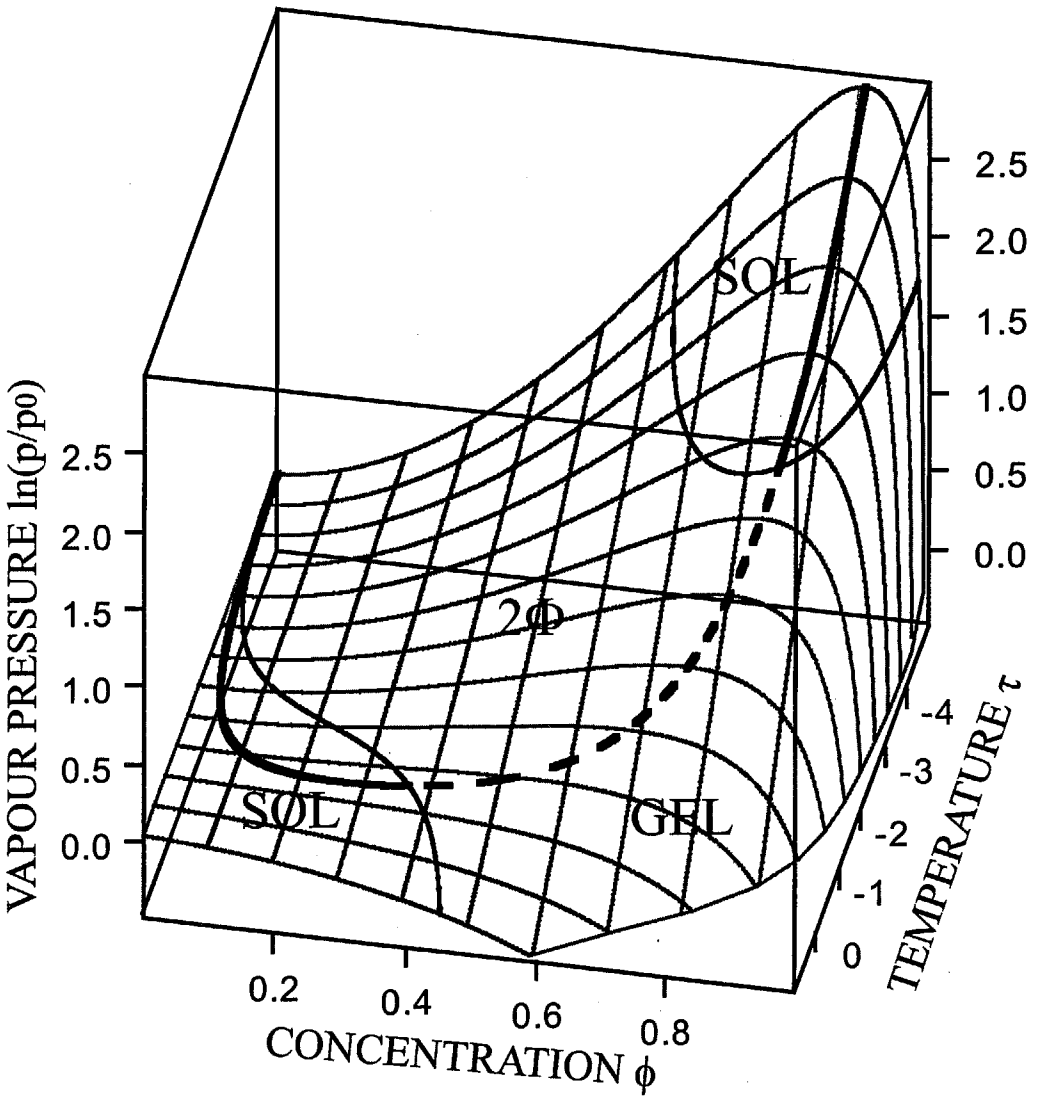

Figure 4.13: The same as in Figure 4.8, but for weak reaction of $\gamma = 0.1$.

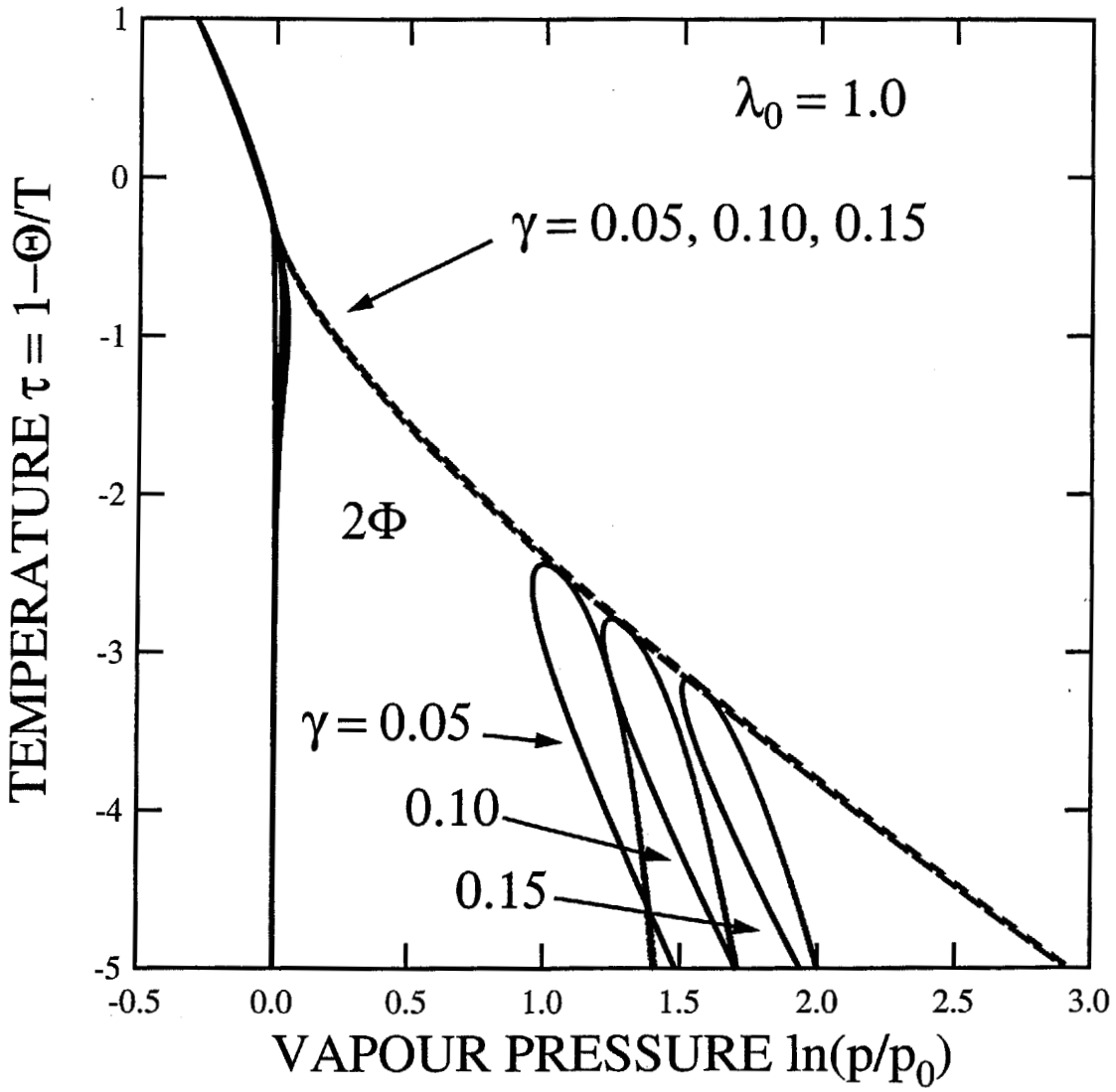

Figure 4.14: The sol/gel transition lines (solid lines) together with the spinodal lines (broken lines) drawn on the temperature-pressure phase plane in the case of weak reaction. The enthalpy of reaction is changed from curve to curve. The two curves (sol/gel and spinodal) cross each other at the top of the spinodal region. The reaction enthalpy is changed from curve to curve.

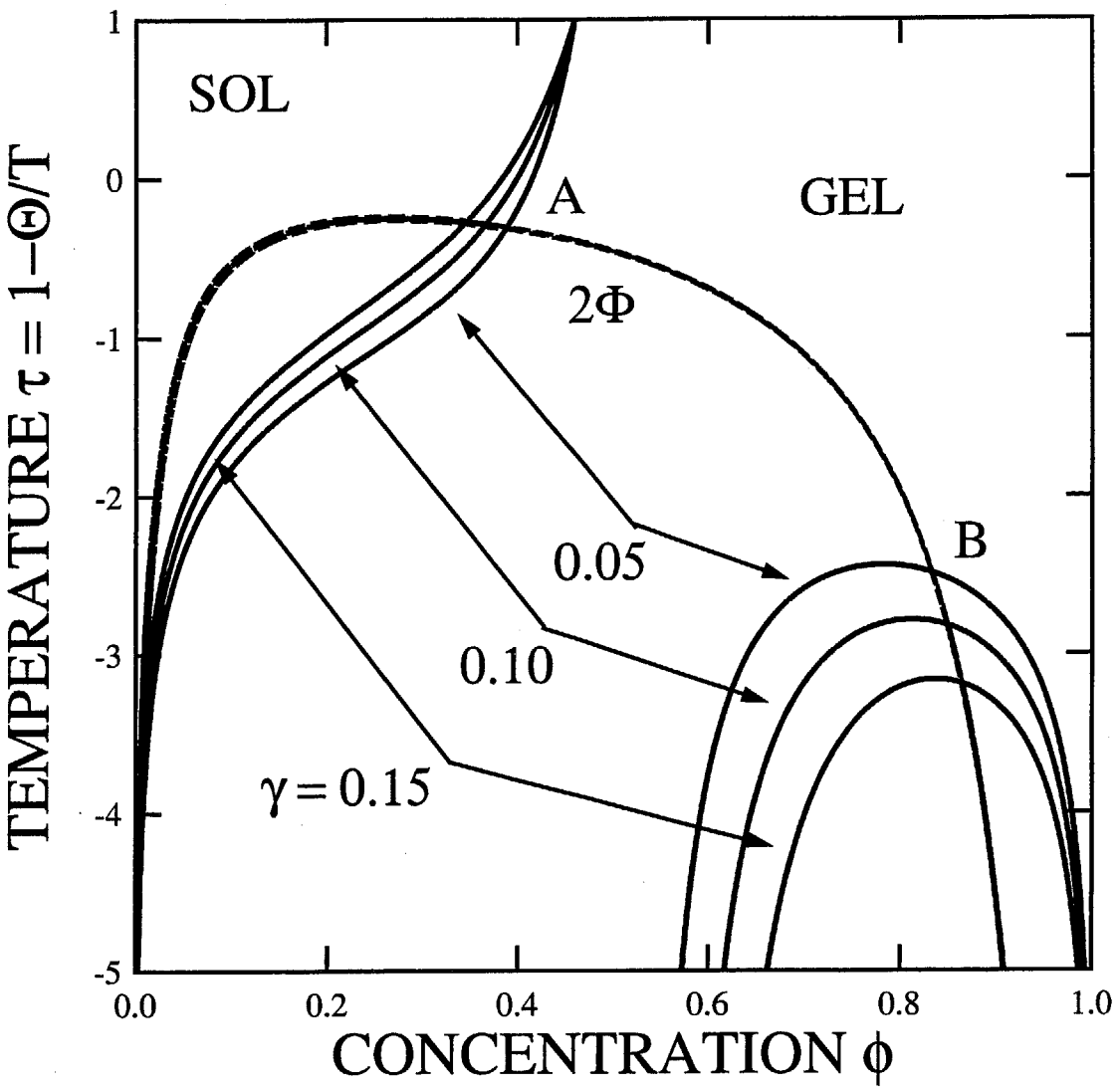

Figure 4.15: The sol/gel transition lines (solid lines) together with the spinodal lines (broken lines) drawn on the usual temperature-concentration plane for weak reaction. The two curves cross each other at the top of the spinodal region (phase separation region). The reaction enthalpy is changed from curve to curve.

4.3.4 Reaction in Closed Systems

When reaction takes place in a closed vessel, the volume is kept constant $\Omega = \Omega_0$, so that we have the relation (4.53). The polymer concentration is reduced by the factor $f_1\alpha/2$ as reaction proceeds due to the production of water molecules. The conversion is then found from Eq.(4.44) as a function of the initial concentration Φ. Explicitly, the equation for α leads to

$$2f_1\lambda\Phi(1-\alpha)^2\exp[\chi(T)(f_1\Phi\alpha+1-2\Phi)] = [2(1-\Phi)+f_1\Phi\alpha]\alpha. \tag{4.65}$$

The spinodal condition remains the same as Eq.(4.61), but the concentration is replaced by the closed system condition (4.53).

Figure 4.16 and 4.17 show the conversion as a function of the initial concentration for a strong and weak reaction. Temperature is varied from curve to curve. Compared to the pressure-controlled open systems, the backward reaction is enhanced due to the elevated pressure by reaction. The reentrant sol phases appear more easily (Figure 4.18).

4.4 Conclusions and Discussion

We have shown the advantage to bring the polycondensing systems to the gel points by controlling the vapour pressure. In a common case of primary molecules with $f = 4$ and $n = 5$, the gel point can easily be reached by depressing the vapour pressure by one order of magnitude. In a weak reaction, we showed that it is possible to move back to a sol from a gel by giving pressure. The thermodynamic conditions to reach the gel point without phase separation can also be found by the theoretical consideration given in this study. Such thermodynamic description, combined with reaction kinetics, therefore turned out to be useful not only for the fundamental research but also for the practical applications.

From the theoretical point of view, the treatment of the postgel regime after the gel point is passed is important because the conversion in the gel part and that in the sol part may be different[4, 18]. Historically, several consistent theoretical treatments have been proposed. The problem requires the inclusion of at least one additional unknown parameter defining the relative

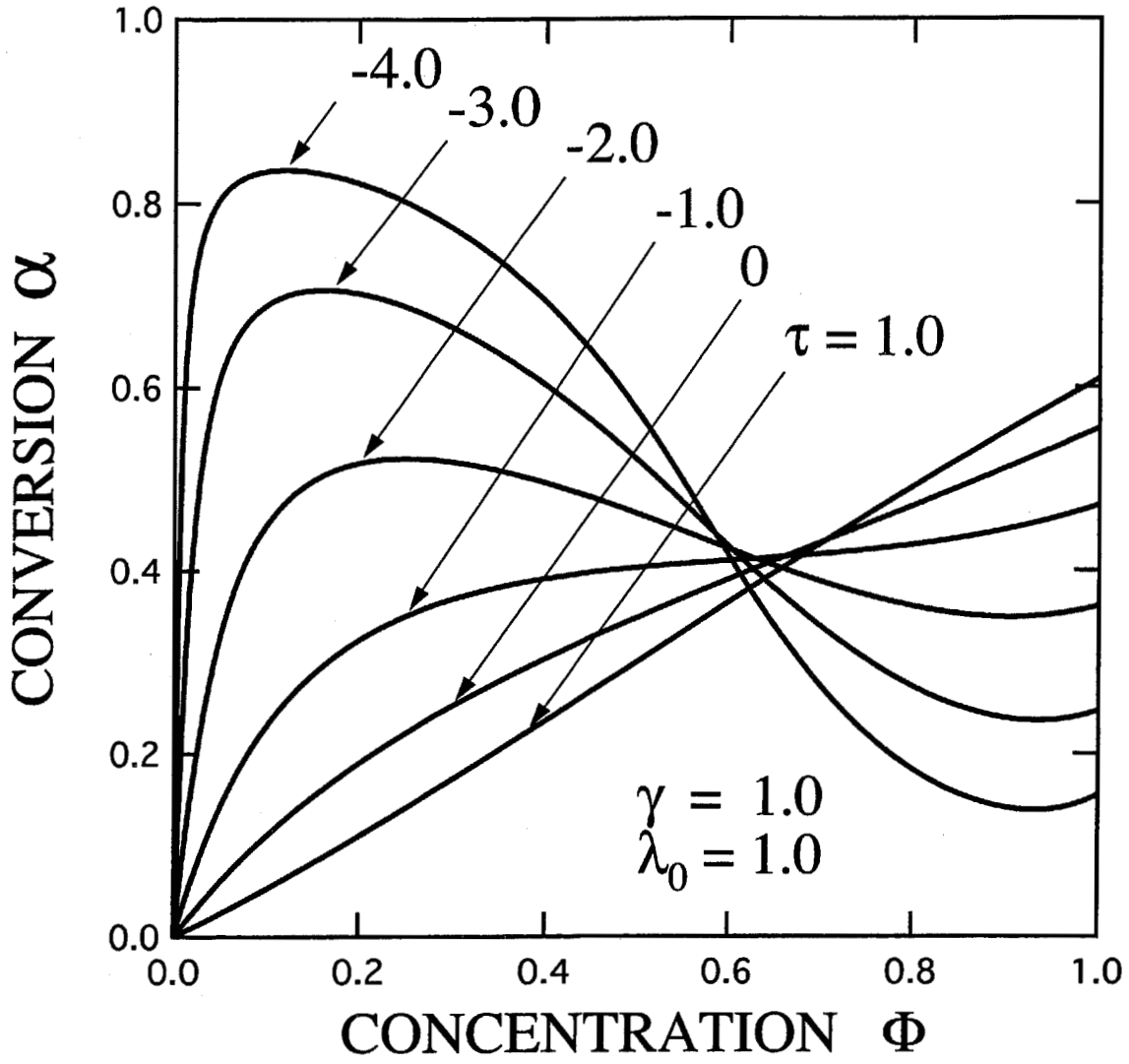

Figure 4.16: The conversion in closed system is plotted against the initial concentration of functional molecules in the strong reaction case. Temperature is varied from curve to curve. The strong backward reaction can be seen at high concentrations.

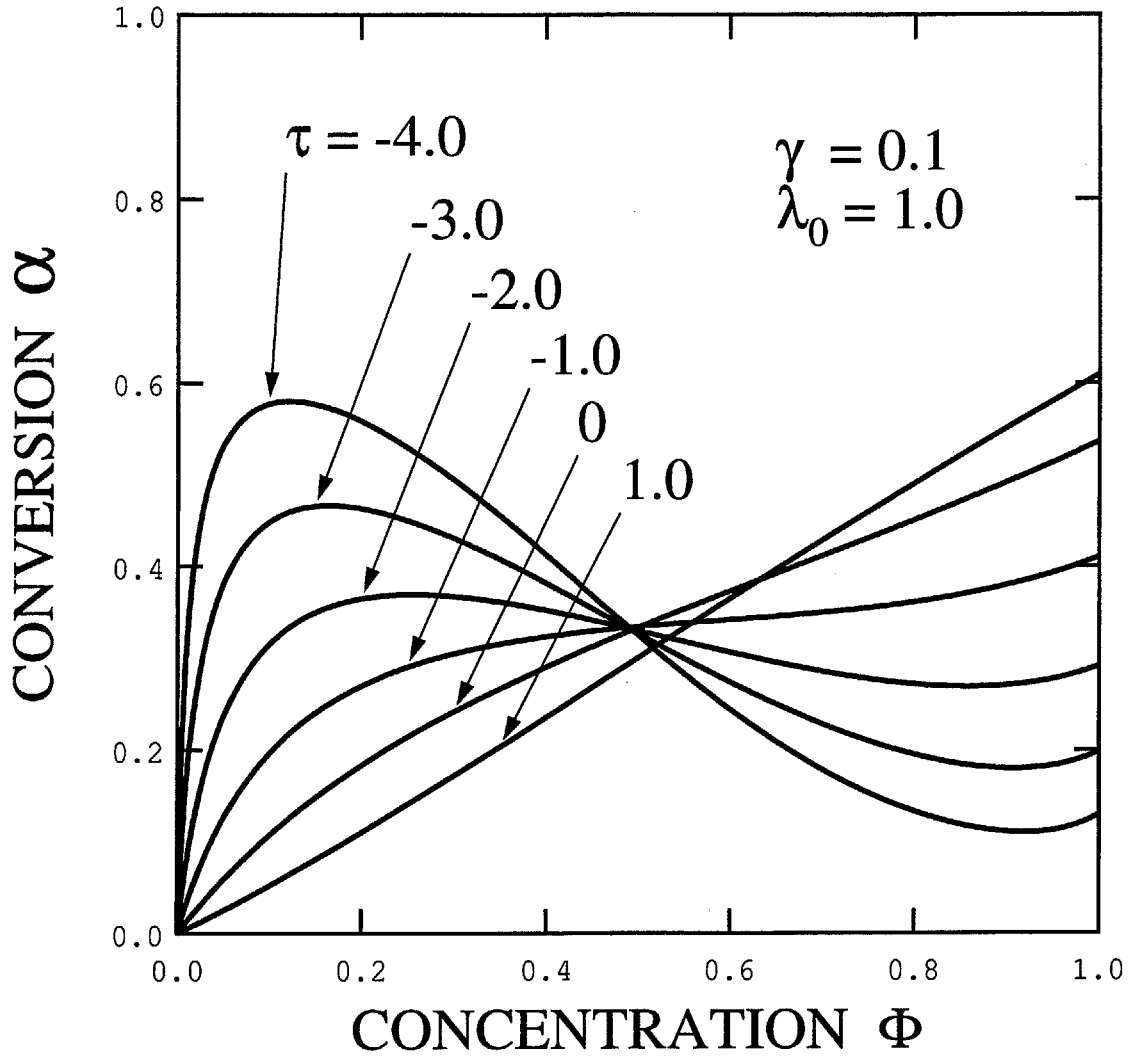

Figure 4.17: The same as Figure 4.16, but in the case of weak reaction.

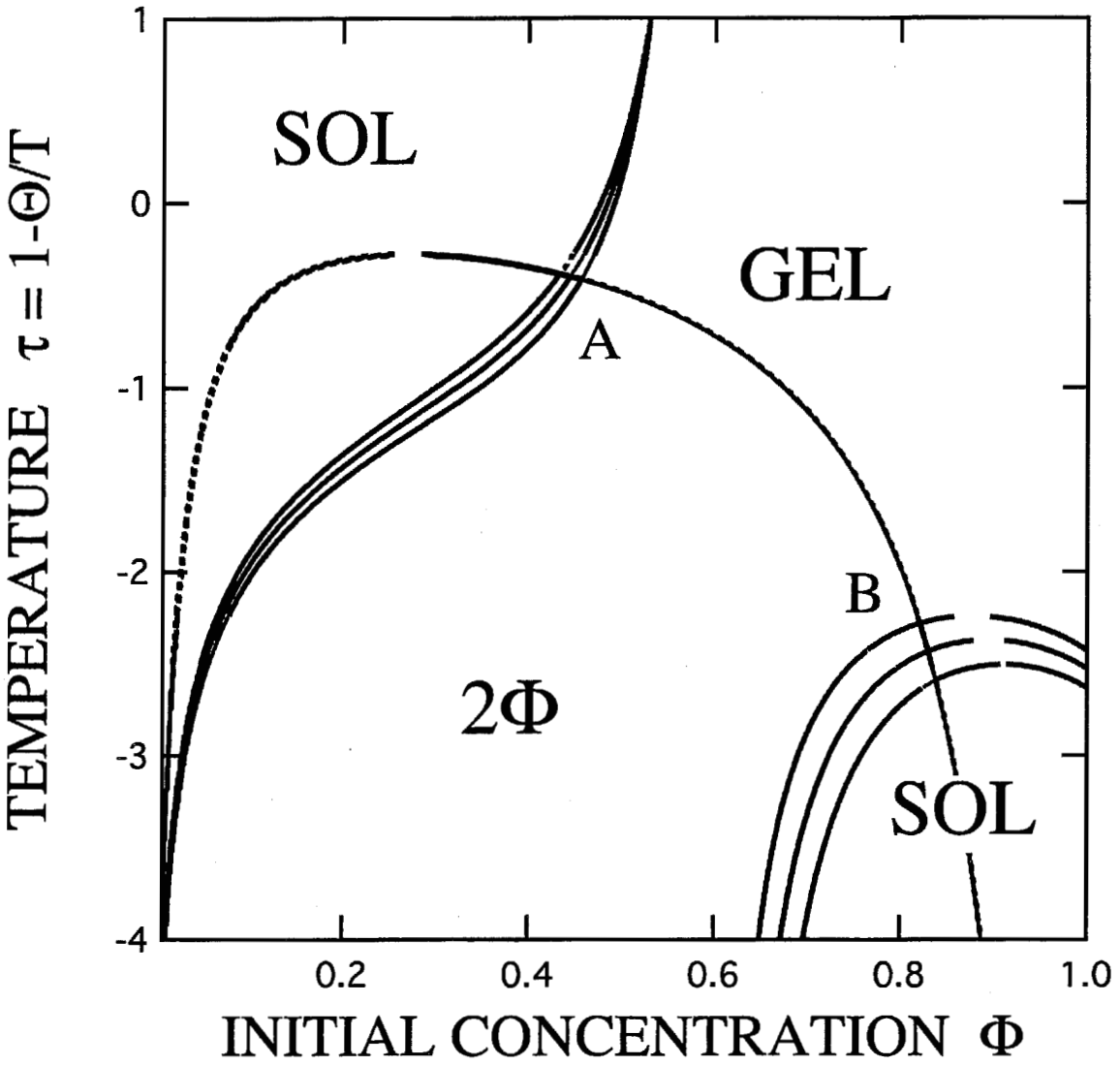

Figure 4.18: Typical phase diagram of a closed system with sol/gel transition lines (thick lines) and the spinodal line (thin broken lines of dome shape) drawn on the temperature and initial concentration plane. The reaction enthalpy is varied from $\gamma = 0.02$ (inner curve), $\gamma = 0.04$ (middle curve), and $\gamma = 0.06$ (outer curve). Large reentrant sol regions appear.

probability of occurrence of intra- and intermolecular reactions. We have avoided this problem, and confined the present study to the pregel regime and the gel point.

Bibliography

[1] Flory, P. J. *Principles of Polymer Chemistry*; Cornell University Press: Ithaca, NY 1953; Chapter.IX.

[2] Vollmert, B. p.207 in *Polymer Chemistry*; Springer-Verlag Inc.: NY 1973.

[3] Flory, P. J. *J. Am. Chem. Soc.* **1941**, *63*, 3091; 3096.

[4] Stockmayer, W. H. *J. Chem. Phys.* **1943**, *11* 45 ; **1944**, *12*, 125.

[5] Sakka, S.; Kozuka, H. *J. Non-Crystal. Solids* **1988**, *100*, 142.

[6] Tanaka, F. *Macromolecules* **1990**, *23*, 3784; 3790.

[7] Tanaka F.; Stockmayer, W. H. *Macromolecules* **1994**, *27*, 3943.

[8] Tanaka, F. *Molecular Gels*; Ed. Weiss, G.; Terech, P., Kluwer Academic Pub.: London 2006; Chapter.1.

[9] Důsková-Smrčková, M.; Dušek, K. *J. Mat. Sci.*, **2002**, *37*, 4733.

[10] Flory, P. J. *J. Chem. Phys.*, **1942**, *10*, 51.

[11] Huggins, M. L. *J. Chem. Phys.* **1942**, *46*, 151.

[12] Ref. [1], Chapter.XII.

[13] Gordon, M.; Scantlebury, G. R. *Proc. Roy. Soc. (London), Ser.A* **1962**, *268*, 240.

[14] Veytsman, B. A. *J. Chem. Phys.* **1990**, *94*, 8499.

[15] Panayiotou, C.; Sanchez, I. C. *J. Chem. Phys.* **1991**, *95*, 10090; *Macromolecules* **1991**, *24*, 6231.

[16] Semenov, A. N.; Rubinstein, M. *Macromolecules* **1998**, *31*, 1373.

[17] Erukhimovich, I.; Thamm, M. V.; Ermoshkin, A. V. *Macromolecules* **2001**, *34*, 5653.

[18] Ishida, M.; Tanaka, F. *Macromolecules* **1997**, *30*, 3900.

[19] Tanaka, F. *Phys. Rev.* E **2006**, *73*, 061405.

[20] London, F. *Superfluids*, Vol. II; Dover Pub., Inc. : New York, 1964; Chapter C, Section.8.

[21] Hill, T.L. *An Introduction to Statistical Thermodynamics*; Dover Pub.: NY 1986; Chapter.14.

[22] Schultz A. R.; Flory, P. J. *J. Am. Chem. Soc.* **1963**, *75*, 3888; 5631.

[23] Koningsveld, R.; Stockmayer, W. H.; Nies, E. *Polymer Phase Diagrams*; Oxford University Press: Oxford, 2001; Part.1, Section.3.

Chapter 5

Time-Dependent Phase Diagrams for Gelation-Induced Phase Separating Systems

5.1 Introduction

In a reactive polymer solution, phase separation region expands as the reaction proceeds (reaction time increases). We usually call such phenomenon "polymerization induced phase separation". In the case of a monomer which has more than 3 reactive sites (functional groups), the solution property changes complicatedly as the reaction proceeds due to the competition between gelation and phase separation. Thus, it is especially called "gelation induced phase separation". It is interesting to predict time-dependent phase behavior from only the conditions such as reaction temperature and initial ratio of monomer and solvent. Then, this prediction gives important knowledge to elucidate both reaction mechanism and phase separation.

There are some studies of time-dependent solution properties. For example, (1) phase separation time is estimated by rheological and DSC measurements as the concentration of reactants are changed then discussed about the mechanism of phase separation[1, 2, 3]. (2) Time-dependent cloud points on the temperature-concentration plain is theoretically derived in simple polymerization systems[4]. (3) Gelation time is estimated when the ratio of monomer concentration is changed[5, 6, 7, 8, 9]. There are few studies, however, that theoretically derived time-dependent phase diagram in the gelation-induced phase separation system and suggest the mechanism of both gelation and phase separation as reaction proceeds.

The purpose of this study is to suggest new analysis showing time-dependent phase diagram with focus on aggregation and reaction by solving time-evolution equations in polycondensation systems. In chapter 4, we theoretically studied on the pressure- and the temperature-controlled thermoreversible gelation and phase separation in polycondensation systems. We also suggested the mechanism of gelation considering the byproduct of water and vapour pressure. From the study, a gel point can be easily reached by depressing the vapour pressure in a strong reaction (the reaction enthalpy is larger than the thermal energy at the reference temperature). In a weak reaction, it is possible to move back to a sol from a gel by giving pressure (reentrant sol phase). The thermoreversible conditions to reach the gel point without phase separation can also be found. By developing this pressure-controlled theory and then combining with kinetics of

reaction, we calculate time-dependent phase diagrams and conversion diagrams of gelation and phase separation and estimate gelation time in associative- and reactive- solutions with focus on the effect of byproduct of water molecules (solvent molecules).

5.2 Kinetic Theory of Reacting Polymer Solutions

5.2.1 Reaction-Controlled Systems and Diffusion-Controlled Systems

In this study, we derive the theory of gelation-induced phase separation paying attention to proceeding of polycondensation. It is difficult to apply the Flory-Huggins equation under non-equilibrium condition. Now, we can apply this equation to such reactive solutions considering rate-controlling step. The rate-controlling step is divided into two systems - reaction controlling system and diffusion controlling system (see Figure 5.1). The diffusion-reaction equation for an l-mer is given by

$$\frac{\partial \nu_l}{\partial t} + \nabla \cdot \mathbf{J}_l = R_l\{\nu\}, \tag{5.1}$$

where ν_l is the number concentration of l-mers, $\mathbf{J}_l$ is flow rate, and $R_l\{\nu\}$ is reaction term, respectively.

The relaxation time of reaction τ_r and of diffusion τ_d are given by

$$\tau_r = k^{-1}, \tag{5.2}$$

$$\tau_d = \frac{R_g^2}{D}, \tag{5.3}$$

where k is the reaction rate for forward reaction, R_g is radius of gyration, D is diffusion constant, respectively. In the case of $\tau_d >> \tau_r$, the time when the system reaches at the diffusion-equilibrium is much longer than that of the reaction-equilibrium, thus it is the diffusion-controlling system. In the case of $\tau_r >> \tau_d$, it is the reaction-controlling system. In this study, we can regard polycondensation as reaction-controlling system. We can neglect the effect of diffusion, then the solution reaches at local equilibrium state immediately. Thus, we can apply the Flory-Huggins equation.

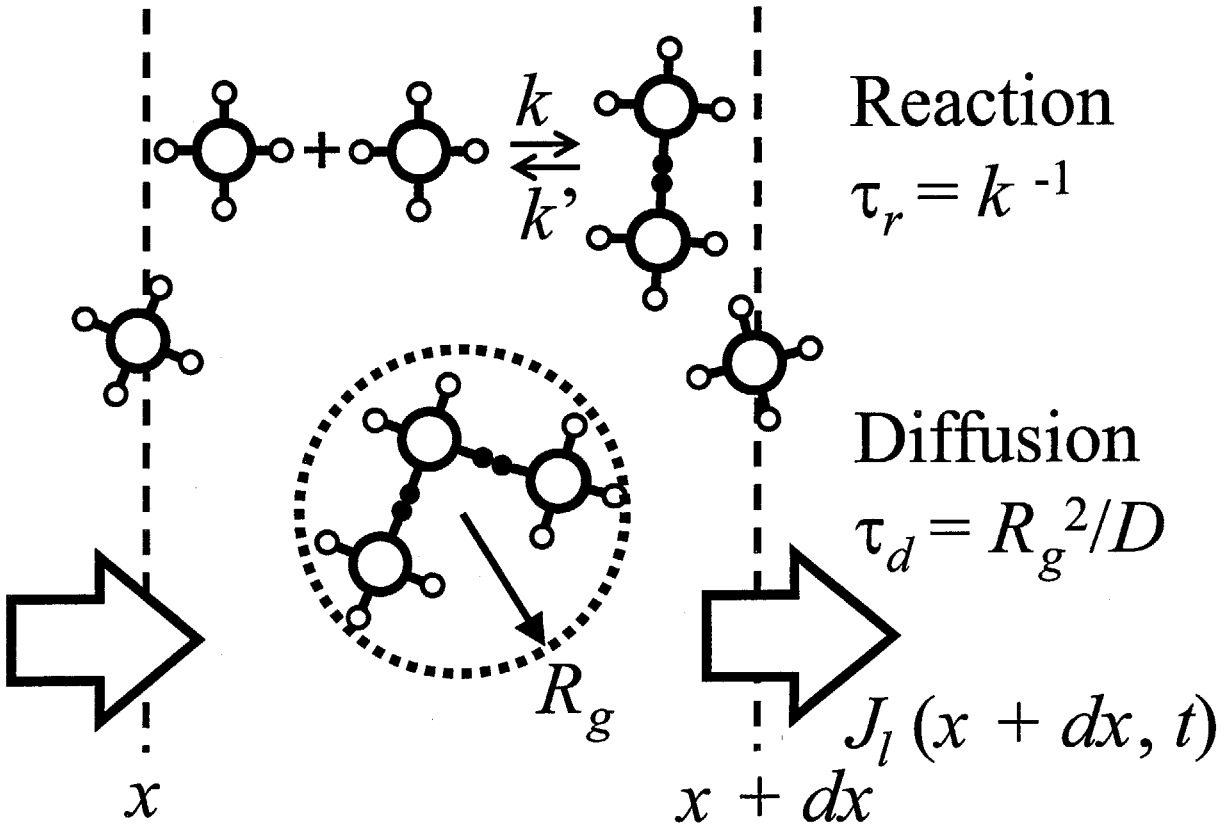

Figure 5.1: Schematic image of reaction controlled system and diffusion controlled system. R_g is radius of gyration, D is diffusion constant, J_l is flow rate, and τ is relaxation time.

5.2.2 Definitions of the Model Solutions

Let us consider functional molecules A (referred to as A molecule) dissolved in water (solvent). To discuss the effect of the byproduct of water molecules in the reaction, we treat two systems - one is that water molecules react with the reactants such as polycondensation, the other is that solvent molecules *do not react* with the reactants. We call simply that the former solvent is active solvent, the latter is inactive solvent.

Let f be the number of functional groups (for example -OH) on an A molecule, and let n be the volume of an A molecule measured relative to the molecular volume a^3 of the solvent molecule (H_2O). We mix the number N of primary A molecules with the number N_0 of the solvent molecules, both in the standard reference state. The volume of the solution is $V = (N_0 + nN)a^3$. In what follows, we study our reactive solutions on the basis of the lattice theory of polymer solution[10, 11, 12], so that the volume is measured in terms of the total number Ω of the lattice cells. Hence we have $\Omega = N_0 + nN$ for the initial volume, and $\Omega = V/a^3$. The volume fraction ϕ of the polymers in active solvent changes as a function of reaction time, and is different from that of the initial solution $\Phi \equiv nN/\Omega_0$. In the case of inactive solvent, ϕ is kept constant $\phi = \Phi$.

We assume the reaction

$$lA \rightleftarrows A_l + \Delta n_l H_2O \tag{5.4}$$

for polycondensation of A molecules, where Δn_l is the number of water molecules produced when an l-mer is formed from the number l of primary molecules by reaction. In inactive solvent, $\Delta n_l = 0$. The volume n_l of l-mer is then given by

$$n_l = ln - \Delta n_l. \tag{5.5}$$

In an active solvent, the number Δn_l may change from the minimum $l-1$ (tree form) to $fl/2$ (complete reaction), but here we simply consider tree forms only and neglect internal loops. We then employ the classical theory of gelation[13, 14, 15]. The effect of cycle formation within

polymers can be taken into consideration step by step by the usual spanning-tree procedure[13], but here we confine tree statistics. We then have $\Delta n_l = l - 1$ and

$$n_l = ln - (l - 1). \tag{5.6}$$

As reaction proceeds, the average molecular weight of the connected clusters grows, and eventually becomes infinite at the gel point. Let N_l be the number of l-mers, and let N^G be the number of A molecules in the gel network. The volume of the solution is then given by

$$\Omega = N_0 + \sum_{l\geq 1}(l-1)N_l + \Delta n^G N^G + \sum_{l\geq 1} n_l N_l + n^G N^G, \tag{5.7}$$

where n^G is the effective volume of an A molecule in the gel network and Δn^G is the number of cross-links on it. The first three terms gives the total number

$$N_{\rm w} \equiv N_0 + \sum_{l\geq 1}(l-1)N_l + \Delta n^G N^G \tag{5.8}$$

of water molecules in the solution. The volume fraction of the polymer in the sol part is given by

$$\phi^S = \sum_{l\geq 1} \frac{n_l N_l}{\Omega}, \tag{5.9}$$

and that in the gel part is

$$\phi^G = \frac{n^G N^G}{\Omega}. \tag{5.10}$$

The total volume fraction of the polymer is given by $\phi = \phi^S + \phi^G$, and the volume fraction of water is

$$\phi_{\rm w} \equiv \frac{N_{\rm w}}{\Omega} = 1 - \phi. \tag{5.11}$$

The gel fraction w is defined by the ratio ϕ^G/ϕ.

5.2.3 Free Energy of the Reactive Solutions

We apply the lattice theory of associating solutions[10, 11, 12] to the present polycondensation system, and start from the free energy

$$\beta\Delta F = N_{\rm w}\ln(1-\phi) + \sum_{l\geq 1} N_l \ln\phi_l + \chi(T)\Omega\phi(1-\phi) + \sum_{l\geq 1}\Delta_l N_l + \delta(\phi)N^G, \tag{5.12}$$

where $\beta \equiv 1/k_B T$, $\chi(T)$ is Flory's interaction parameter, and

$$\Delta_l \equiv \beta(\mu_l^\circ - l\mu_1^\circ) \tag{5.13}$$

is the free energy change in forming an l-mer from the number l of separated primary molecules in the standard reference state. The volume fraction of the l-mers is given by

$$\phi_l \equiv \frac{n_l N_l}{\Omega}, \tag{5.14}$$

and its number density is given by

$$\nu_l \equiv \frac{N_l}{\Omega}. \tag{5.15}$$

We can find the chemical potential for each component by taking derivatives of the free energy with respect to the corresponding number of molecules. We find

$$\beta\Delta\mu_{\mathrm{w}} = \phi + \ln(1-\phi) - \nu + \chi\phi^2 \tag{5.16}$$

for the water, and

$$\beta\Delta\mu_l = 1 + \Delta_l + \ln\phi_l - n_l(1-\phi+\nu) + \chi n_l(1-\phi)^2 \tag{5.17}$$

for an l-mer, where

$$\nu \equiv \sum_{l\geq 1} \nu_l \tag{5.18}$$

is the number of monomers and clusters that possess center of mass translational degree of freedom[10, 11, 12].

5.2.4 Equilibrium Conditions

In each state of reaction, the reaction reaches a chemical equilibrium, we have the condition in the sol part and gel part, respectively

$$l\Delta\mu_1 = \Delta\mu_l + (l-1)\Delta\mu_{\mathrm{w}}, \tag{5.19}$$

$$\Delta\mu_1 = \Delta\mu_1^G. \tag{5.20}$$

Substituting the chemical potentials into this equilibrium condition, we find that the volume fraction of the l-mers is given by

$$\phi_l = K_l(\phi)\frac{{\phi_1}^l}{{\phi_w}^{l-1}}, \tag{5.21}$$

where

$$K_l(\phi) \equiv \exp\left[-\Delta_l + (l-1)\chi(T)(1-2\phi)\right] \tag{5.22}$$

is the equilibrium constant of the reaction, and ϕ_1 is the volume fraction of the primary molecules that remain unreacted. In contrast to the simple association without production of the solvent molecules, the equilibrium constant depends on the concentration through the interaction term with χ-parameter. Such concentration dependence appears from the change in the number of monomer-solvent contacts during the reaction.

5.2.5 Rate Equations of the Polycondensation Reactions

Let us define and solve the rate equation in an inactive solvent system. We assume the reaction

$$-\mathrm{A} + \mathrm{A}- \rightleftarrows -\mathrm{A} - \mathrm{A}-. \tag{5.23}$$

The rate equation for (5.23) is that

$$\frac{d(\psi\alpha)}{dt} = k[\psi(1-\alpha)]^2 - k'\psi\alpha. \tag{5.24}$$

where $\psi \equiv f\phi/n$ is the total concentration of functional groups, α is the conversion, and k, k' are the rate constant of forward and backward reaction, respectively. Thus, $\psi\alpha, \psi(1-\alpha)$ is the concentration of reactive and un-reactive functional groups, respectively. The equilibrium constant λ is defined by $\lambda \equiv k/k'$. We solve Eq.(5.24), α is expressed as a function of reaction time $k't$. We notice that the reaction time t is scaled by k'. In this system, the total concentration of monomer and polymer are not changed during the reaction, thus $\phi = \Phi, \psi = \Psi$, where Φ, Ψ are the initial volume fraction and the initial number density of monomer, respectively.

$$\alpha(t) = \frac{\alpha_1(\alpha_0-\alpha_2) - \alpha_2(\alpha_0-\alpha_1)e^{-\Gamma t}}{(\alpha_0-\alpha_2) - (\alpha_0-\alpha_1)e^{-\Gamma t}}. \tag{5.25}$$

α_1, α_2 are the solutions of the equation $\lambda\psi(1-\alpha)^2 - \alpha = 0$, then expressed by Eqs.(5.26) and (5.27).

$$\alpha_1 = \frac{1}{2\lambda\psi}(1 + 2\lambda\psi - \sqrt{1+4\lambda\psi}) \tag{5.26}$$

$$\alpha_2 = \frac{1}{2\lambda\psi}(1 + 2\lambda\psi + \sqrt{1+4\lambda\psi}) \tag{5.27}$$

$0 \leq \alpha_1 \leq 1 \leq \alpha_2$, thus, α_1 is the stable solution and α_2 is the unstable solution. Γ is defined by $\Gamma = \Gamma(\psi) = \sqrt{1+4\lambda\psi}$. α_0 is the initial conversion, usually $\alpha_0 = 0$. At the equilibrium state, $\alpha(\infty) = \alpha_1$ by substituting $t \to \infty$ into Eq.(5.25). We have three compositions - monomer, polymer, and water (solvent). These concentration ϕ_1, ϕ_p, ϕ_w are

$$\phi_w = 1 - \phi, \tag{5.28}$$

$$\phi_1 = \phi(1-\alpha)^f, \tag{5.29}$$

$$\phi_p = \phi[1 - (1-\alpha)^f]. \tag{5.30}$$

In the case of an active solvent system, we assume the reaction

$$-\mathrm{A} + \mathrm{A}- \rightleftarrows -\mathrm{A} - \mathrm{A}- + \Delta_n \mathrm{H_2O}. \tag{5.31}$$

To simplify, we assume $\Delta_n = 1$, the rate equation for (5.31) is that

$$\frac{d(\psi\alpha)}{dt} = k[\psi(1-\alpha)]^2 - k'\psi\alpha(1-\phi). \tag{5.32}$$

A water molecule is formed on forward reaction, thus $\phi = (1 - f_1\alpha/2)\Phi \neq \Phi, \psi = \Psi(1-\alpha) \neq \Psi$ where $f_1 \equiv f/n$. We can rewrite Eq.(5.32),

$$\frac{d\alpha}{dt} = \lambda\Psi(1-\alpha)^2 - \alpha(1-\phi). \tag{5.33}$$

At equilibrium state $d\alpha/dt = 0$, α is expressed by

$$\lambda\frac{f\phi}{n(1 - f_1\alpha/2)} = \frac{\alpha}{(1-\alpha)^2}(1-\phi). \tag{5.34}$$

Compared with Eq.(4.54) in the pressured-controlled system at the equilibrium state, λ should be $\lambda = \lambda e^{\chi(1-2\phi)}$. Now the rate equation is

$$\frac{d\alpha}{dt} = \lambda\Psi e^{\chi(1-2\phi)}(1-\alpha)^2 - \alpha(1-\phi) \tag{5.35}$$

This equation is highly non-linear. ϕ_1, ϕ_p, ϕ_w are

$$\phi_w = 1 - \left(1 - \frac{f_1}{2}\alpha\right)\Phi, \tag{5.36}$$

$$\phi_1 = \Phi(1-\alpha)^f, \tag{5.37}$$

$$\phi_p = \Phi\left[1 - \frac{f_1}{2}\alpha - (1-\alpha)^f\right]. \tag{5.38}$$

5.2.6 Gel Point, Gelation Time, and Spinodal Condition

We employ the same definition of section 2.5 in chapter 4 as the definition of gel point. Gel point is a percolation point where the largest cluster grows to macroscopic dimensions and spans the entire solution. Simple calculation gives $\alpha = 1/(f-1) \equiv \alpha^*$ as in the classical Flory-Stockmayer theory. We then find from Eq.(4.54) that the concentration ϕ^* of the solution at the gel point is given by the condition.

The gelation time is the time required to reach the gel point from an arbitrarily given initial state. t_g satisfies the condition $\alpha(t_g) = \alpha^*$. In an inactive solvent system, from Eq.(5.25), t_g is given by

$$t_g = \frac{1}{\Gamma}\ln\frac{(1-f'\alpha_1)(\alpha_0-\alpha_2)}{(1-f'\alpha_0)(\alpha_0-\alpha_1)}. \tag{5.39}$$

To study phase separation, let us derive the spinodal condition in the pregel regime. We can neglect the chemical potential of the gel part. The derivation is same as in section 2.5 in chapter 4. The spinodal condition is given by

$$\beta\left(\frac{\Delta\mu_1}{n} - \Delta\mu_w\right) = \frac{\kappa(\phi)}{n\phi} + \frac{1}{1-\phi} - 2\chi = 0 \tag{5.40}$$

where a new function κ is defined by

$$\kappa(\phi) \equiv \frac{\partial \ln \phi_1}{\partial \ln \phi}. \tag{5.41}$$

It is explicitly given by

$$\kappa = \frac{1-f'\alpha}{1-\alpha} D_1(x), \tag{5.42}$$

where $x = 2\lambda\phi$ and $D_1(x)$ is

$$D_1(x) = \frac{\alpha(\alpha_2 + \alpha_1 e^{-\Gamma t}) + (1-\alpha\alpha_1)xte^{-\Gamma t}}{\Gamma(1-e^{-\Gamma t})}. \tag{5.43}$$

Thus, $\alpha(t)$ is a time-dependent parameter, we develop the phase separation theory depending on the reaction time t.

In the postgel regime, we have to consider the gel part, thus $\kappa(\phi)$ is given by

$$\kappa(\phi) = \frac{\partial}{\partial \ln \phi}\left(1 + w^G \frac{\partial}{\partial \ln \phi}\right) \ln \phi_1, \tag{5.44}$$

where w^G is the ratio of gel phase.

We employ two treatments in the postgel regime - Stockmayer's treatment[15] and Flory's treatment[13, 14] (the difference is written in section 2.3 in chapter 1 and section 2.5 in chapter 3).

Stockmayer's treatment is very simple spinodal condition, $\kappa(\phi) = 0$.

In the case of Flory's treatment, we have to solve the rate equation of both sol and gel part. We need to introduce these equations to an unknown function $Q(t)$ related that sol cluster converts into gel cluster by reaction and its reverse conversion. To define $Q(t)$ is very complex problem. We avoid this problem, then we use the relation at the equilibrium condition,

$$\frac{\lambda f}{n}\phi = \frac{\alpha}{(1-\alpha)^2}, \tag{5.45}$$

$$\frac{\lambda f}{n}\phi^S = \frac{\alpha^S}{(1-\alpha^S)^2}, \tag{5.46}$$

where α^S, ϕ^S is the conversion and the volume fraction of sol phase, respectively. Thus, $\kappa(\phi)$ is given by

$$\kappa(\phi) = \frac{1 - f'\alpha}{1+\alpha}\left[w^G - w^S \frac{(1+\alpha^S)(a - f'\alpha)}{(1+\alpha)(a - f'\alpha)}\right] - f w^G \frac{\alpha(1-\alpha)}{(1+\alpha)^3}. \tag{5.47}$$

w^S is the ratio of sol phase. $w^S = \phi^S/\phi$ is given by Eqs.(5.45) and (5.46).

5.3 Numerical Results

For numerical calculation of the temperature-concentration phase diagrams, we fix the necessary parameters in the following way. We first assume the conventional Schultz-Flory form $\chi(T) = 1/2 - \psi\tau$ for the χ-parameter[16], where $\tau \equiv 1 - \Theta/T$ is the reduced temperature deviation measured from the reference theta temperature Θ satisfying the condition $\chi(\Theta) = 1/2$,

and ψ is a material parameter of order unity. The equilibrium constant is then expressed as $\lambda(T) = \lambda_0 \exp(|\epsilon|/k_B T) = \lambda_0 \exp[\gamma(1-\tau)]$, where λ_0 gives the entropy part of the standard reaction free energy, and $\gamma \equiv |\epsilon|/k_B\Theta$ the reaction enthalpy in the unit of the thermal energy at the reference temperature. The reference temperature Θ is not the true theta temperature. Throughout the present numerical calculation, we fix at $\psi = 1.0$, $\lambda_0 = 2.0$, $\gamma = 0.1$. The functionality and the molecular weight of the primary molecules are fixed at $f = 4$ and $n = 5$ as a typical example in attempting to apply the present study to time-dependent sol/gel transition in polycondensation of silicic acid $Si(OH)_4$ in water.

5.3.1 Inactive Solvent

We first study an inactive solvent system where the solvent molecules (water) do not react with the reactants. At this system, when the monomer concentration is higher, the conversion α is higher and the reaction rate is faster. Figure 5.2 shows the time-dependent phase diagram of an inactive solvent system showing phase separation and gelation as functions of initial concentration (horizontal axis) and reaction temperature (vertical axis). At lower temperature, phase separation precedes gelation. For instance, at the condition of $\Phi = 0.35, \tau = -0.4$, at $k't = 0.5$, this point enters the phase separated region and the concentrated phase have not reached a gel point, so the solution is sol/sol phase separated solution. At $k't = 3.0$ where is near termination of reaction, the concentrated phase reaches a gel point, the solution changes sol/gel phase separated solution. In the case of higher temperature, however, the solution is not phase separated. For instance, at the condition of $\Phi = 0.35, \tau = -0.1$, even at $k't = 3.0$, the solution keeps homogeneous sol phase.

Figure 5.3 shows the triangular time-dependent phase diagram and the conversion phase diagram in an inactive solvent system showing phase separation and gelation. The reaction temperature is fixed at $\tau = -0.4$. The component consists of monomer, polymer, and water. From this figure, the base line shows the initial condition. In the case of inactive solvent, the total concentration of monomer and polymer are constant, so the state point advances towards leaning to the left from the base line in parallel with the P-M line when the reaction proceeds.

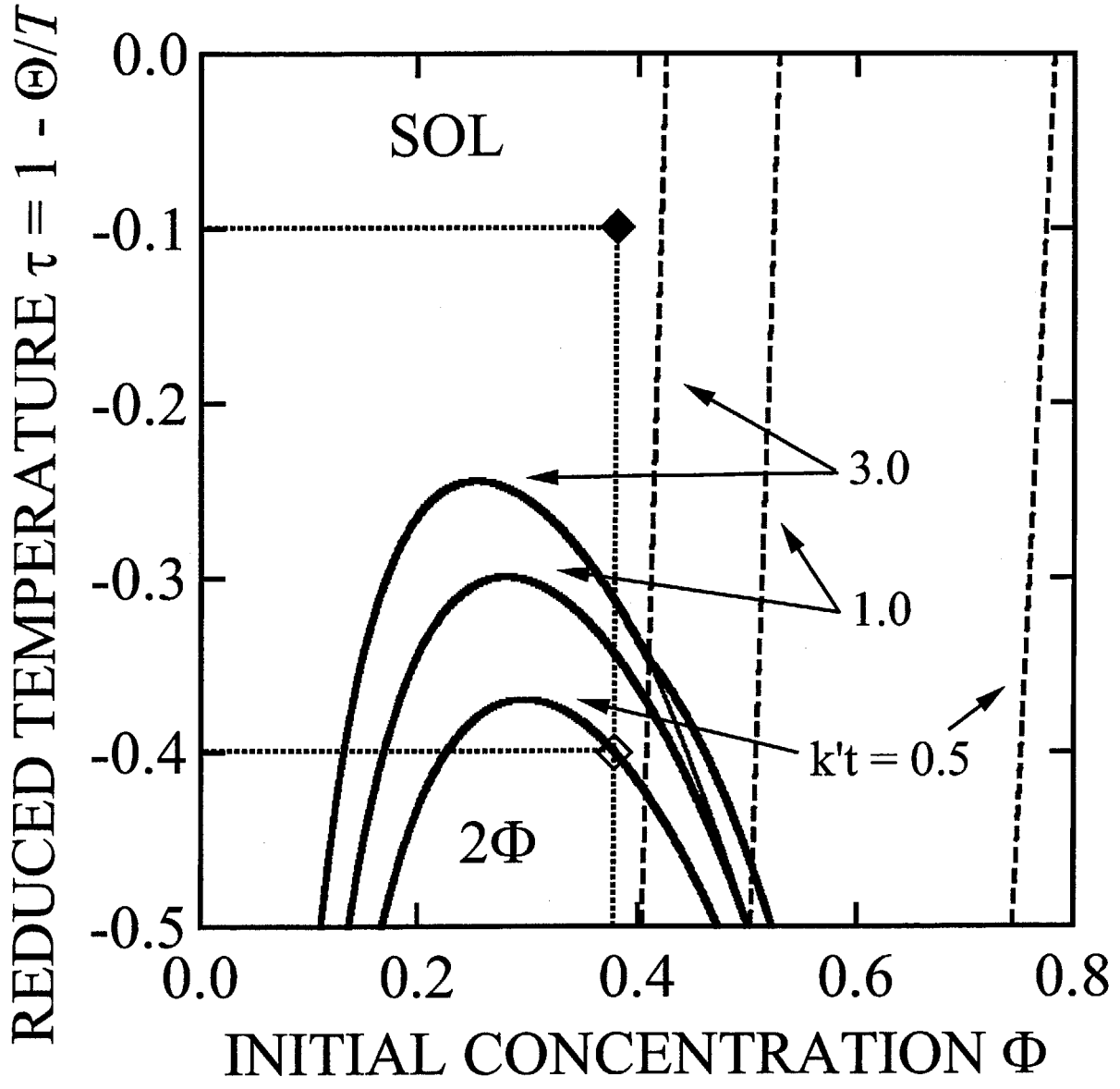

Figure 5.2: Time-dependent phase diagram showing phase separation and gelation in an inactive solvent system. Sol/gel transition lines (dash lines) together with the spinodal lines drawn on the usual temperature-initial concentration plane. Spinodals in the postgel regime are calculated by two treatments: Flory's treatment (thick line), Stockmayer's treatment (thin line). The reaction time $k't$ is changed from curve to curve.

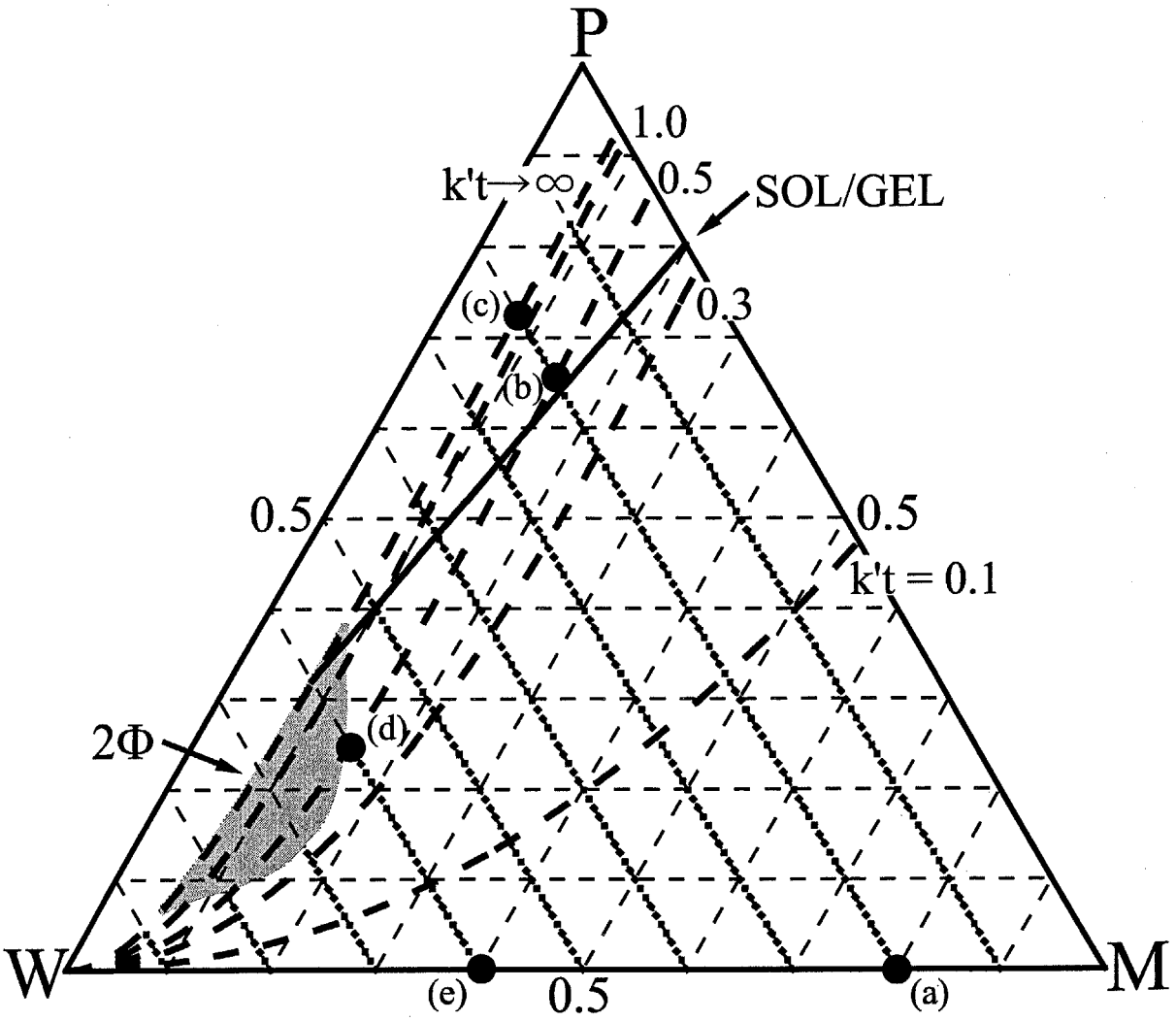

Figure 5.3: Time-dependent triangular phase diagram showing phase separation and sol-gel transition curve (solid line) in an inactive solvent system. Conversion curves (dotted lines) and state line at the same time (dash lines) are drawn. P, M, and W stand for the composition of Polymer, Monomer, and Water, respectively.

At higher concentration, for instance in the case of $\Phi = 0.8$, the solution changes as follow; (a) initial condition ($t = 0$), (b) the solution reaches a gel point at $k't = 0.5$, (c) the reaction is terminated at equilibrium condition ($k't \rightarrow \infty$). At lower concentration, for instance in the case of $\Phi = 0.4$, when the reaction proceeds, (d) initial condition ($k't = 0$), (e) the solution is phase separated into sol/sol phase at $k't = 0.5$.

5.3.2 Active Solvent

We next study an active solvent system where the water molecules react with the reactants. Figure 5.4 shows the time-dependent phase diagram of an active solvent system showing phase separation and gelation as a function of initial concentration (horizontal axis) and reaction temperature (vertical axis). There is different behavior from the inactive solvent system. At lower temperature, the active solvent system changes at the same way as the inactive solvent system with the progress of the reaction. For instance, at the condition of $\Phi = 0.35, \tau = -0.4$, at $k't = 0.5$, the solution is phase separated into sol/sol phases. At $k't = 1.0$, the concentrated phase reaches a gel point, the solution changes sol/gel phase separated solution. In the case of higher temperature, however, there is significant difference between these systems; gelation precedes phase separation. For instance, at the point of $\Phi = 0.35, \tau = -0.1$, at $k't = 1.0$, the solution is homogeneous gel phase. At $k't = 3.0$ where is near the termination of the reaction, in addition to gelation, the solution is phase separated. Even in the dilute phase the solution reaches a gel point, the solution changes gel/gel phase separated solution.

Figure 5.5 shows the triangular time-dependent phase diagram and the conversion phase diagram in the active solvent system. The reaction temperature is fixed at $\tau = -0.4$. In the case of active solvent system, the water molecules are formed and the concentration of water is increased when the reaction proceeds. From this effect, the trace of state point curves in the left from the base line. Let us compare the inactive solvent system to the active solvent system. In the inactive solvent, if the concentration increases, the reaction proceeds faster. On the other hands, in the active solvent, if the concentration increases, the reaction proceeds slower. At the

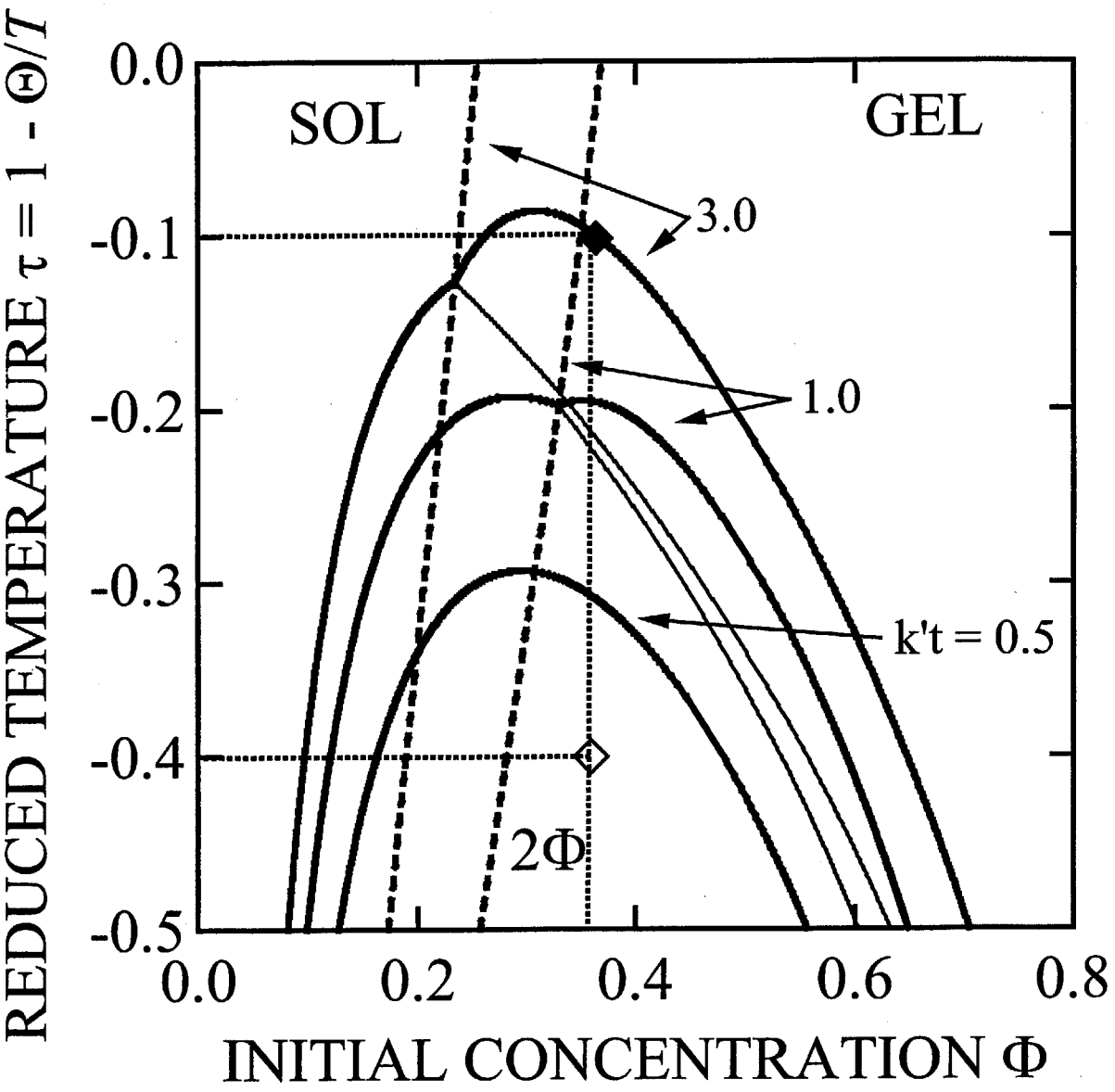

Figure 5.4: Same as in Figure 5.2, but in an active solvent system.

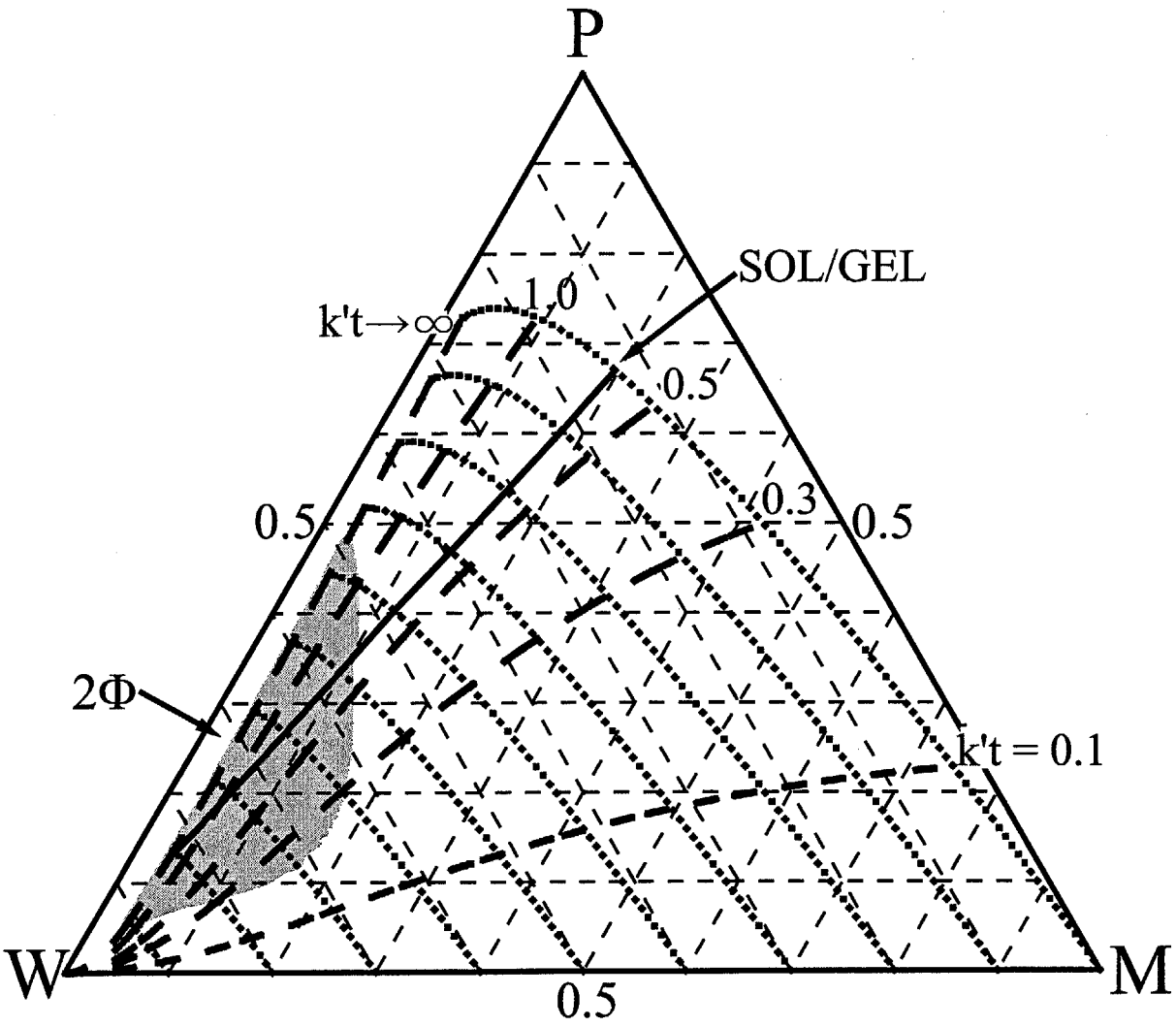

Figure 5.5: Same as in Figure 5.3, but in an active solvent system.

equilibrium state, the reaction in the active solvent proceeds better than in the inactive solvent. The active solvent system is easier phase separated than the inactive solvent system.

5.3.3 Gelation Time

We define the gelation time how long does the solution reach a gel point from the start of the reaction. We note that the gelation time t_g is scaled by the rate constant of backward reaction k'.

Figure 5.6 shows the gelation time (horizontal axis) plotted as a function of the initial monomer concentration (vertical axis) in an inactive solvent system. The gelation time decreases monotonously as the initial concentration of monomer increases. The reaction temperature τ is lower, the gelation time is shorter at the same initial concentration. However the difference of the gelation time by the reaction temperature is very small. We can also determine the critical concentration of gelation. It is estimated approximately $\Phi^* = 0.41$.

Figure 5.7 shows the gelation time plotted as a function of the initial monomer concentration in an active solvent system. The gelation time decreases and it has a minimum point as the initial concentration of monomer increases, then it increases at high concentration. We can find the most efficient concentration for gelation time. At $\Phi = 0.6$, the gelation time has the constant value if the reaction temperature is changed. In the dense region, if the reaction temperature increases, the gelation time is longer. Figure 5.8 shows the initial concentration which has the minimum gelation time plotted as a function of the reaction temperature. The relation between the temperature and the concentration is nearly linear.

Let us compare the active solvent system to the inactive solvent system. Figure 5.9 shows the gelation time for both systems plotted as a function of the initial monomer concentration at the reaction temperature $\tau = -0.3$. At lower concentration, the gelation time in the active solvent is shorter than in the inactive solvent. On the other hand, at higher concentration, there is reverse relation because the gelation time in the active solvent has a minimum point.

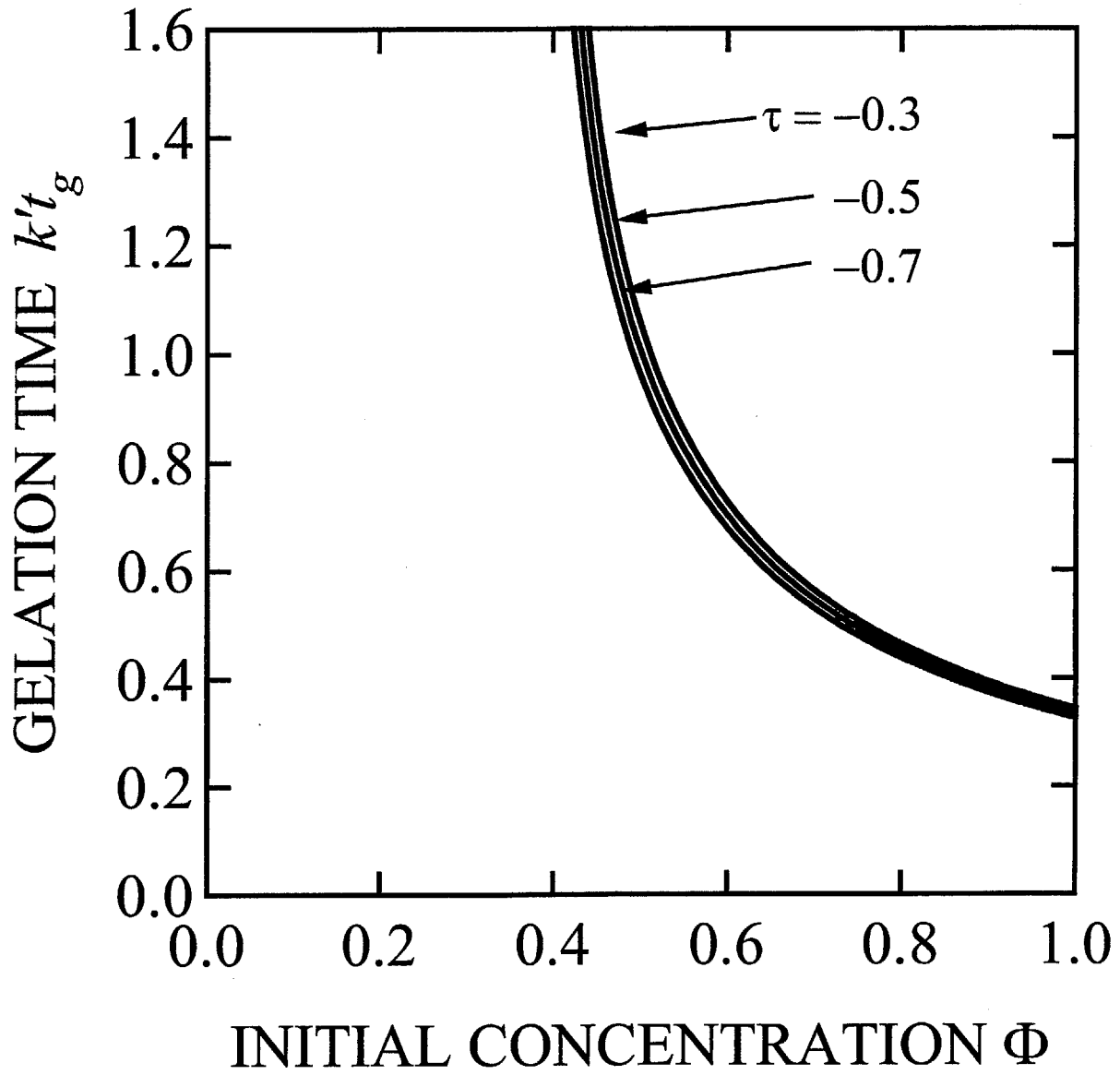

Figure 5.6: Gelation time plotted as a function of the initial concentration in an inactive solvent system. The reaction temperature is changed from curve to curve.

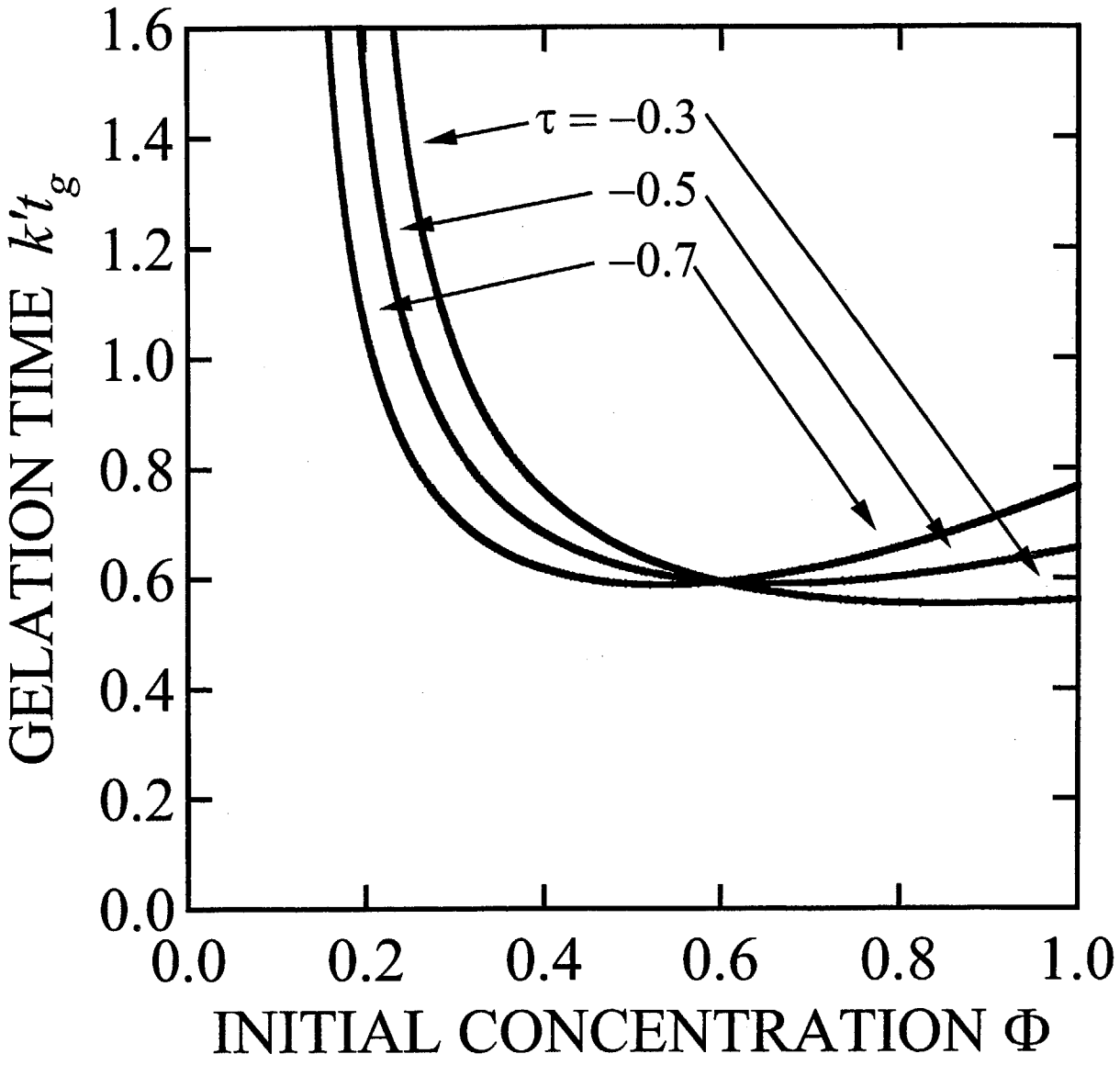

Figure 5.7: Same as in Figure 5.6, but in an active solvent system.

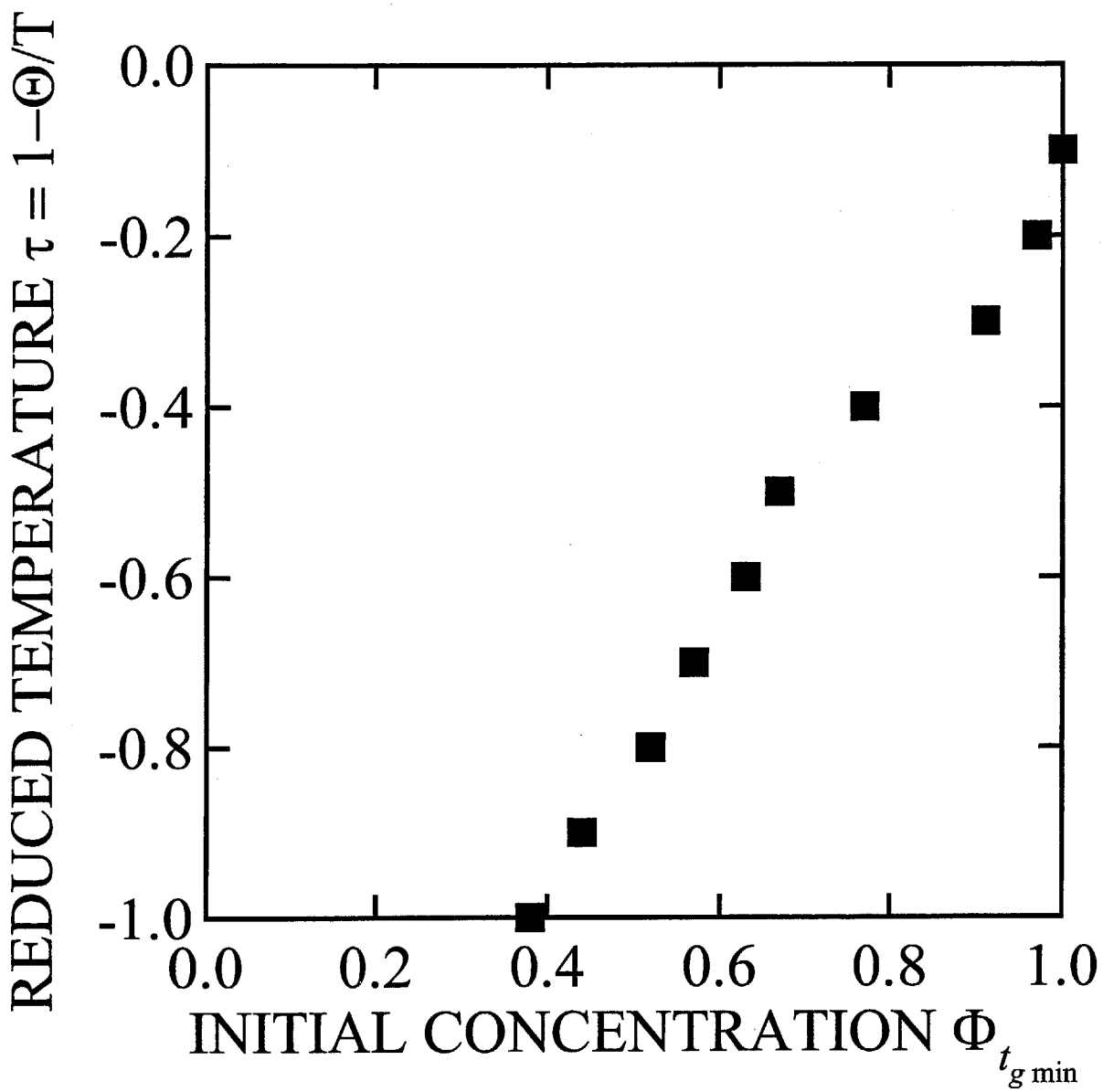

Figure 5.8: Reaction temperature plotted as a function of initial concentration Φ_{tgmin} which has minimum gelation time in an active solvent system.

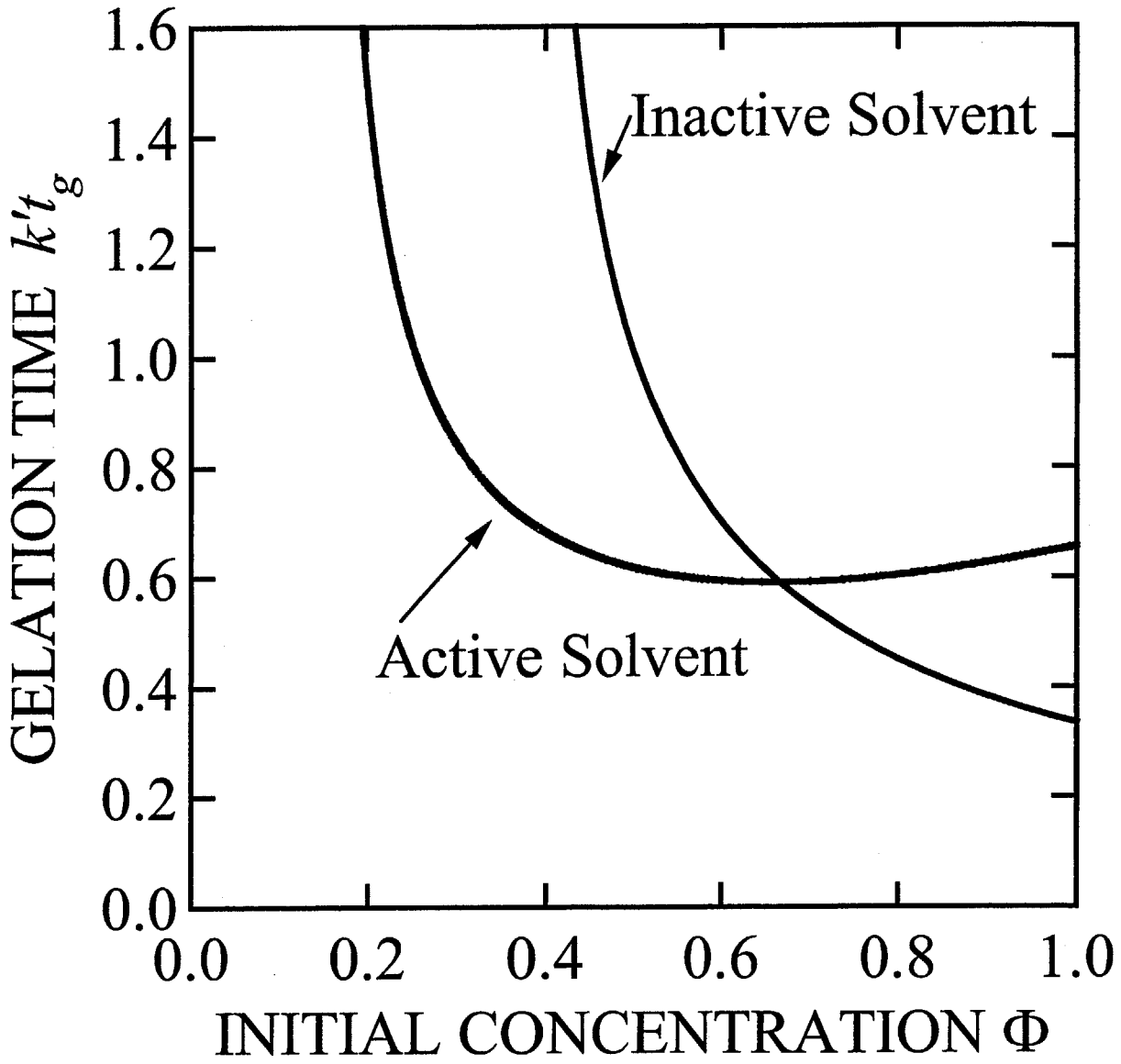

Figure 5.9: Gelation time plotted as a function of initial concentration in both systems.

5.4 Conclusions and Discussion

We have theoretically studied the gelation-induced phase separation by using time-dependent phase diagrams in a common case of primary molecules with $f = 4$ and $n = 5$. We can predict the change of the solution properties with the progress of polycondensation from the initial concentration and the reaction temperature, for example, we can find the initial conditions where a gel point is reached without phase separation. There are two types in the solution of phase separation and gelation - phase separation precede type and gelation preceding type. In the phase separation preceding type (inactive solvent system), the solution changes from homogeneous sol, sol/sol phase separated, then sol/gel phase separated solution. At the termination of the reaction, since a gel point is not reached in the dilute phase, the solution remains sol/gel phase separated solution. In the gelation preceding type (active solvent system), the solution changes from homogeneous sol, homogeneous gel, then gel/gel phase separated solution.

We also calculate the gelation time in both systems. The gelation time in the inactive solvent system decreases monotonously as the initial concentration of monomer increases. This is because it is easy to contact each functional group, then the reaction rate is faster and the conversion α is higher. In the active solvent, the gelation time has a minimum point where is the most efficient concentration for gelation. At higher concentration, we have to consider the formation of the water molecules by forward reaction. The opportunities that contact each functional group are decreased by the formation of the solvent molecules. This effect makes both the reaction rate slower and phase separation easier.

Bibliography

[1] Tran-Cong, Q.; Harada, A. *Phys. Rev. Lett.* **1996**, *76*, 1162.

[2] Verchere, D.; Sautereau, H.; Pascault, J. P.; Riccardi, C. C.; Moschiar, S. M.; Williams, R. J. J. *Macromolecules* **1990**, *23*, 725.

[3] Girard-Reydet, E.; Pascault, J. P. *Macromolecules* **2000**, *33*, 3084.

[4] Kyu, T.; Lee, J. H. *Phys. Rev. Lett.* **1996**, *76*, 3746.

[5] Ponton, A.; Griesmar, P.; Barboux-Doeuff, S.; Sanchez, C *J. Mater. Chem.* **2001**, *11*, 3125.

[6] Ponton, A.; Warlus, S.; Griesmar, P. *J. Colloid Interface Sci.* **2002**, *249*, 209.

[7] Mal, S.; Maiti, P.; Nandi, A. K. *Macromolecules* **1995**, *28*, 2371.

[8] Mal, S.; Nandi, A. K. *Polymer* **1998**, *30*, 6301.

[9] Mal, S.; Nandi, A. K. *Langmuir* **1998**, *14*, 2238.

[10] Tanaka, F. *Macromolecules* **1990**, *23*, 3784; 3790.

[11] Tanaka F.; Stockmayer, W.H. *Macromolecules* **1994**, *27*, 3943.

[12] Tanaka, F. *Molecular Gels*; Ed. Weiss, G.; Terech, P., Kluwer Academic Pub.: London 2006; Chapter.1.

[13] Flory, P. J. *Principles of Polymer Chemistry*; Cornell University Press: Ithaca, NY 1953; Chapter.IX.

[14] Flory, P. J. *J. Am. Chem. Soc.* **1941**, *63*, 3083; 3091; 3096.

[15] Stockmayer, W. H. *J. Chem. Phys.* **1943**, *11*, 45.

[16] Schultz A. R.; Flory, P. J. *J. Am. Chem. Soc.* **1963**, *75*, 3888; 5631.

Chapter 6

Conclusions and Perspectives for the Future

In chapter 2, the author has theoretically studied sharp phase separation in aqueous thermosensitive polymer solutions of poly (*N*-isopropylacrylamide). The author assumed that sharp phase separation with flat cloud point curve, which is almost independent on the molecular weight and concentration, is caused by the cooperative hydration (dehydration), i.e., bound water molecules covering the polymer chain are sharply dehydrated in one cluster after another. The author analyzed the experimental results along with this hypothesis. Thus, he developed a general thermodynamic theory of phase transition in aqueous polymer solutions under cooperative hydration analogous to the Zimm-Bragg coil-helix transition model. As the results, he found the coverage of bound water is independent of both molecular weight and polymer concentration. Thus, hydration can be regarded as single chain problem. If the cooperativity of hydration is stronger, the spinodal curves are flatter and more independent of both molecular weight and polymer concentration, the shape of phase separation region becomes a box type due to sharp dehydration near the phase separation temperature. The spinodal curves found in this theory agree well with the experimental ones obtained by light scattering. Thus, the author concluded that sharp phase separation is caused by cooperative hydration.

In chapter 3, the author theoretically studied gelation and phase separation in solutions of hydrophobically end-capped polymers. The author built a new theory that combine the theory for hydration in chapter 2 with Tanaka-Stockmayer theory for thermoreversible gelation with micellar crosslinks by hydrophobic aggregation. When the author applied the theory to telechelic associating polymers, he found that the spinodal curve shifts to lower temperature along with sol/gel transition line. In the case of both high molecular weight and strongly cooperative hydration, the downward shift of spinodal curve is small. When molecular weight is higher, the density of hydrophobic groups is lower, then hydrophobic interaction is weaker; thus it is difficult to form large clusters. When cooperativity in hydration is stronger, sharper dehydration occurs at the near single chain coil-globule transition temperature; thus, it is difficult to form large clusters of polymer chains by hydrophobic interaction up to the temperature very close to the coil-globule transition temperature. These results show a good qualitative agreement with the experimental data. In the case of weak cooperativity for low molecular

weight polymers, there is a special molecular weight of polymers where a loop-shaped high temperature phase separated region merges with a dome-shaped low temperature phase separated region. This point is called *double critical point.* The shape of phase separation region turns into an hourglass type.

In chapter 4, the author applied the theory of chapter 3 to polycondensation systems with focus on the sol/gel transition under controlled vapour pressure. The thermodynamic conditions, i.e., pressure and temperature, to reach the gel point without phase separation are found. In the case of strong reaction where reaction enthalpy is larger than the mixing enthalpy, the gel point can be easily reached by depressing the vapour pressure at high temperature. At low temperature, however, the gel point is not reached due to the high vapour pressure where the solution tends to be phase separated. In the case of weak reaction, there is a condition where the solutions turns back to a sol phase from a gel (reentrant sol phase) by giving pressure due to the strong backward reaction.

In chapter 5, the author developed a new theory that the theory in chapter 4 is combined with reaction kinetics, then the author theoretically studied the time dependence of gelation and phase separation in associative and reactive solutions by analyzing the time-dependent phase diagram and the conversion diagram. The author also found the gelation time, i.e., the time required to reach the gel point from an arbitrarily given initial state. In the time-dependent phase diagram and the conversion diagram, he could predict the time dependence of solution properties from reaction temperature and initial molar ratio of monomers and solvent. He also found the initial condition to reach a gel point without phase separation. To study the effect of the byproduct of water molecules as solvent, the author compared inactive solvent systems to active solvent systems. The difference of these systems lies in whether the water molecule is formed or not in the forward reaction. In an inactive solvent, the reaction proceeds faster at higher concentration of the monomer. In active solvent, however, the reaction is slow at concentrated regime. In this regime, due to the formation of water, the probability that the reaction site contacts each other decreases, then the reaction rate is slow at the initial stage. Thus active solvent system is easier to phase separate than inactive solvent system. In inactive

solvent, gelation time monotonously decreases when the concentration of monomer increases. In the case of active solvent, there is the concentration where gelation time becomes minimum, thus the author could find the most effective initial composition for gelation.

In conclusions, the author theoretically studied gelation and phase separation in associative and reactive solutions with focus on hydration, hydrophobic interaction, vapour pressure of solvent, and reaction time. Through the present study of many simple reactive and associating solutions from the unified theoretical point of view, the author obtained many pieces of fundamental knowledge on the mutual interference between phase separation and thermoreversible gelation in aqueous polymer solutions. Thus the author confirms that the theory can be applied to more complex system such as water-soluble polymers carrying many hydrophobes, associating polymer/surfactant mixtures, ternary systems such as TEOS(monomer)/H_2O(active solvent)/EtOH(inactive solvent) and hetero-polycondensation systems. There remain, however, many problems to be solved to understand their molecular mechanisms more precisely, such as interference phenomena between hydration and association in associating polymer solutions, formation and aggregation of flower micelles in telechelic associating polymer solutions at dilute regime, calculation of cloud points, and phase separation in polycondensation at postgel regime. The author hopes that some solutions of these problems will be addressed in his future papers.

List of Publication

Full Papers

Chapter 2

Y. Okada and F. Tanaka

Cooperative Hydration, Chain Collapse, and Flat LCST Behavior in Aqueous Poly(*N*-isopropylacrylamide) Solutions

Macromolecules **38**, 4465-4471 (2005).

Chapter 3

Y. Okada, F. Tanaka, P. Kujawa and F. M. Winnik

Unified model of association-induced lower critical solution temperature phase separation and its application to solutions of telechelic poly(ethylene oxide) and of telechelic poly(*N*-isopropylacrylamide) in water.

J. Chem. Phys. **125**, 244902 (2006) (11 pages).

P. Kujawa, F. Segui, S. Shaban, C. Diab, Y. Okada, F. Tanaka and F. M. Winnik

Impact of End-Group Association and Main-Chain Hydration on the Thermosensitive Properties of Hydrophobically Modified Telechelic Poly(*N*-isopropylacrylamides) in Water

Macromolecules **39**, 341-348 (2006).

Chapter 4

Y. Okada and F. Tanaka

Pressure-Controlled Thermoreversible Gelation

Macromolecules **39**, 8153-8162 (2006).

Chapter 5

Y. Okada and F. Tanaka

Time-Dependent Phase Diagrams for Gelation-Induced Phase Separating Systems

Submitted to *Macromolecules*.

Review Articles

F. Tanaka and Y. Okada
Theoretical Study of Phase Diagrams in Associating Polymer Solution Systems
- I. Nongelling System -
Netsu Sokutei **32**, 178-185 (2005).

F. Tanaka and Y. Okada
Theoretical Study of Phase Diagrams in Associating Polymer Solution Systems
- II. Gelling System -
Netsu Sokutei **32**, 249-255 (2005).

Proceedings of International Conference

Y. Okada and F. Tanaka
Hydration and Thermoreversible Gelation in Solutions of Telechelic Associating Polymers
Polymer Networks Group Conference, M18 (2006)
Sheffield University, Sheffield, UK, 3-7 September, 2006.

Acknowledgements

The present thesis is based upon the study carried out under the supervision of Professor Fumihiko Tanaka, at Department of Polymer Chemistry, Graduate School of Engineering, Kyoto University, during the years 2000 - 2003 and 2004 - 2007.

First of all, the author wishes to express his sincere gratitude to Professor Fumihiko Tanaka for his continuous and patient guidance, encouragement, valuable suggestions and discussions during this study.

The author is extremely grateful to Professor Tomonari Dotera, Professor Tsuyoshi Koga, and Dr. Tsutomu Indei (Fukui Institute for Fundamental Chemistry, Kyoto University) for their useful advice, encouragement and valuable suggestions. The author also acknowledges Dr. Masahiko Shoji for valuable suggestions and supports.

Professor Takenao Yoshizaki (Department of Polymer Chemistry, Kyoto University) and Professor Toshikazu Takigawa (Department of Material Chemistry, Kyoto University) are especially acknowledged for their critical review of this thesis.

The author acknowledges all of the professors and staffs of Department of Polymer Chemistry, Kyoto University to support his researcher and student life.

The author wishes to his thanks to Professor Françoise M. Winnik (Faculty of Pharmacy, University of Montréal) for her helpful suggestions and support from experimental point of view and Dr. Piotr Kujawa (Department of Chemistry, University of Montréal) for his collaboration in the light scattering and DSC measurements of aqueous solutions of *telechelic* PNIPAM.

The author acknowledges a lot of foreign and domestic scientists for their critical comments, discussions and encouragement at international and domestic conferences. The author is very sorry that their names are not mentioned due to the lack of space. The author also thanks the 21st. Century Centers of Excellence (COE) for a United Approach to New Materials Science from Japan Society for the Promotion of Science and Trinity Chemistry Education from Ministry of Education, Culture, Sports, Science and Technology of Japan for giving an opportunity to participate in the international conference Polymer Networks Group 2006.

The author would like to thank all of the students of Professor Fumihiko Tanaka's Laboratory in the past and current, especially his classmates; Professor Yohei Otani (Department of Electronic Systems Engineering, Tokyo University of Science, Suwa), Dr. Kazuhiko Ikeuchi (Solid State Science for Quantum Structure, KANSAI Institute, Japan Atomic Energy Agency), Mr. Makoto Kawamoto (Nihon L'ORÉAL Co. Ltd.) and Mr. Tatsuya Enomoto for their useful suggestions and cooperation.

The author wishes acknowledge to Ms. Naoko Oda, a secretary of Professor Fumihiko Tanaka's Laboratory for her kind help.

The author had worked in The Bank of Kyoto, Ltd. Shoji Branch for about one year after he finished his master course. The author would like to thank his boss Mr. Kou Nishizawa (former branch manager of Shijo branch, current director of securities and international division), Mr. Ryoji Morishita (office manager), Mr. Masaharu Usui, Mr. Hirohisa Yasu (acting branch manager), Ms. Kyoko Morishita (chief teller), Mr. Kohei Sunazawa (his instructor), his coworker Mr. Masayuki Yoshida, Ms. Megumi Kakuda, Ms. Kaori Nishiguchi and all of the members of Shijo branch for encouraging at his farewell party.

The author has been supported by a lot of relatives and friends, especially close friends Professor Osamu Tonomura (Department of Chemical Engineering, Kyoto University), Professor Akira Makino (Department of Material Chemistry, Kyoto University), Mr. Yuichi Idomoto (Sumitomo Electreic Industries, Ltd.), Mr. Kazuhisa Takeda, Mr. Taro Kawarasaki from his undergraduate days, Mr. Takayuki Ohtuka and Mr. Yasuyoshi Katayama from his high school days.

Finally, the author expresses his heartfelt thanks to his parents, Kouichi and Takemi Okada for their care and constant encouragement during his studies.

January, 2007

Yukinori Okada